AdriaClim

Climate change information, monitoring and management tools for adaptation strategies in Adriatic coastal areas

Project ID: 10252001

D5.4.5 Multi-risk assessment in the Veneto Region pilot area: comparative analysis and prioritization of main impacts, vulnerabilities and risks related to climate change

PP09 – CMCC, PP02 – ARPA Veneto

Final version

Public document

June, 2023

Project Acronym:	AdriaClim
Project ID Number:	10252001
Prject Title:	Climate change information, monitoring and management tools for adaptation strategies in Adriatic coastal areas
Priority Axis:	2 - Climate change adaptation
Specific objective:	2.1 - Improve the climate change monitoring and planning of adaptation measures tackling specific effects, in the cooperation area
Work Package Number:	5
Work Package Title:	Adaptation Plans
Activity Number:	5.4
Activity Title:	Veneto Coastal Pilot: Adaptation/Mitigation/Intervention Plan
Partner in Charge:	P02 ARPA Veneto
Partners involved:	P01 CNR, P09 CMCC, P14 AULSS3, P17 COV
Status:	Final
Distribution:	Public
Date:	30/06/2023

Work Package:	5. Adaptation plans
Activity:	5.4 Veneto Coastal Pilot: Adaptation/Mitigation/Intervention Plan
Deliverable:	D.5.4.5 Multi-risk assessment in the Veneto Region pilot area: comparative analysis and prioritization of main impacts, vulnerabilities and risks related to climate change
Authors	ARPA Veneto: Francesco Rech, Giovanni Massaro, Fabio Zecchini; IUAV: Francesco Musco, Denis Maragno, Filippo Magni, Gianfranco Pozzer, Nicola Romanato; CMCC@Ca'Foscari: Silvia Torresan, Maria Katherina Dal Barco, Davide Mauro Ferrario, Ngoc Diep Nguyen, Margherita Maraschini, Heloisa Labella Fonseca, Olinda Rufo, Stefania Gottardo, Andrea Critto.
Due month	M42
Delivery month	M42

Table of contents

1.Introduction

Risk can be defined as the probability of occurrence of hazardous events or trends multiplied by the impacts if these events or trends occur. The risk originates from the interaction among hazard, vulnerability and exposition (IPCC, 2014).

In this deliverable two approaches for estimating the risk are described.

The first approach (Section 2. "A Machine Learning approach to support climate multi-risk assessment and adaptation planning in the Veneto region") is based on a Machine Learning (ML) approach and is valid for the whole Veneto coastal area. The ML approach is proposed to assess climate risks caused by extreme weather events affecting the coastal municipalities of the Veneto region. Thanks to the ability to integrate large volumes of heterogeneous information and to model non-linear relations among multiple factors, ML models offer an innovative path to analyse multi-hazard events.

The ML model was designed according to a tiered approach composed of two subsequent phases. At first, the identification of the most influencing factors triggering the daily risk score allowed to understand the relationships between the observed atmospheric and marine hazards, and the impacts recorded in the reference timeframe (2009-2019). Moreover, the Veneto coastal municipalities were clustered to understand the intrinsic relationships between the occurrence of impacts and the characteristics of exposure and vulnerability. Secondly, the estimation of the annual risk frequency was made possible by integrating in the designed ML model the output of the AdriaClim modelling chain developed under RCP8.5 future climate change scenarios until year 2050. The developed ML model predictes an increasing trend of future climate risks, as a result of the combination of extreme levels of sea surface height, seasonal precipitation, and wind strength along the investigated case study. The performed assessment could represent valuable information to drive adaptive policy pathways in the context of coastal zone management and climate adaptation in the Veneto coastal area.

The second approach (Section 3. "Spatial multi-criteria risk assessment approach for climate change adaptation and mitigation policies") is valid at urban scale and consists in the evaluation of the predisposition to the risk at some coastal municipalities. The areas more predisposed to suffer possible impacts (heat in urban areas, urban flooding and coastal flooding) are identified through a multi-criteria analysis in GIS environment. In parallel, an analysis on the exposure through OpenStreetMap data is conducted. The intersection of the vulnerability and exposure point-based data leads to the indication of areas potentially subject to a climate change-induced risk. This second

approach also gives valuable information to support adaptation policies and territory planning in the Veneto coastal area.

2. A Machine Learning approach to support climate multi-risk assessment and adaptation planning in the Veneto region

Over the past three decades, the global climate has experienced a significant and unprecedented increase in temperature, which has led to the occurrence of several extreme events worldwide (Lange et al., 2020). The frequency of high-temperature events (i.e., hot days and tropical nights) and extremely high rainfall events (triggering pluvial and fluvial floods) has already increased in many parts of the world (IPCC, 2021; Goswami et al. 2006; Schickhoff et al. 2016). Similarly, in many regions, the number of rainy days has significantly decreased causing severe water scarcity and drought conditions (Rani and Sreekesh, 2017). These hazards interact and affect the environment and society in complex ways. Furthermore, it is proved that the cumulative impact of multiple interacting hazards is greater than the total effects of the single ones (Terzi et al., 2019). This can result in an underestimation of risk. Eventually, these complex hazards are likely to have significant effects on populations, infrastructures, and ecosystems due to the poor level of preparedness (de Ruiter et al., 2020).

Coastal areas are particularly vulnerable to the impacts of climate change, due to the high population density, interconnected economic activities and the presence of fragile habitats and ecosystems (Richards and Nicholls, 2009). The analysis of extreme events that occurred in the last decades shows that these are often generated by multiple hazards, acting at different temporal and spatial scales (Lange et al., 2020). The growing impacts that natural disasters and climate change have on people and ecosystems make the ability to model and predict the relationships between multiple risks and their evolution over time critical expertise (Halsnæs & Trærup, 2009; Simpson et al., 2021; Van Aalst, 2006). Accordingly, an integrated approach is needed to estimate the relationship between the risk factors (i.e., hazard, exposure, and vulnerability), evaluate the multiplicity of impacts, and estimate the potential risk from climate change in the future that may occur at the land-sea interface.

The use of classical deterministic approaches may be very challenging as the relationship between hazards, exposure and vulnerability, and the presence of impacts is highly non-linear and site-dependent (Rivera-Velasquez et al., 2013; Tao et al., 2018). In recent times, data-driven tools (e.g., Artificial Intelligence and Machine Learning algorithms) are becoming increasingly implemented as they offer a new path to tackle the analysis of multi-risk events, due to their ability to integrate great volumes of heterogeneous data, as well as to model non-linear relations between multiple factors (Zennaro et al., 2021). Understanding the relationship between weather-induced impacts and risk

factors is an important tool in the hands of governing bodies to develop mitigation strategies and early warning systems. Machine Learning (ML) models have been developed to detect rare and extreme climate events (Daizong Ding et al., 2019) and to investigate patterns of risks (Richman & Leslie, 2018; Schlef et al., 2019). Furthermore, when applied in conjunction with future climate change models (e.g., Representative Concentration Pathways – RCP scenarios produced by the Intergovernmental Panel on Climate Change – IPCC; IPCC, 2014), it can be leveraged to improve confidence in estimating the social cost of climate change. However, only few studies were conducted through the implementation of ML algorithms to estimate climate risks in the medium-term and long-term future under the impacts of climate change (Lee et al., 2020; Maina et al., 2021).
The proposed study was aimed at designing and implementing a ML model able to assess multiple climate change related risks in the coastal area. The study was developed in the frame of the EU-Interreg Italy-Croatia AdriaClim project[1], aiming at enhancing climate change adaptation capacity in coastal areas developing advanced tools, indicators, and information systems.
Specifically, a two-tier ML approach is proposed to assess climate risks caused by extreme weather events affecting the coastal municipalities of the Veneto Region, Italy. The first tier was applied with atmospheric and oceanographic observed data as well as vulnerability and exposure factors over the reference timeframe of 2009-2019, aiming to identify the most influencing factors triggering the daily risks (i.e., risk score, to the potential occurrence of damages on population, infrastructures, and the territory). Moreover, the understanding of the intrinsic relationships between the occurrence of impacts and the exposure and vulnerability characteristics was made by an analysis of impacts according to groups of municipalities sharing similar patterns in territorial and geographical features. The second tier further explore the annual risk frequency under a baseline (i.e., historical situation of the system using as input modelled data for the 2009-2019 timeframe) and a climate change scenario (i.e., RCP8.5 till the year 2050), by integrating in the ML model the data developed from the AdriaClim climate downscaling modelling chain (as described in the deliverables *D.3.2.1* and *D.3.2.2* of the AdriaClim Project). The variations of estimated risks were explored under different combinations of single and multiple extreme hazard factors, allowing the understanding of the nature of multi-risks and multi-hazards over the study site.
Following the characterization of the case study area (**Section 2.1**), the application of the first tier is detailed in **Section 2.2,** integrating observed data for the daily estimation of impacts from extreme events for the reference timeframe 2009-2019. Further applications of the algorithms developed in

[1] https://www.italy-croatia.eu/web/adriaclim

the first tier in the prediction of annual risks for both baseline (2009-2019) and future climate change RCP8.5 scenario (2020-2050) are described in **Section 2.3.** The conclusions on the applicability of the ML approach in climate risk assessment and the implications for climate adaptation in the coastal areas of the Veneto Region are detailed in **Section 2.4.**

2.1. Study area: the coastal zone of the Veneto region

The coastal area of the Veneto region stretches approximately 156 km along the Adriatic Sea and overlooking the Gulf of Venice. It borders Emilia Romagna region to the South and Friuli Venezia Giulia region to the North (Ruol et al., 2016). The eleven Veneto coastal municipalities (**Figure 1**) belong to the provinces of Venice (i.e., San Michele al Tagliamento, Caorle, Eraclea, Jesolo, Cavallino-Treporti, Venice, and Chioggia) and Rovigo (i.e., of Rosolina, Porto Viro, Porto Tolle, and Ariano nel Polesine).

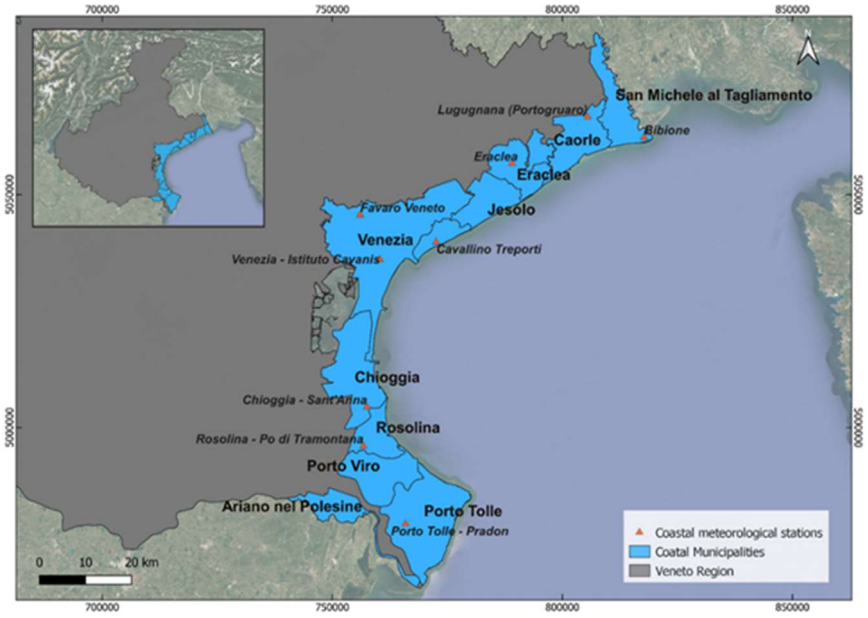

Figure 1: Coastal municipalities of Veneto Region and their meteorological stations.

The littoral zone of the Veneto region belongs to the subcontinental temperate zone (Barbi et al., 2013), characterised by annual mean temperatures (around 14°C) higher than the average 13°C of the internal zones (Barbi et al., 2013), and by fewer rain days, lower rainfall accumulations, and more days with heavy precipitation (Barbi et al., 2012). From a geomorphological point of view, the low-lying coast, fragmented by the presence of seven river mouths (i.e., Tagliamento, Livenza, Piave,

Sile, Brenta, Adige, Po, from north to south), presents gentle-slope and sandy beaches resulting from alluvial plain coasts that evolved during the Holocene into three lagoons (i.e., Caorle lagoon, Venice lagoon, and lagoons of the Po River Delta), barrier beaches, deltas, and spits. Moreover, the sedimentary shore can be subdivided into a northern, central, and southern trait. Specifically, the northern trait is characterized by straight littorals, where the longshore transport has a south-westerly direction, which is progressively increasing (Ruol et al., 2018). The central stretch belongs to Venice and includes the sandy barrier islands of Lido and Pellestrina, with a quite null net longshore sediment transport given by the convergent site (Bezzi et al., 2018). The southern trait comprehends the Po Delta system, the largest wetland area of Italy, dominated by several river outlets and salt marshes (Regione del Veneto, 2012; Torresan et al., 2008). Despite the natural evolution of the coast, starting from 1950, the Veneto littoral has been subjected to abrupt urbanization and anthropic pressure, a condition that, over time, has brought to a considerable change in land use (e.g., to industrial, urban, and touristic buildings). On the other hand, 60 km of the overall littoral have conserved their natural status, mainly because they cover lagoonal and fluvial estuary areas, which are difficult to urbanize (Legambiente, 2012).

The overbuilding of the coast, together with an improper management of the area (e.g., intensive water withdrawal from rivers, gravel and sand excavation, presence of several dams) has decreased the sedimentary budget for beach and dune accretion, resulting in coastal erosion which is exacerbated by sea-level rise and storm surge conditions. However, in recent times, there has been a period of recovery, thanks to the beach nourishment interventions accomplished between 1997-2011 (MATTM, 2017), as well as other soft adaptation strategies, including foredune restoration.

Regardless of these management improvements, in this zone, the relative sea-level rise is due to the combined effects of natural eustasy (i.e., sea level increases because of the change in the ocean water volume due to ice melting, thermal expansion of the water, or change in the ocean floor consequent to tectonic activity) and subsidence (i.e., downward vertical movement of the bottom level, which along the Veneto coast has both natural and human causes) (Camuffo, 2021; Cavalieri, 2020).

The coastal municipalities of the Veneto region comprehend several natural protected areas, regional parks and reserves (e.g., Bocche di Po, Valle Averto, Delta Po regional park, Bosco Nordio), and areas included in the European ecological network Natura 2000 (Regione del Veneto, 2012; Ruol & Pinato, 2016). On the other hand, the socio-economic capital is mainly related to maritime traffic, fisheries, aquaculture, agriculture, industrial activities (e.g., Porto Marghera), offshore activities and tourism (Torresan et al., 2012). Specifically, the primary sector (i.e., agriculture, forestry, and fishing)

covers an average share of 7.42% of the total regional employment, against the 0.59% of the non-coastal areas. The tertiary sector, comprehending mainly tourism, is very important and particularly associated to the city of Venice, as well as to beach destinations, which are chosen for the high quality of water (Rizzi et al., 2016).

The Veneto coastal area is subjected to multiple natural and anthropic pressures, which are now intensified by climate change. Precisely, the average temperature rose by +0.55°C per decade, a higher value compared to the global trend, with summer and autumn seasons recording the highest increment of +0.7°C. Rising temperature determines, on one hand, the widespread of intense rainfalls with strong wind gusts, flooding, and storm surge, on the other, the magnification of heatwaves which create health risks for the population and drought conditions. In addition, these extreme events aggravate the natural coastal inundation phenomenon, which is one of the principal natural hazards affecting the case study area. In particular, the occurrence of extreme sea-levels, along the North Adriatic, is expected to increase in the upcoming years as a combination of tides, storm surges and wave energy (Ferrarin et al., 2013, 2022; Umgiesser et al., 2021).

2.2. Design of a Machine Learning model to evaluate the risks related to extreme weather events along the Veneto coastal municipalities

2.2.1. Data characterization for the daily risk evaluation

The implementation of the ML model requires the analysis of the occurrence of impacts related to extreme weather events along the coastal municipalities of the Veneto region during the 2009-2019 decade with daily temporal scale. In particular, for each municipality and for each day, a series of features (i.e., indicators, henceforth) which constitutes the input variables of the algorithm were collected, as well as the output labels, i.e., a Boolean indicator of the presence/absence of impact.

The indicators are a set of spatio-temporal heterogeneous variables that can influence the likelihood of an impact to occur in an area, which can be related to hazard, exposure, and vulnerability. As far as the output variables are concerned, the presence or absence of an impact was estimated in each municipality on a given day. The data cleaning, which consists in filling of missing data and identifying errors in the input datasets, played a major role, as a correct execution of this step has major effects on the performances of the model.

Moving toward the application of the methodology, data collection was divided into input features (**Section 2.2.1.1**) related to hazards, and impacts (**Section 2.2.1.2**), as well as to exposure and

vulnerability information to characterise the coastal municipalities of the Veneto region (**Section 2.2.1.3**).

2.2.1.1. Input features

In order to estimate the impacts along the Veneto coastal municipalities, the ML-based approach must include hazard-related indicators, such as atmospheric (i.e., precipitation, wind, humidity, and solar radiation) and oceanographic features (i.e., sea surface height and significant wave height). The hazard information is related to the day when the impact did and did not occur, as well as to the delay of reactions related to the occurrence of extreme events. Indicators of precipitation and solar radiation (Table 1) were also calculated considering the previous three days in order to take into account the delayed reaction to hazards. Another factor that indirectly influences the likelihood of having an impact, and hence it is useful to consider as input for the ML, is the month of the year. Regarding vulnerability and exposure characteristics of the investigated case study (e.g., land use, population, soil types, topography), they are available as a snapshot in time (e.g., annual or multi-year scale), and in any case their percentage variation with time is very small. As the vulnerability and exposure indicators are almost constant over time, and only one value per municipality is available, their contribution to the creation of the impact is conveyed by the municipality index. Therefore, it is possible to estimate the influence that each municipality has in creating the impact, but it was not possible to determine which of the vulnerability and exposure factors are causing it. In order to reduce the risk of overfitting, during the ML analysis we started with a wide range of indicators, and we iteratively reduced their number, gradually removing the indicators that did not play a key role in the estimation of the impacts (see **Section 2.2.3** for more details). The final list of input features is summarised in **Table 1**.

Table 1: List of input data to characterize the Veneto coastal case study.

Acronym	Definition
Month	*Month related to the impact*
Municipality	*Location where the impact occurred*
MSSH	*Maximum hourly sea surface height in a day*
MWIH	*Maximum hourly significant wave height in a day*

WIH	*Daily average significant wave height*
PRCMAX	*Maximum hourly precipitation in a day*
PRCTOT	*Total daily precipitation*
PRCTOT_TOT_MAX_3	*Maximum daily total precipitation in the previous 3 days*
RAD_MAX_3	*Maximum daily total solar radiation in the previous 3 days*
RX-1day	*Maximum daily precipitation in a month*
URmax	*Maximum hourly relative humidity in a day*
VRFDd	*Maximum hourly wind velocity in a day*

The atmospheric data were derived from the monitoring network of the Regional Agency for Environmental Protection and Prevention of the Veneto Region (ARPAV)[2], which acquires precipitation, temperature, humidity, wind and solar radiation data at hourly or daily basis. Each municipality has at least one monitoring station, except for Jesolo, Porto Viro, and Ariano nel Polesine (**Figure 1**). Considering the proximity of the municipalities and the low variation in the values of the atmospheric parameters, in accordance with the data provider, the *Nearest Neighbour Rule* was applied to infer their atmospheric conditions. In particular, the average values of the two closest stations were calculated or replaced with the values of the nearest missing station in case of a municipality bordering another region (i.e., Ariano nel Polesine). On the other hand, Venezia has two stations within its territory, and similar values were recorded, except for humidity. However, since specific parameters were missing in 2009 and 2017 at the Favaro Veneto station, for the data analysis and the implementation of the ML-based methodology, the Venezia - Istituto Cavanis station was the only one to be used. Additionally, wind indicator data from the monitoring stations has been integrated with information from the European Severe Weather Database[3], as local events (e.g., tornadoes) may not be detected by the stations.

On the other hand, oceanographic hazard indicators for the Veneto case study were collected from the Copernicus Marine Service (CMEMS)[4] provided by the European Union's Earth Observation Programme. The above-mentioned indicators were retrieved from the Mediterranean Sea Physics Reanalysis products (i.e., MEDSEA_MULTIYEAR_PHY_006_004), which is the product of a numerical composed hydrodynamic model, supplied by the Nucleous for European Modelling of the Ocean (NEMO) and a variational data assimilation scheme (OceanVAR). The reanalysis is forced by hourly ECMWF ERA5 atmospheric forcing fields and assimilates reprocessed data. Specifically, SSH and WIH data are provided under a regular grid of 1/24˚ (about 4 km) at hourly resolution. In agreement with

[2] https://www.arpa.veneto.it/

[3] https://eswd.eu/

[4] https://marine.copernicus.eu/

atmospheric parameters, the values of the closest pixels to the municipalities' coastline were extracted and aligned with the local data at the *Acqua Alta* platform, by adding the mean difference with the observation data during the reference period. A detailed description of the input datasets was described within the deliverable *D5.4.6 'Definition of primary risk information layers for the Veneto Pilot area'* of the AdriaClim project.

2.2.1.2. Impact data

The impact data indicator includes both damages (e.g., agricultural losses, shoreline erosion, damage to buildings) and services interruption (e.g., blackouts, impaired viability), caused by extreme climate events within the coastal municipalities of the Veneto region. In particular, data on impacts were extracted from the *Decreto del Presidente della Giunta Regionale* (DPGR, namely Decree of the President of the Regional Council)[5] reports which witness the activation of the regional state of crisis, namely *'Stato di crisi'*. These documents reveal the qualitative information on damages and issues of the elements at risk on the municipal level after the occurrence of extreme events. Typologies of the damages reported include physical damages related to urban flooding, agriculture/fisheries, people (e.g., fatalities, injuries, displacements), beaches (e.g., shoreline erosion, debris accumulation), structures/infrastructures, economic activities, and tertiary sector. Ideally, in order to accurately determine the quantitative extent of impacts, more detailed data and reports on the investigated extreme event, including coordinates, typology, monetary cost of restoration would be required. However, detailed quantitative data on impacts and their economic costs are not in the public domain. Therefore, the risk indicator that we used in the present analysis is characterised by the list of coupled 'Date' and 'Municipality' where an impact occurred.
Moreover, to avoid the risk of misleading information on the consistency between location and time of reported impacts, each positive sample has been checked against local newspapers, in order to identify the correct coupling between dates and municipalities. Additionally, local newspapers have also been used to identify events that were not reported in the *'Stato di crisi'* database, but still led to damages to population or infrastructures. Eventually, the impact dataset comprises a total of 447 days of impacts from extreme weather events over eleven Veneto coastal municipalities during the 2009-2019 timeframe (**Figure 2**).

[5] http://bur.regione.veneto.it/BurvServices/Pubblica/sommarioDecretiPGR.aspx?expand=19

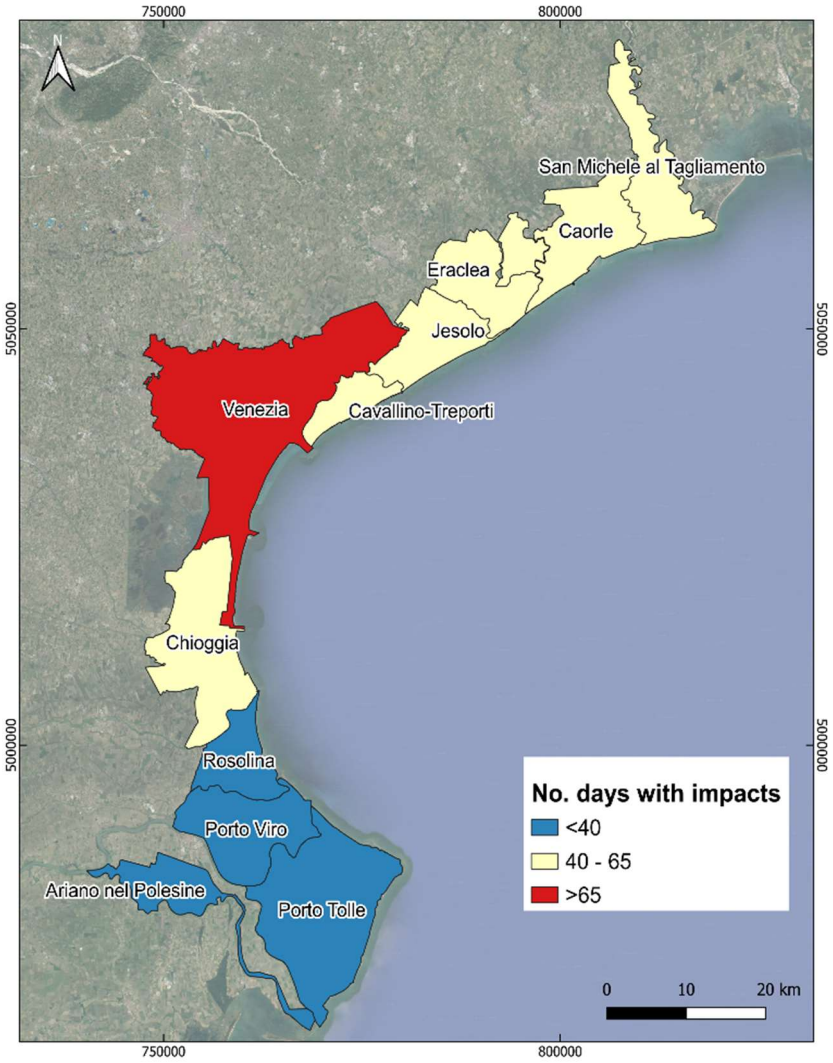

Figure 2: Frequency of the impacts recorded within the reference timeframe (2009 – 2019) along the coastal municipalities of the Veneto region.

2.2.1.3. Characterization of coastal municipalities

In order to support the analysis of the factors that drive the occurrence of impacts, which will be introduced within the *feature importance* (**Section 2.2.2.3**), the coastal municipalities of the Veneto region were clustered based on the occurrence of impacts, as well as on exposure and vulnerability features.

Firstly, the former analysis highlighted the frequency of days with recorded impacts (**Figure 2**), based on the impact data described in **Section 2.2.1.2**., pointing out how the different coastal municipalities of the Veneto region are affected by extreme weather events.
On the other hand, it is of pivotal importance characterising the area to analyse the intrinsic relationships of impacts occurrence against exposure and vulnerability characteristics, and thereby understanding the reason for this trend. Consequently, the municipalities were clustered into four groups, as detailed in **Figure 3**.

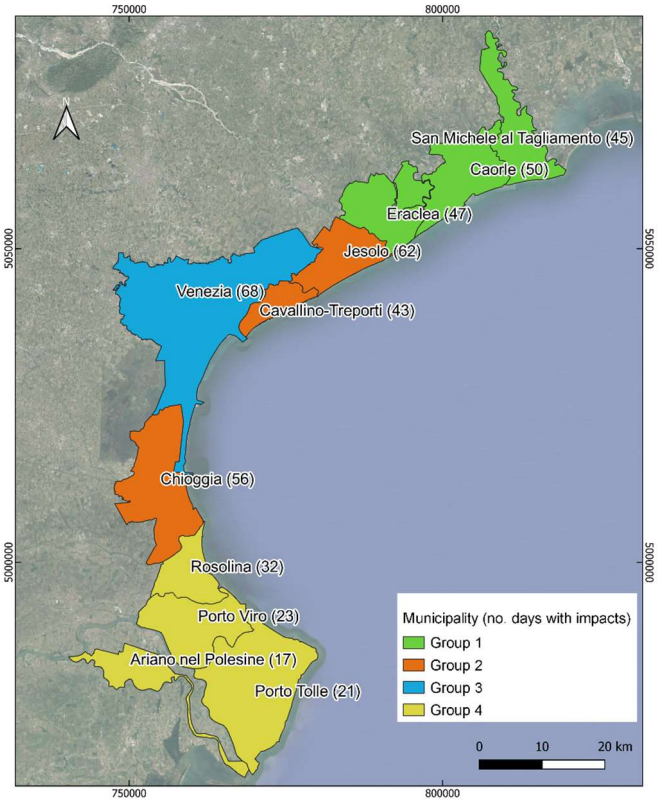

Figure 3: Classification of the coastal municipalities according to the occurrence of the impacts, as well as on the characteristics of exposure and vulnerability.

The total area of each municipality, the land-use types (i.e., anthropic, agriculture, natural, water bodies), soil characteristics (i.e., permeability, dune ridges and lagoon islands, reclaimed lagoon areas artificially drained), population (i.e., total population and density), and topography (i.e., elevation, slope) were investigated. In particular, the municipality extension deserves a special mention, as it is reasonable to expect that bigger municipalities are affected by more impacts.

However, it is impossible to normalize the number of days with impacts using the municipality size, as it is not recorded if more than one impact happens on a given day.

Topography data of the study site were derived directly from the Digital Elevation Model (DEM) of 10m x 10m obtained by the National Institute of Geophysics and Volcanology. Data on soil types and permeability were retrieved from ARPAV Geoportal[6] with a scale of 1:50.000. Population and land-use data were collected from the JRC web portal[7] with a resolution of 1km x 1km. Exposure and vulnerability characteristics were extracted as average value for each municipality and normalized to a scale from 0 to 1. The resulting outputs of the analysis are shown in **Figure 4** and described below from North to South.

Group 1 consists of the municipalities of San Michele al Tagliamento, Caorle and Eraclea. The territory is mainly covered by agricultural fields, which are former lagoon areas that have been reclaimed and artificially drained, lowering the soil permeability coefficient (**Figure 4**). The lagoonal municipalities of Jesolo, Cavallino-Treporti and Chioggia have been assembled in *Group 2*. Although the dunes have been reinforced to protect the mainland, they have the second highest number of impacts. However, this may be referred to anthropic land use, as buildings and facilities have been built for tourism purposes (**Figure 4**). The municipality of Venice, identified as *Group 3,* is by far the biggest municipality, the most densely populated and urbanised, and it covers the highest extension of water (i.e., lagoon and coast), which increases the inundation risks concurrently with storm surge events (**Figure 4**). Finally, the municipalities located in the province of Rovigo (i.e., Rosolina, Porto Viro, Porto Tolle and Ariano nel Polesine – *Group 4*) are the least developed, since the area is covered by rural fields and natural parks (e.g., River Po Delta Regional Park; **Figure 4**).

[6] https://gaia.arpa.veneto.it/

[7] Joint Research Centre Data Catalogue - Land-Use based Integrated Sustainability Assessmen... - European Commission (europa.eu)

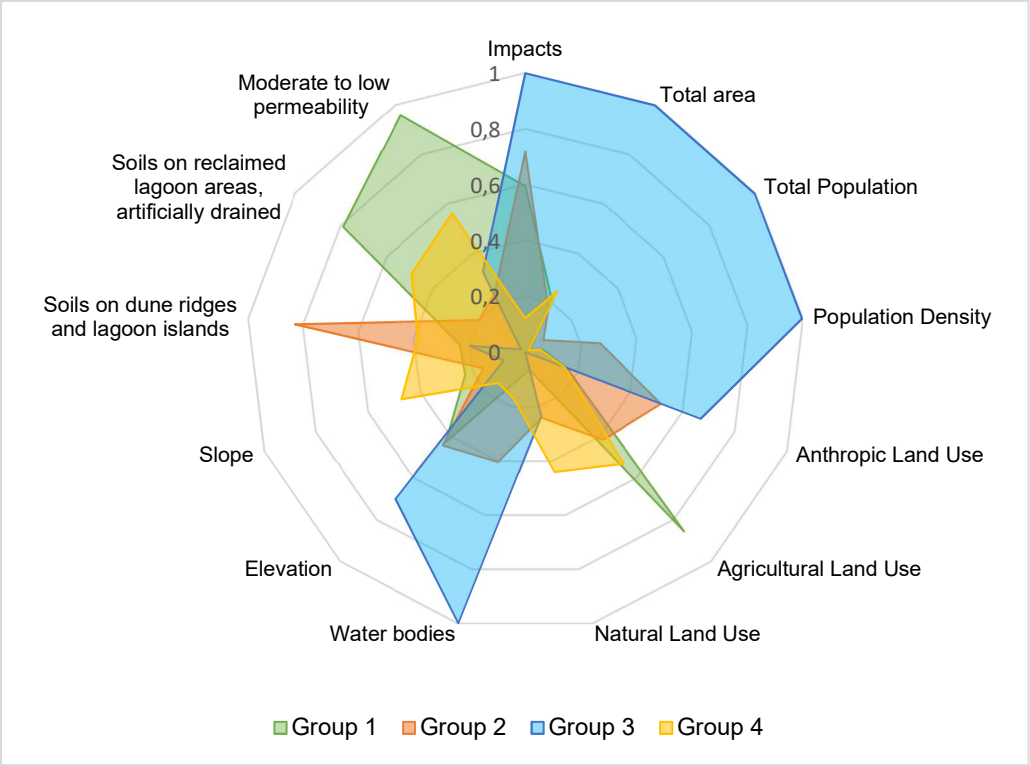

Figure 4: Visualisation of the analysis combining the historical impacts and territorial features carried out to characterise the coastal municipalities of the Veneto region.

A detailed description of both impact, exposure and vulnerability datasets were described within the deliverable *D5.4.6 'Definition of primary risk information layers'* of the AdriaClim project.

2.2.2. Method

Artificial Intelligence (AI) and Machine Learning (ML) algorithms offer a new path to address the analysis of multiple environmental hazards due to their ability to model complex feedbacks and non-linear interactions between different factors without the need for an explicit modelling. In the frame of this work, several Supervised ML methods for binary classification, whose goal is learning a function that maps input features to their associated binary labels Goodfellow et al. (2016), were tested. Each of these algorithms takes as input the value of the hazard-related indicators (e.g., the atmospheric and oceanographic indicators) in each municipality on each day and as output label the presence, (represented by the value 1) or absence (represented by the value 0) of an impact in the same municipality and day; the output of the algorithm is the risk score (i.e., a value describing the

likelihood of a positive outcome, represented by the occurrence of impacts on a given day and municipality) associated to a set of input values.

The challenges for the application of binary classification algorithms along the coastal municipalities of the Veneto region are the skewness of the dataset, the quality of the impact data (i.e., coarse, sparse, inaccurate impact records), and the non-independence of samples. In particular, the skewness of the dataset makes the estimation of impacts in the Veneto coastal area fall into the category of rare event estimation (i.e., a classification problem in which occurrences of one class take place with a significantly lower frequency compared to more common events) (Maalouf & Trafalis, 2011). The problems related to the general binary classification are common and can be solved easily, however the skewness of the dataset adds a degree of complexity, as some adjustments are needed to correctly estimate the risk score of the elements in the minority class. Moreover, any classification result of a binary classification on a skewed dataset will be affected by a high number of false positive cases compared to the true positives. The coarse spatial resolution and the low quality of the dataset will thus result in a low sensitivity to vulnerability and exposure factors, as well as in a general lower performance. In machine learning it is impossible to improve data quality with processing. However, we propose a method robust for dealing with low-quality impact datasets (often referred to weather-related impact estimation), bearing in mind that the quality of the results is always data-dependent.

2.2.2.1. Metrics

After the definition of the problem, the following step of the Machine Learning (ML) design consists in the choice of the metric, i.e. a scalar function that takes as input the estimated and the observed output for the whole dataset and outputs the error, i.e. a single real number that describes the distance of the algorithm result from the target: the lower the error value, the better the algorithm performance (**Figure 5**). The metric is then used to optimize the values of the algorithm parameters and to compare the performances of different algorithms.

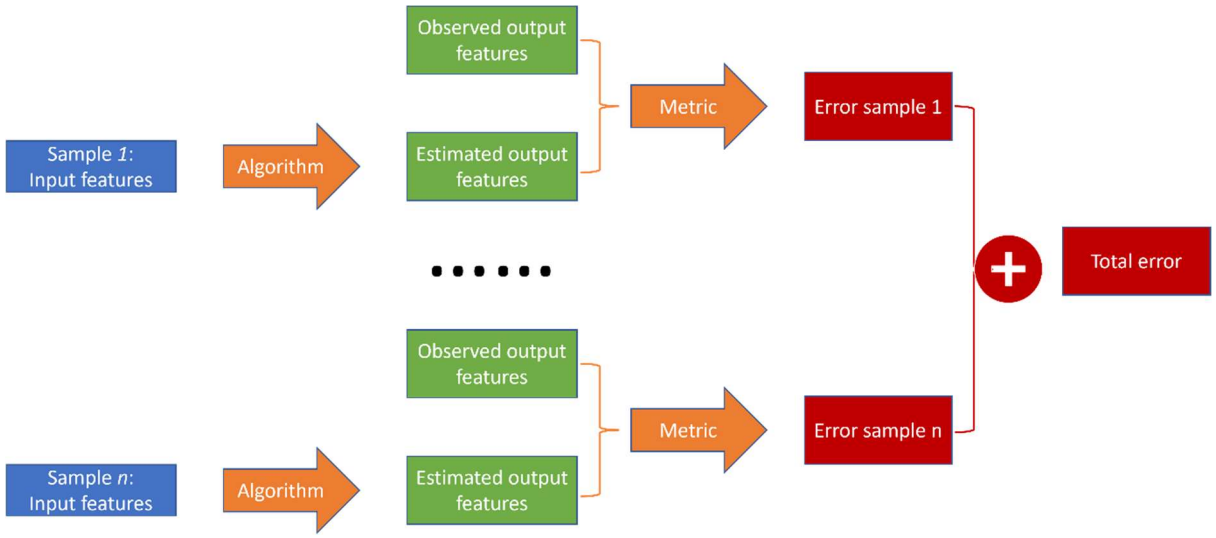

Figure 5: Scheme of the calculation of the error for each algorithm: for each sample of a given dataset the algorithm calculates the estimated output features. The distance between the estimated and the calculated output features for each sample is calculated by the metric, and the weighted sum of the sample error over the dataset represents the performance of the algorithm on the dataset.

The choice of the metric is extremely important as it would set the objective of the analysis and define which errors are worse than others, influencing the results more than any of the other choices. In order to define the metric for this specific case study (i.e., a binary classification problem of an extremely skewed dataset), we need to address two issues: *(i) how to calculate the error of each sample? (ii) which weight to attribute to each class?*

Considering the estimation of the error for a single sample first, most algorithms for binary classification (including the one implemented in this study) calculate a probability p_i that a sample i is associated with the positive class. Consequently, it is possible to associate a sample i to the positive class if this estimate p_i is above a threshold T and to the negative class otherwise, but it is also possible to divide the predicted class in more categories (i.e., positive, negative, undetermined). The metric that estimates the error for each sample can be based on the difference between the observed and the estimated class **Figure 6-a** or on the difference between the observed class and the estimated probability value **Figure 6-b**. The main difference between these approaches is that, when using a metric based on the number of samples that fell into each class (like accuracy, precision, recall, F1 score), the same loss can be attributed to events with very different values of risk score (points P1 and P2 in **Figure 6-a** have the same loss, while their probability is very different)

. On the other hand, if a metric (such as the log-loss) is used, two elements belonging to the same class but with different predicted probabilities have different losses (points P1 and P2 in **Figure 6-b** have the different losses).

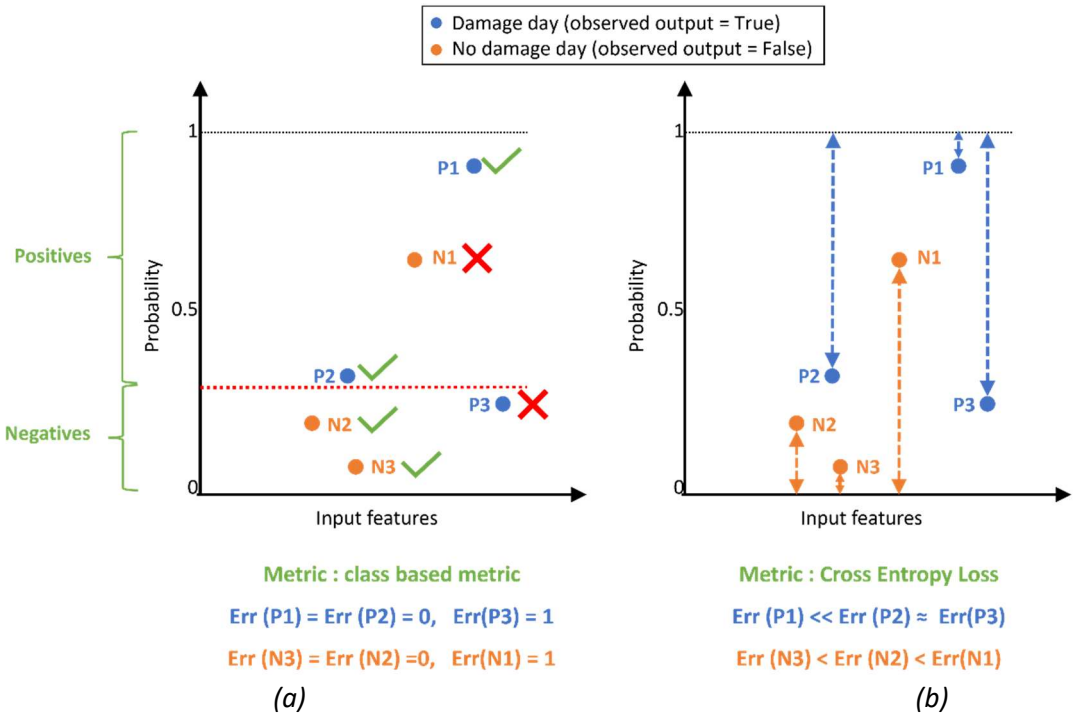

Figure 6: Schematization of a class-based metric (a) versus a probability-based metric (b). In (a) the probability value estimated for each sample is only used to be compared against a threshold (red dotted line). All samples with probability higher than the threshold are considered positives, and the others are considered negatives, irrespectively of the value of the probability inside the range. In (b) the error of each sample is associated with the probability value of the sample, and no threshold is considered.

The probability-based metric 'Cross Entropy Loss' has been used, because this function can better represent the uncertainty of the problem, and allows for more flexibility in the use of the results (a binary classification can be determined afterward by setting a threshold). However, as the knowledge of the class (i.e., if a sample is likely associated with an impact) is useful in most applications, the weighted F1 score is also used to analyse the results. The threshold is defined by maximizing the weighted F1 score on the test dataset.

In rare-event-estimation tasks most classification algorithms can sharply underestimate the probability events belonging to the minority class (King et al., 2001): possible solutions of the unbalance problem can be the application of weights, the under-sampling of the majority class or the oversampling of the minority one (Cahyana et al., 2019; Ertekin et al., 2007; He et al., 2021).
In light of these considerations, the explicit formula of our chosen metric, the (binary) cross entropy with weights inversely proportional to the cardinality of each class, is:

$$loss = \frac{1}{n}\sum_{i=1}^{n} \quad w[y_i \, ln\,(f(x_i))\,] + (1 - y_i)\, ln\,(1 - f(x_i))\,,$$

where *w* is the ratio between the number of elements in the negative class and in the positive class and $f(x_i)$ is the predicted value of the probability for sample x_i .
It is important to note that the probability calculated by the algorithm is not the probability of having an impact on a given day because the weights are not 1.

2.2.2.2. Algorithm

In order to design a Machine Learning (ML) model for the analysis of impacts of atmospheric and marine indicators, the available data must be divided into training/validation and test sets. In this study, the data was split chronologically (Lam et al., 2022). Specifically, the train and validation dataset corresponds to the years from 2010 to 2016, and the test dataset is related to the years after 2016. This choice, although not ideal from a ML point of view, is justified by the non-independence of data samples: some indicators are monthly or yearly, and others are based on the values that the indicator assumed in the previous days, hence indicators of adjacent days are correlated.
Then, several ML algorithms were coded (using ScikitLean[8]), trained, tuned and compared*: (i)* a neural network (i.e., Multi-Layer Perceptron – MLP; Murtagh, 1991), *(ii)* a Random Forest (RF; Breiman, 2001), and *(iii)* a Support Vector Classifier (SVC; Chang & Lin, 2001). Other options were also considered, including autoencoders (Baldi, 2012) and isolation forest (Liu et al., 2008) for anomaly detection, but the preliminary results were not promising, these options were dropped in the early stages.
Given the relatively small amount of data available, to reduce the high redundancy of clusters of features (e.g., precipitation features, sea features) and the risk of overfitting, during the ML analysis

[8] https://scikit-learn.org/

the number of indicators were iteratively decreased, gradually removing the indicators that, accordingly to the feature importance, did not play a key role in the estimate of the result. After each step of this procedure, the validation set was used to check that the algorithm performances did not decrease. Similarly, an error analysis was performed iteratively on the training set, and outliers were identified and cross-checked.
After the tuning, the final parameters of the algorithms are summarized in **Table 2**. Note that oversampling of the positive events in the training dataset is performed before training.

Table 2: Algorithm parameters

RF		**MLP**		**SVC**	
Number of Trees	200	**Maximum # of iterations**	2000	**Kernel**	rbf
Max depth	4	**# hidden layers**	2	**C**	0.01
Criterion	Log Loss	**Hidden layer sizes**	5	**Probability**	True
Minimum sample split	5	**Alpha**	3	**Degree**	3

The algorithms are then applied to the test dataset, and results are summarized in the **Section 2.3.2**.

2.2.2.3. Feature importance

The permutation method was implemented for feature importance, which was defined by Breiman (2001) as the decrease of the metric value when the values of a single feature are randomly shuffled. Features are important if they contain valuable information, hence the more important a feature is, the more the prediction results will be affected by incorrect values, and this decrease of performances may be a measure of the importance of that specific feature.
The implementation of the method consists of randomizing one input variable at a time, calculating the corresponding loss value for the metric and repeating the process several times to reduce the sensitivity to the randomized set. The decrease in algorithm performance due to randomising a feature is a measure of the importance of this feature.
The feature importance was conducted over the whole domain of the study site in order to understand the driving factors of the impacts. In particular, the contribution of the atmospheric,

oceanographic, temporal and geographical factors to impacts was explored. In addition, in order to better understand the contribution of vulnerability and exposure to the dynamics of risks, the feature importance was performed explicitly to groups of municipalities sharing similar patterns, as detailed in **Section 2.2.1.3**. The results of these analyses are illustrated in **Section 2.3.2.1.**

2.2.3. Results

As described in **Section 2.2.2**, the proposed study was organised into a preliminary data analysis and the following implementation of the ML algorithms. In particular, the results of hazard and impact data analysis are presented in **Section 2.2.3.1**, whereas **Section 2.2.3.2** highlights the result of the ML model application along the coastal municipalities of the Veneto region. Finally, **Section 2.2.3.3** outlines the results of the feature importance for the whole Veneto region and the group of municipalities described in **Section 2.2.1.3**.

2.2.3.1. Data analysis results

The collected hazard indicators (described in Section 2.2.1) were analysed, in order to study the occurrence and characteristics of different single and multi-hazards events in the 2009-2019 timeframe. In particular, the values for extreme precipitation events (PRCPTOT), extreme wind (VRFDd), extreme sea surface height (SSH, as proxy for storm surges) and extreme heat (TDd) were extracted for each municipality of the Veneto coastal area.

With regards to extreme precipitation, different percentiles were tested (such as 95th percentile, 99th percentile, excluding or including days with no precipitation) and finally the 95th total percentile (calculated over the whole distribution) was used to identify extreme precipitation events (Tilloy et al., 2022; Yu et al., 2022). The 95th total percentile was selected also for identifying extreme sea surface height events. On the other hand, with regards to extreme wind events, after several testing the 99th total percentile was selected (Tilloy et al., 2022). With regards to extreme heat, a moving window was applied to daily data (3-days in the final analysis), and then a daily-based percentile (90th percentile) was calculated to extract the extremes: each calendar day (e.g., 1st January) has a different percentile-threshold, calculated over all the days (e.g., 1st January) in the timeframe, in order to better account for the seasonality of temperature data (Barriopedro et al., 2023). Moreover, an extreme heat event was identified only if its duration persisted for more than a certain number of days (i.e., at least three consecutive days over the percentile) and an

empirical threshold was applied to select only heat extremes happening between May and September (Sutanto et al., 2020; Yu et al., 2022).

The anomalies for single hazards were combined in order to identify multi-hazard events and their characteristics, checking for the simultaneous presence of extreme values happening in the same municipality. As described in **Section 2.2.1.3**, the results were then aggregated for each municipality group, calculating for each single or multi-hazard combination the more relevant associated indicators.

The intensity of each combination of single and multi-hazard event was calculated: for each day and municipality in which the extreme event happened, the maximum value of the involved indicators was extracted. Then, arithmetic average and maximum were calculated for each single and multi-hazard combination to extract the mean and most extreme event associated with each type of event. In the following tables we show a subset of these values, in particular: the mean total daily precipitation (PRCPTOT), mean maximum wind velocity (VRFDd), mean maximum daily temperature (TDd) and Maximum Sea Surface Height (MSSH max). Moreover, also the number of days in which a municipality was impacted by the event and the most frequent month and season associated with each specific event are presented in the tables.

Table 3: Multi-hazard events characteristics in the northern municipalities (i.e., Group 1, including San Michele al Tagliamento - M1, Caorle - M2, Eraclea - M3)[9]

Name	Events in M1	Events in M2	Events in M3	PRCPTOT (mm/day)	VRFDd (m/s)	TDd (°C)	MSSH max (m)	Month	Season
Extreme Precipitation	305	213	216	24.45	-	-	-	9	3
Extreme Wind	47	51	44	-	14.50	-	-	2	1
Extreme Heat	170	185	174	-	-	29.36	-	8	3
Extreme SSH	154	147	153	-	-	-	0.41	11	4
W+S	16	15	13	-	**15.83**	-	0.34	11	4
W+H	1	1	1	-	13.08	**30.69**	-	7	3
R+H	2	2	5	18.62	-	29.48	-	7 & 8	3
R+S	62	76	73	24.47	-	-	-	11	4
R+W	16	26	24	**30.02**	14.03	-	0.44	8	3
R+W+S	24	26	23	28.13	15.43	-	**0.75**	11	4

Table 4: Multi-hazard events characteristics in the lagoon municipalities (i.e., Group 2, including Jesolo - M4, Cavallino-Treporti – M5, Chioggia – M7)[9]

Name	Events in M4	Events in M5	Events in M7	PRCPTOT (mm/day)	VRFDd (m/s)	TDd (°C)	MSSH max (m)	Month	Season
Extreme Precipitation	198	172	245	21.30	-	-	-	9	3
Extreme Wind	50	35	47	-	16.08	-	-	2	1
Extreme Heat	180	181	216	-	-	29.09	-	8	3
Extreme SSH	157	164	168	-	-	-	0.47	11	4
W+S	16	11	14	-	**16.75**	-	0.30	12	4
W+H	3	1	5	-	15.77	29.43	-	7	3
R+H	2	2	5	17.00	-	29.43	-	7,8,9	3
R+S	67	67	69	22.03	-	-	-	11	4
R+W	24	25	21	26.25	16.24	-	0.52	5,7,8	3
R+W+S	24	23	25	**28.66**	16.69	-	**0.74**	11	4
R+W+H	1	**0**	0	14.01	15.59	**30.13**	-	8	3

Table 5: Multi-hazard events characteristics in the Venice Municipality (i.e., Group 3)[9]

Name	Events in M6	PRCPTOT (mm/day)	VRFDd (m/s)	TDd (°C)	MSSH max (m)	Month	Season
Extreme Precipitation	305	24.85	-	-	-	9	2
Extreme Wind	64	-	17.02	-	-	3	1
Extreme Heat	213	-	-	29.49	-	8	3
Extreme SSH	148	-	-	-	0.33	11	4
W+S	15	-	18.14	-	0.15	11	4
W+H	6	-	15.78	**30.31**	-	7	3
R+H	10	20.86	-	29.78	-	7	3
R+S	77	26.66	-	-	-	11	4
R+W	55	**34.43**	17.53	-	0.50	8	3
R+W+S	33	32.17	**18.24**	-	**0.76**	11	4
R+W+H	5	16.28	17.92	29.71	-	7	3

Table 6: Multi-hazard events characteristics in the southern municipalities (i.e., Group 4, including Rosolina - M8, Porto Viro - M9, Porto Tolle - M10, Ariano nel Polesine - M11)[9]

[9] The different hazard combinations resulting from the analysis are presented in the following tables and thus labelled:

Name	Events in M8	Events in M9	Events in M10	Events in M11	PRCPTOT (mm/day)	VRFDd (m/s)	TDd (°C)	MSSH max (m)	Month	Season
Extreme Precipitation	200	210	221	233	19.64	-	-	-	9	3
Extreme Wind	33	44	46	52	-	16.60	-	-	2	1
Extreme Heat	202	207	218	178	-	-	28.69	-	8	3
Extreme SSH	178	174	177	173	-	-	-	0.50	11	4
W+S	15	9	13	9	-	17.42	-	0.24	12	4
W+H	1	2	3	4	-	15.21	**30.08**	-	7	3
R+H	1	5	7	1	16.76	-	29.20	-	7,8,9	3
R+S	67	68	73	71	20.23	-	-	0.37	11	4
R+W	11	24	38	28	23.38	17.04	-	-	5,7,8	3
R+W+S	19	17	23	20	**24.05**	**17.44**	-	**0.63**	11	4

Across all the different groups of municipalities, we note that the most common multi-hazard events are those involving storm surges and extreme precipitation (R+S), extreme precipitation and wind (R+W) and storm surges, extreme precipitation and extreme wind (labelled as R+ W+S in the figures). Moreover, while single hazard events were more common, the most extreme values of total precipitation, wind velocity and sea surface height (highlighted in **bold** in the tables) were consistently recorded during multi-hazard events. In particular, compound rain, wind and storm surge events (R+W+S) recorded the highest values for SSH across all municipalities, while PRCPTOT and VRFDd were still close to the maximum in most cases. The seasonality of the multi-hazard events highlights how events associated with sea surface height are most common during the last three months of the year, regardless of whether they are single hazards or associated with others. Instead,

- Extreme precipitation: single-hazard events where only PRCTOT was above the threshold;
- Extreme Wind: single hazard events where only VRFDd was above the threshold;
- Extreme Heat: single hazard events where only TDd was above the threshold;
- Extreme SSH: single hazard events where only SSH was above the threshold;
- W+S: multi-hazard events in which VRFDd and SSH were above the threshold;
- W+H: multi-hazard events in which VRFDd and TDd were above the threshold;
- R+H: multi-hazard events in which PRCPTOT and TDd were above the threshold;
- R+S: multi-hazard events in which PRCPTOT and SSH were above the threshold;
- R+W: multi-hazard events in which PRCPTOT and VRFDd were above the threshold;
- R+W+S: multi-hazard events in which PRCPTOT, VRFDd and SSH were above the threshold;
- R+W+H: multi-hazard events in which PRCPTOT, VRFDd and TDd were above the threshold.

wind extremes are most common during winter months when associated with no other hazard, while they are most often linked to summer months when associated with either extreme heat or extreme precipitation. Alternating dry and wet events, characterised by the presence of high temperature, extreme wind and/or extreme precipitation have also been identified during the summer months, even if they are comparably rare in the analysed timeframe.

After analysing the multi-hazard combination, the comparison of different hazard indicators was done, focusing on their distribution and, especially to the days when an impact was recorded, or not (**Figure 7**). Temperature related indicators were dropped from successive analyses since most of the impacts were associated with events connected with extreme wind, extreme precipitation or extreme sea surface height.

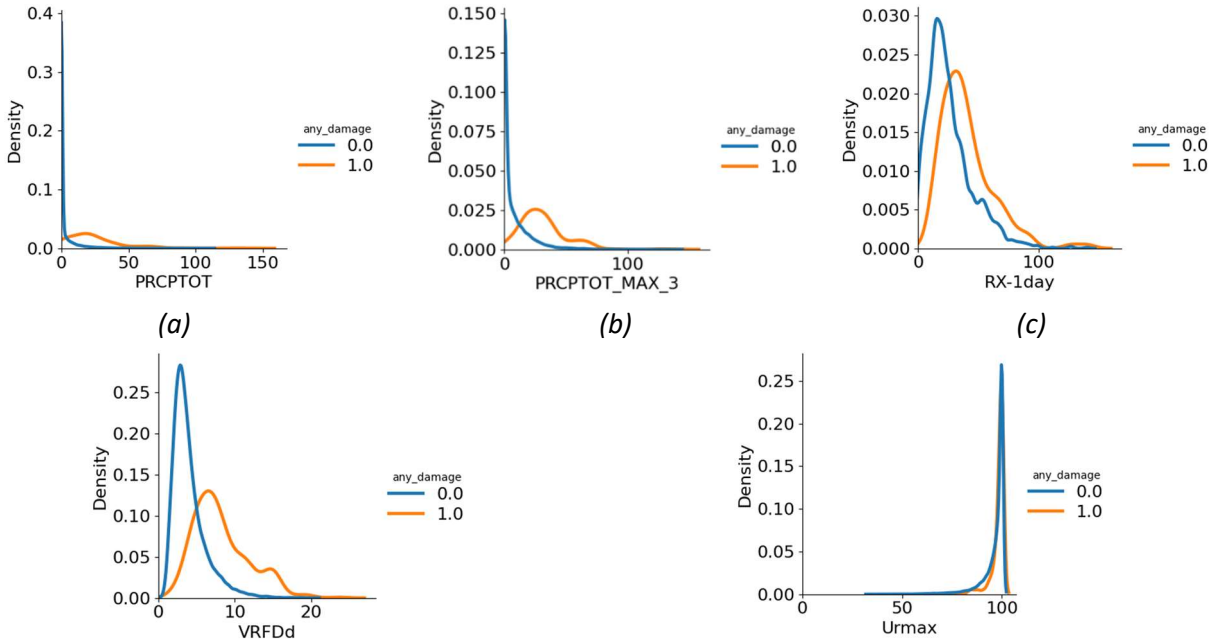

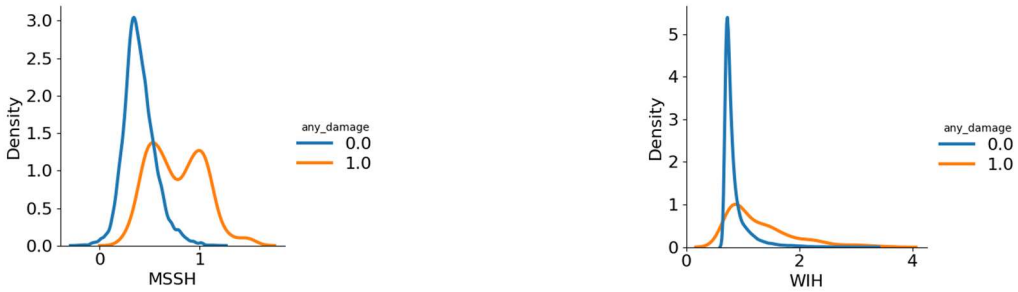

(f) *(g)*

Figure 7: Distribution of indicators during days with and without impacts.

The indicators related to precipitation (i.e., PRCTOT, PRCMAX, PRCTOT_TOT_MAX_3, and RX-1day) show that the distribution of the values associated with impacts is more shifted towards higher levels of precipitation when compared to absence of impacts. In practical terms, this means that impacts are more likely to occur if the amount of precipitation is higher. Similar considerations can be drawn for maximum sea surface height (MSSH), wave height (MWIH and WIH), and maximum wind velocity (VRFDd).

The difference in the distribution of the maximum solar radiation over the previous 3 days and the maximum humidity (i.e., RAD_MAX_3 and URmax, respectively) is more subtle, suggesting that these indicators are not strongly correlated with the presence of an impact, and therefore will not be very useful in the ML analysis.

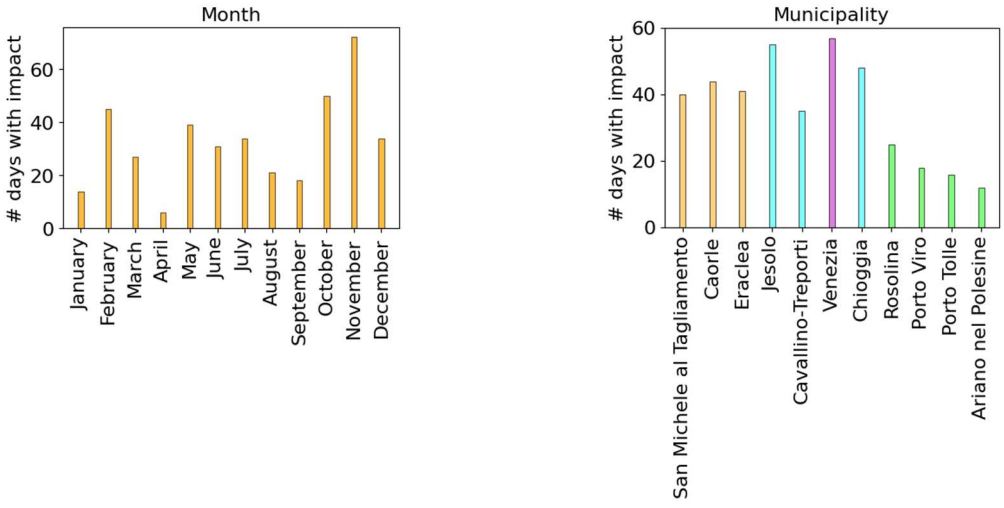

(a) *(b)*

Figure 8: Distribution of indicators during days with and without impacts.

Finally, the monthly histogram shows that summer and autumn months, especially July, October and November, are more affected by impacts than any other months (**Figure 8-*a***). As far as the

investigated coastal municipalities are concerned, Venice, Jesolo, and Chioggia show a higher number of impact days, while the southern town (i.e., Rosolina, Porto Viro, Porto Tolle, and Ariano nel Polesine) had lowest impacts (**Figure 8-*b***).

2.2.3.2. Classification results

The objective of this application is the estimate of a risk score for each sample, i.e. the potential occurrence of impacts for each couple day, municipality; the risk score is calculated by the implemented ML algorithm using the climate-relate hazard indicators (i.e. atmospheric and marine drivers of impact) as inputs.

The results obtained in terms of probability of impacts for the three algorithms are shown in **Figure 9**. Each point corresponds to a sample in the input data (i.e., a couple of dates and municipality). In particular, blue points represent the samples associated with an impact and orange points represent samples associated with no impact. The vertical position of the point represents the risk score: if a point has a high risk score, it is more likely to be affected by an impact.

In the training process, each algorithm determines its parameter by minimizing the error between the calculated and the measured outcome (i.e., by trying to move all the blue points to the top of the plot, and all the orange points to the bottom), while in the training phase the information on the impact is only used to measure the quality of the results. Ideally, blue points in both training and in testing should be placed as close as possible to 1 and all orange points to 0. The results of Support Vector Classifier (SVC) and Multi-Layer Perceptron (MLP) are quite similar and with most orange points very close to 0 and most blue points on the upper side of the plot. On the other hand, the Random Forest (RF) algorithm has blue and orange points in the central part of the plot.

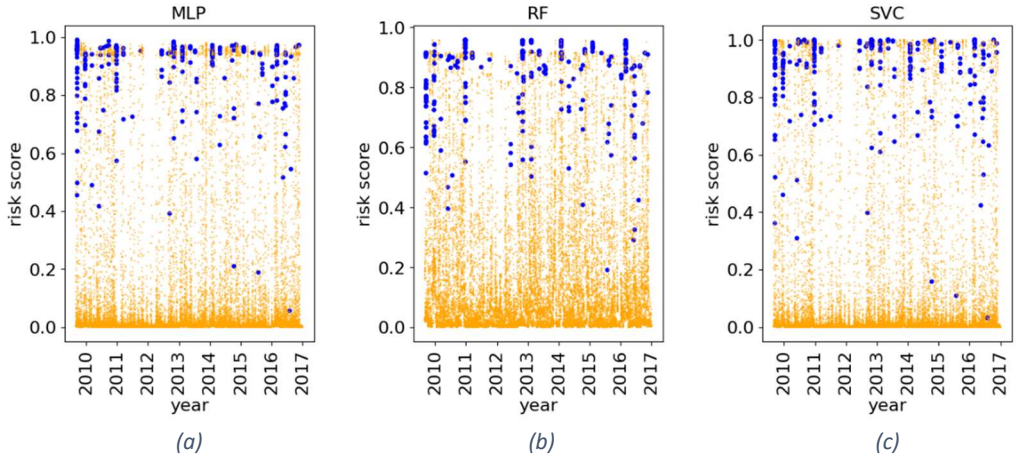

(a) *(b)* *(c)*

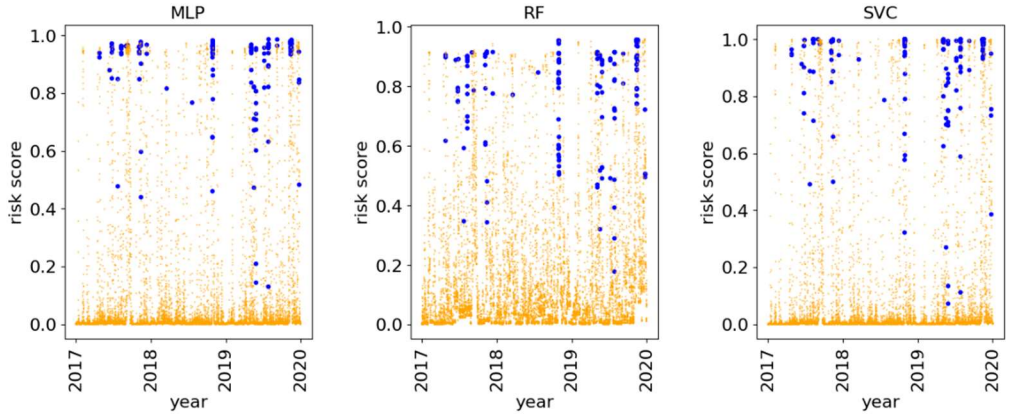

(d) *(e)* *(f)*

Figure 9: Predicted risk score on the train dataset for Multi-Layer Perceptron (MLP, a), Random Forest (RF, b), Support Vector Classifier (SVC, c) algorithms and predicted impact probability on the test dataset for MLP (d), RF (e), SVC (f) algorithms. Blue point represents dates associated with impacts, and orange point represents dates not associated with impacts.

For some applications it may be useful to decide, based on the risk score of the year sample, if the sample is at high risk of impact or not. In order to do that, we need to set a threshold, such that all the samples that have a risk score higher than this value are considered at high risk damages, while samples with a risk score lower than this threshold are not. The value of this threshold can be chosen by the end-user. If a conservative measure is needed (i.e., if it is important to flag every sample that can be reasonably associated with an impact) a low value for the threshold will be chosen. The drawback of this choice will be a high number of false positives (i.e., samples flagged as high risk that did not present any impact). On the other hand, if some false negatives are acceptable (i.e., days not flagged as high risk that were eventually affected by an impact), the number of false positives can be reduced.

In the frame of this study a threshold was selected by maximizing the value of the weighted F1-score of the MLP algorithm, which is a standard metric used on binary classification. **Figure 10** shows the F1 score on the training test plotted against different values of the threshold. The F1 score is maximum and presents a plateau between 0.4 and 0.6, i.e. its value is almost constant for this range of threshold values. The value of 0.5 was set as a threshold, as it is located in the middle of the plateau.

The confusion matrix, calculated using the same threshold of 0.5 (**Figure 11**) illustrates the performance of the algorithm: the top left square (true label = 0, predicted label = 0) contains the number of True Negatives (i.e., the number of samples correctly labelled as low risk). The top right square (true label = 0, predicted label = 1) contains the number of False Positives (i.e., the number of samples incorrectly labelled as high risk). The bottom left square (true label = 1, predicted label = 0) contains the number of False Negatives (i.e., the number of samples incorrectly labelled as high risk). Finally, the bottom right square (true label = 1, predicted label = 1) contains the number of True Positive (i.e., the number of samples correctly labelled as high risk).

As a result, MLP and SVC algorithms identify as low risk only 8 samples where an impact occurred (from a total of 161 days with impacts), against the 14 samples detected by RF. Moreover, all algorithms incorrectly label approximately 1000 samples over 11000 as high risk.

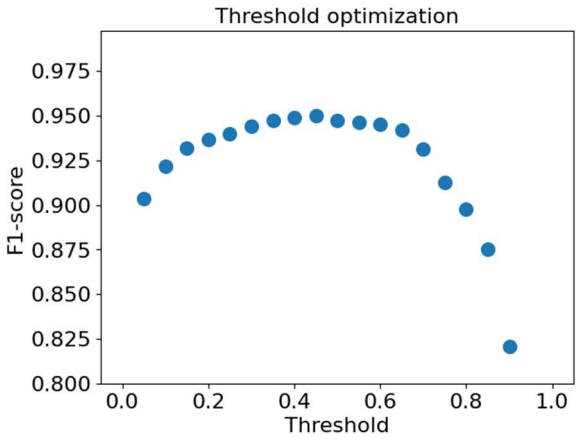

Figure 10: F1 score on the trained dataset for different values of the threshold.

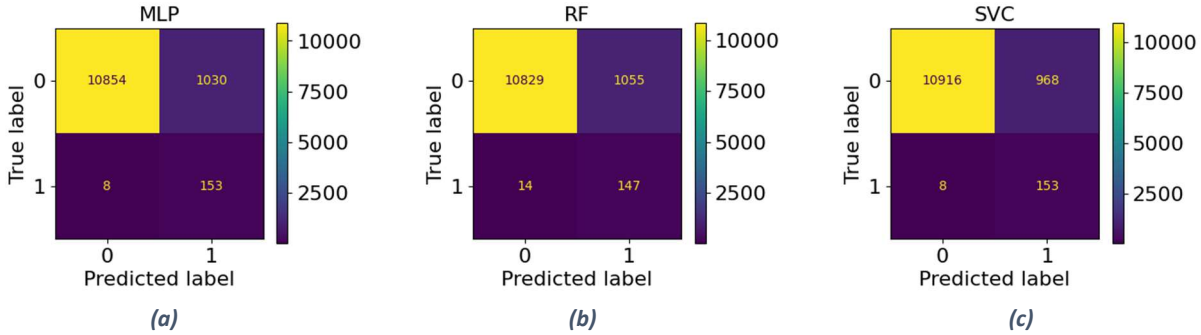

Figure 11: Confusion matrix for a threshold of 0.5 for Multi-Layer Perceptron (MLP, a), Random Forest (RF, b), Support Vector Classifier (SVC, c) algorithms.

The calculated weighted log losses and the corresponding weighted F1 score for a threshold of 0.5 for the three algorithms is summarized in **Table 7**, confirming a similar performance for Support Vector Classifier (SVC) and Multi-Layer Perceptron (MLP), and a slightly worse performance of the Random Forest (RF).

Table 7: Performances for Multi-Layer Perceptron (MLP), Random Forest (RF), Support Vector Classifier (SVC) algorithms

Algorithm	Weighted Log-Loss (train)	Weighted Log-Loss (test)	Weighted F1-score (test) (threshold 0.5)
MLP	**0.33**	**0.40**	**0.94**
RF	**0.42**	**0.59**	**0.88**
SVC	**0.36**	**0.45**	**0.95**

However, it is very important that the quality of the results is similar between the training and the test, because if the results of the former are much better, it would mean that the algorithm is overfitting the data, and is therefore unreliable.

2.2.3.3. Feature importance

The *feature importance*, introduced in **Section 2.2.2.3**, is aimed at identifying the variables that influence the occurrence of extreme events, and the cascading impacts that have generated damage along the coastal municipalities of the Veneto region. It consists in calculating the loss function when a feature is randomly shuffled: the more the value of the metric increases, the more important the shuffled feature is.
In accordance with the classification results discussed in **Section 2.2.3.2**, of the three ML algorithm trained, validated and tested (i.e., Multi-Layer Perceptron – MLP, Random Forest – RF, Support Vector Classifier – SVC) within the 2009-2019 timeframe, only the results for the MLP algorithm are shown in **Figure 12**.

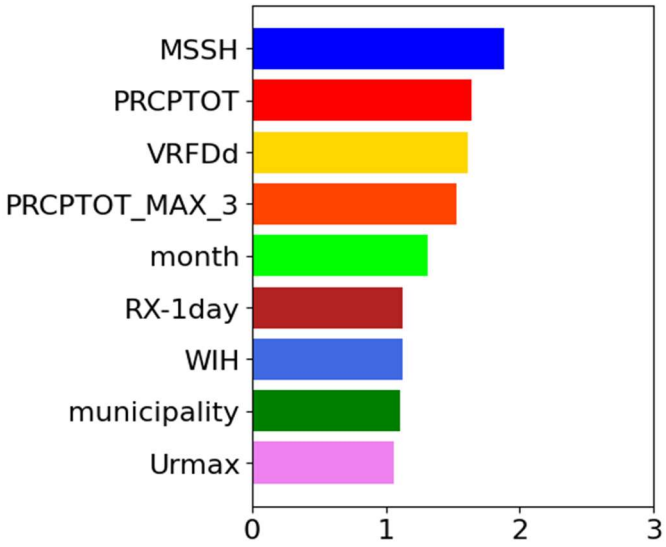

Figure 12: Results of feature importance obtained applying the MLP algorithm to all the municipalities of the Veneto region.

The most important factors triggering impacts in the investigated case study are indicators of sea level, total precipitation and wind intensity, in terms of *maximum sea surface height* (i.e., MSSH), *total precipitation* (i.e., PRCPTOT), and *wind intensity* (i.e., VRFDd). These results are in agreement with the conditional distributions, detailed in **Figure 7**. In particular, Bora and Sirocco wind jets expose the coastal area of the Veneto region to strong winds, heavy rainfall, strong sea storms and flooding, of low frequency but extremely intense (Stocchi & Davolio, 2017). Moreover, the presence of several indicators of precipitation leads to a high level of redundancy, thus reducing the importance of each feature. If a feature shows different conditional distributions according to the presence or absence of impacts, the same feature will have high importance in the corresponding machine learning algorithm.

Furthermore, in accordance with the characterization of the coastal municipalities presented in **Section 2.2.1.3**, **Figure 13** depicts the feature importance for each cluster of municipalities. This helps to understand how exposure and vulnerability play a key role in determining the drivers of impacts.

Group 1, composed of the coastal municipalities of San Michele al Tagliamento, Caorle and Eraclea, presents an overall homogeneity of the most important features. The only exception is given by the total precipitation, which dominates the importance ranking, as shown in **Figure 13-*a***. This behaviour is corroborated by (Stocchi & Davolio, 2017) where several extreme events occurred in the area have been analyzed. The study highlights how summer and autumn seasons are characterized by marked convective activities, with precipitation systems also affecting the lowland area that faces the Adriatic coast.

Group 2 (i.e., Jesolo, Cavallino-Treporti and Chioggia) and *Venice* (Group 3) are mainly governed by extreme sea-level related events (**Figure 13-*b*** and **Figure 13-*c***). These phenomena are exacerbated by the combined effect of sea-level rise and subsidence (Lionello et al., 2020), that makes these areas more impacted (as

detailed in **Section 2.2.1.3**). Besides that, although Group 2 is influenced by the intense precipitation coming from North (as seen for *Group 1*), Venice is famously affected by winds (i.e., Bora and Scirocco) which represents the major cause of *Acqua Alta* (i.e., high tide).

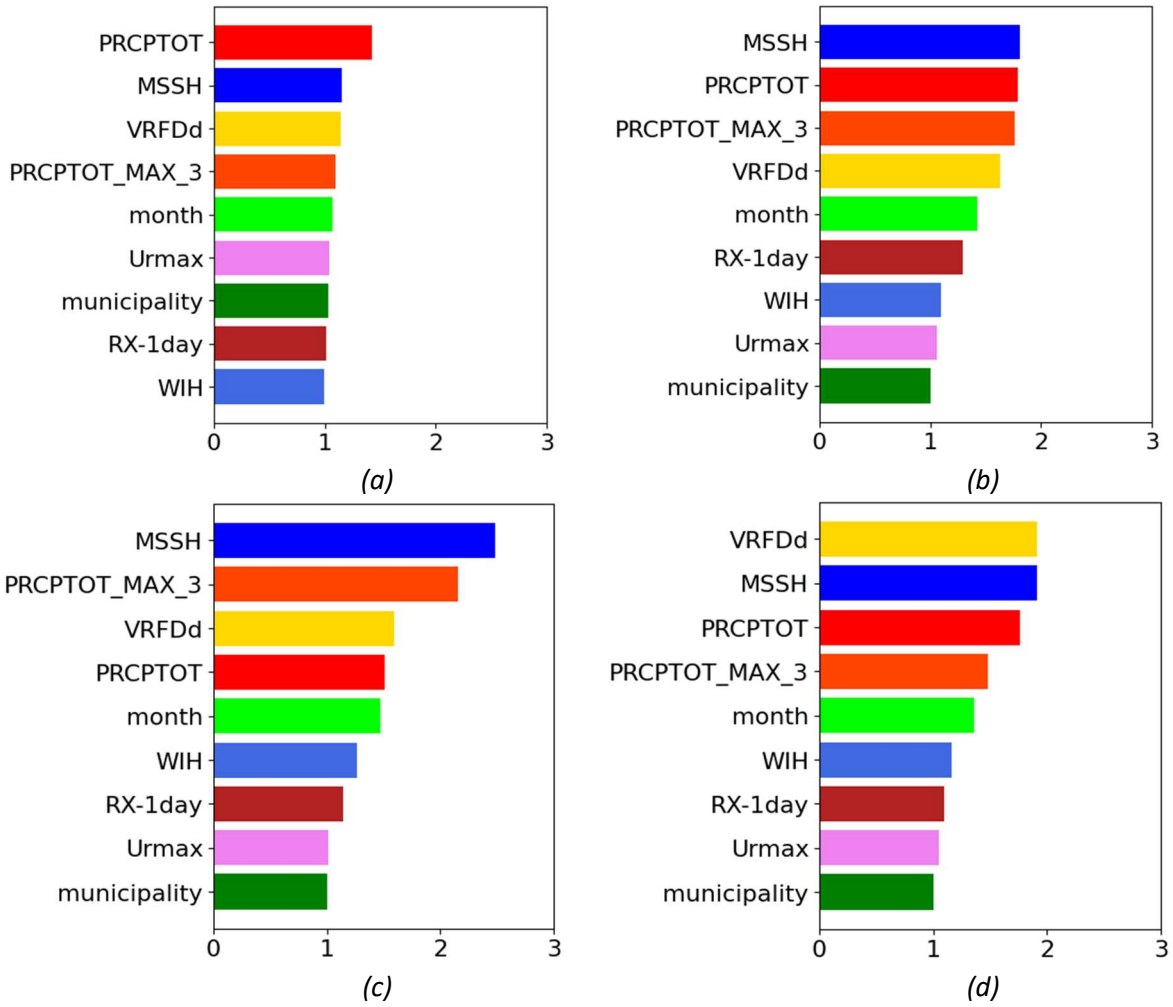

Figure 13: Feature importance obtained for each group of municipalities. In particular, (a) is related to Group 1, which includes San Michele al Tagliamento, Caorle and Eraclea; (b) Group 2 covers the lagoonal municipalities of Jesolo, Cavallino-Treporti and Chioggia; (c) Group 3 is entirely devoted to Venice; and Group 4 represented in (d) contain the Rovigo municipalities of Rosolina, Porto Vito, Porto Tolle and Ariano nel Polesine.

On the other hand, impacts recorded in *Group 4* (i.e., Rosolina, Porto Viro, Porto Tolle and Ariano nel Polesine) are equally triggered by winds and sea-level related events. These make the River Po Delta area a famous hotspot for saltwater intrusion, especially during dry seasons, exposing the vast cultivated fields (Paolo Tarolli et al., 2023).

2.2.4. Discussion

The study was developed to create an algorithm able to estimate, given a set of environmental indicators, a risk score for each coastal municipality of the Veneto region, and to understand the extreme events that caused the occurrence of impacts, through the analysis of feature importance in the reference timeframe (2009-2019).

The resulting outputs, reported in **Section 2.2.3**, show that despite the low data quality of the input data, the performances of the tested algorithms are quite good. Moreover, the similar performances between the training and the test set results prove that the risk of overfitting is avoided.

The designed algorithm follows the main criteria for robustness, replicability, transparency and explicability, as it was tested on new data, it uses mainly open-source python libraries, and identifies the most important features for impact evaluation. For these reasons, the algorithm could be implemented as an early warning tool for weather forecast applications. However, it is recommended to retrain the algorithm whenever new data becomes available.

Compared with other available decision support systems for climate change adaptation in coastal areas (e.g., DSS-DESYCO and THESUS; Torresan et al., 2016; Zanuttigh et al., 2014), the novelty of the Machine Learning (ML) model developed within AdriaClim is that, to the authors' knowledge, for the first time Artificial Intelligence (AI) methodologies are used to estimate the risks as a result of extreme weather events, especially along the coastal municipalities of the Veneto region. Therefore, the developed model represents an early prototype decision support tool underpinning climate change risk assessment and the definition of adaptation strategies at the regional scale.

Even if the first results obtained applying the ML model for the coastal area of the Veneto region are promising, some improvements could be achieved with the use of impact data with higher spatial and temporal granularity. As detailed in **Section 2.2.1.2**, in fact, the impact data used in this analysis (i.e. the data recorded by the *'Stato di crisi'* emergency reports of the Veneto Region), show some limitations and gaps. In fact, the list of impacts reported for the set of analysed municipalities often doesn't report specific details on magnitude and economic damage, exact location and date, among others. Moreover, the reports do not include the climate-related impacts that have not triggered the *'Stato di crisi'*.

The magnitude and number of impacts recorded in each coastal municipality is not measured, thus hindering the ability to normalize impacts by municipality size or population. Therefore, any analysis

of exposure and vulnerability, based on the characteristics of the investigated municipalities, will reveal that larger and more populated municipalities are more likely to be affected by impacts.
For these reasons, it is necessary for local authorities and the scientific community to collaborate in order to create a standardized impact dataset. In fact, the existence of such a dataset would greatly improve the results and their quality, especially in multi-risk studies, thereby simplifying the sharing of such achievements useful for local communities.

2.3. A two-tier approach to estimate future climate risk in the coastal area of the Veneto region

2.3.1. Data characterization to estimate future climate risks

The implementation of a Machine Learning (ML) approach for the evaluation of impacts along the coastal municipality of the Veneto region requires the collection and processing of a huge amount of data. Specifically, in order to feed the ML algorithms, the data was divided into input indicators (i.e., atmospheric and marine hazards) and output features (i.e., impacts caused by extreme events), as shown in **Table 8**.

Table 8: Descriptions of input data for the application of the Machine Learning Algorithms.

	Parameters	Reference (2009-2019)	Baseline scenario (2009-2019) Future RCP8.5 scenario (2020-2050)
Hazard	**Atmospheric domain** ● Precipitation ● Wind velocity	**CERRA**[10] ● Spatial resolution: 5.5 km ● Temporal resolution: 3h	**Adriaclim-WRF**[11] ● Spatial resolution: 6 km ● Temporal resolution: 6h
	Sea domain ● Sea surface height	**CMEMS**[11] ● Spatial resolution: 1/24˚ (ca. 4-5 km) ● Temporal resolution: hourly	**Adriaclim-NEMO**[12] ● Spatial resolution: 2km ● Temporal resolution: 3h
Risk	**Impacts** ● Impacts	**DPGR**[13] ● Spatial resolution: municipality ● Temporal resolution: daily	*-- output of the ML algorithms --*

[10] https://climate.copernicus.eu/climate-reanalysis

[11] https://cds.climate.copernicus.eu/cdsapp#!/dataset/reanalysis-cerra-single-levels?tab=overview

[12] https://programming14-20.italy-croatia.eu/web/adriaclim?id=undefined

[13] http://bur.regione.veneto.it/BurvServices/Pubblica/sommarioDecretiPGR.aspx?expand=19

The ML algorithms were trained, validated, and tested with *reanalysis* input data (i.e., combination of past observations with models to generate consistent time series of multiple climate variables) for the 2009-2019 decade, hereafter referred to as *reference*. Consequently, the refined algorithms were applied to the subregional earth system modelling data (hereafter *modelled)* from climate *baseline* (2009-2019 timeframe) and *future RCP 8.5 scenarios* (2020-2050), developed in the frame of the Interreg Italy-Croatia AdriaClim Project. Detailed descriptions of the modelling chain are presented in the **Section 2.3.1.1**. Impacts are defined as damages observed on the territory after the occurrence of an extreme weather event (e.g., agricultural losses, damages to buildings/infrastructures, problems to the population) and service interruptions (e.g., blackouts, impaired viability), recorded with the activation of the *'Stato di crisi'* from the Veneto region emergency archive (DPGR, *Decreto del Presidente della Giunta Regionale*)[5], and validated through a local newspapers review.

2.3.1.1. The AdriaClim subregional earth system

Outputs from the subregional earth system developed within the Work Package 3 of the AdriaClim Project were used to create the input to the ML model for the projection of risks until year 2050 under the RCP8.5 climate change scenario. It includes atmospheric, hydrologic, oceanographic, waves and biogeochemical components which are represented in **Figure 14**.

By providing a more thorough and higher resolution representation of all relevant physical and biogeochemical processes and by resolving their two-way feedbacks, the modelling system advances the state-of-the-art of regional earth system modelling. The climate downscaling from regional (i.e., MEDCORDEX) to subregional (i.e., AdriaClim Earth system) scale was driven by one of the ensembles of coupled air-sea models over the Mediterranean region provided by the Med-CORDEX coordinated initiative (Ruti et al., 2016), namely the LMDZNEMOMED (L'Hévéder et al., 2013). A detailed description of this modelling chain is in the deliverables *D.3.2.1* and *D.3.2.2* of the AdriaClim Project.

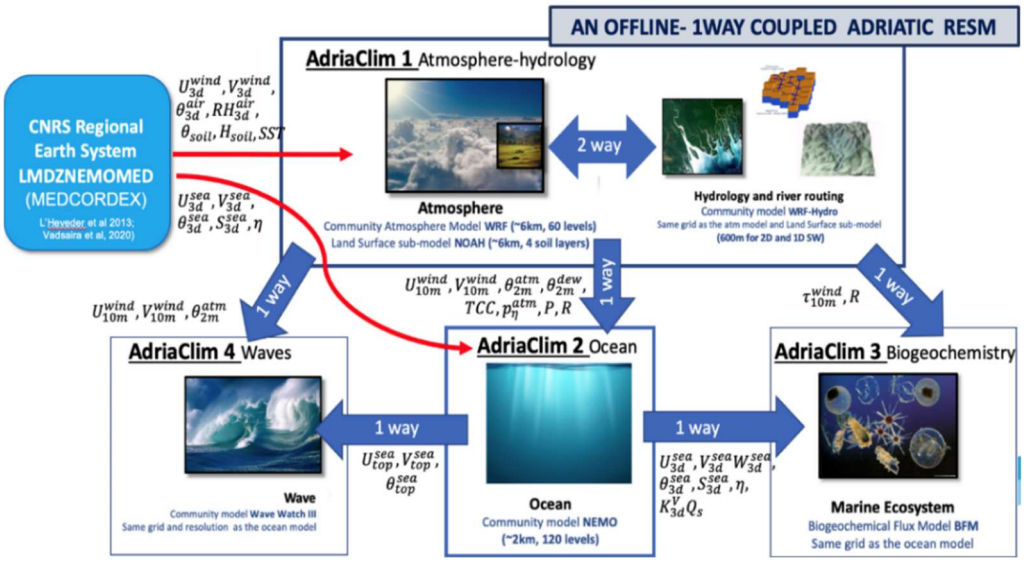

Figure 14: Modelling components of the AdriaClim subregional earth system and 1-way coupling architecture (source: Deliverable D.3.2.1, AdriaClim Project).

As components of the AdriaClim subregional earth system (**Figure 14**) the AdriaClim Atmosphere (WRF) comprises a large set of atmospheric variables, including temperature, wind, precipitation, humidity. On the other hand, the Ocean (NEMO) model describes the dynamics in the Adriatic Sea, such as sea surface height (SSH), salinity, temperature, and current velocity. The WRF climate simulations have the historical run over the time window 1990-2020, and the projection spans the 2020-2050 range, with the first year of both simulations (1990 and 2020) as spin-up period. The quantile mapping method, which uses non-parametric transformations through empirical quantiles, was applied for the bias-correction to the selected parameters (i.e., 2-meter temperature, 10-meter zonal wind speed, 10-meter meridional wind speed, 6-hourly cumulative precipitation and daily cumulative precipitation). For this purpose, two reanalyses were used: UERRA (Ridal et al., 2017) and ERA5 (Hersbach et al., 2020), with a horizontal resolution of about 5.5 and 30 km respectively (see *Deliverable D3.2.1* for more details). Within the scope of the ML application in this study, the 10-meter zonal wind speed and the 6-hourly cumulative precipitation were used to calculate the daily maximum wind speed (VRFDd), daily cumulative precipitation (PRCPTOT), and maximum daily cumulative precipitation in a month (RX-1day) within the spatial scale of the 11 coastal municipality of the Veneto Region.

The distributions of the maximum daily wind velocity (VRFDd) for each decade from 2009 to 2050 for the Veneto coastal municipality under the RCP8.5 scenario are shown in **Figure 15**. In particular, the red dash line of the represents the median, the lower and upper hinges of the boxes are the 25th

and 75th percentiles (interquartile range), the lower and upper whiskers depict the interval within 1.5-fold of the interquartile range, and finally circles account for the outliers.

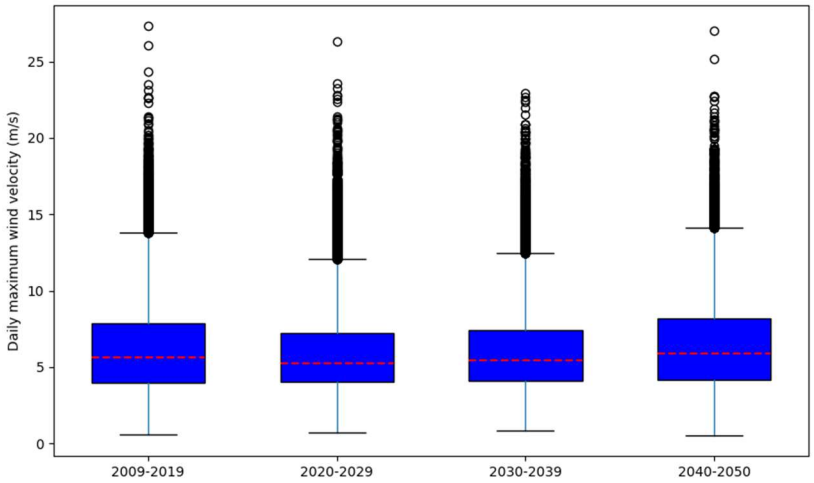

Figure 15: Comparisons between the baseline and future variations of daily maximum wind (VRFDd) under climate change scenario RCP8.5 produced from AdriaClim-WRF model.

There is a slight reduction in wind speed in the decades 2020-2039 compared to the reference timeframe (2009-2019), whereas a slight increasing trend is found toward the last decade (i.e., 2040-2050). **Figure 16** and **Figure 17** represent the distributions of the daily cumulative precipitation (PRCPTOT) and the maximum daily cumulative precipitation in a month (RX-1day), respectively. It has been observed that in the future (2020-2050) there will be a decrease in the number of days without low precipitation, while an increase in the number of days with precipitation above 50 mm is observed, especially in the decade 2040-2050 (**Figure 16**). Similarly, an increase of magnitude of the extreme rain value (RX1-day) is observed in the same decade (2040-2050) with a higher value of 75th percentiles compared to the reference timeframe (2009-2019; **Figure 17**). However, a high range of uncertainty in the last 5 years of the climate simulation leads to a drop and inversion in the time series of precipitation from 2045-2050.

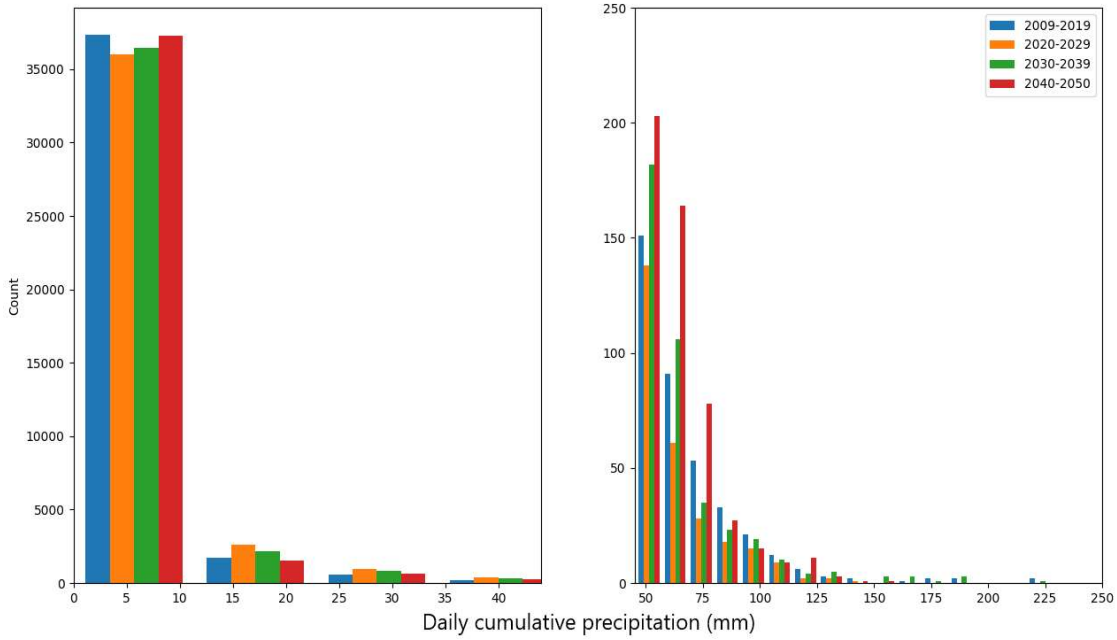

Figure 16: Comparisons between the baseline and future variations of daily cumulative precipitation (PRCPTOT) under climate change scenario RCP 8.5 produced from AdriaClim-WRF model. The left panel represents the low precipitation values (0-50 mm), while the right panel is a continuation of the left one with precipitation from 50 mm.

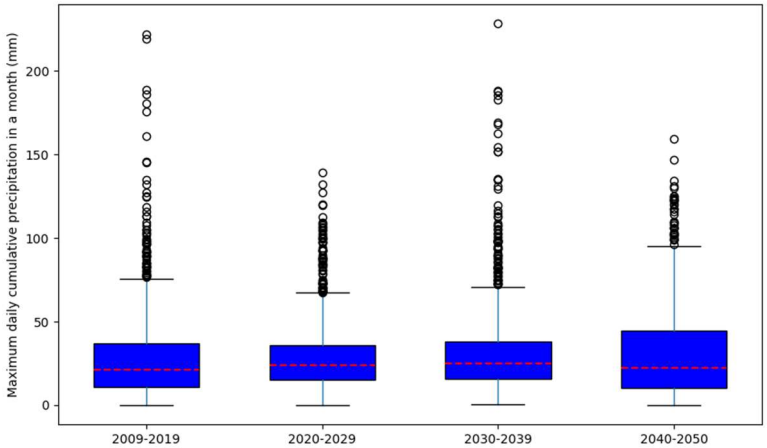

Figure 17: Comparisons between the baseline and future variations of maximum daily precipitation in a month (RX-1day) under climate change scenario RCP 8.5 produced from AdriaClim-WRF model.

Regarding the marine dataset, NEMO climate historical and projection simulations cover the time window 1992-2020 and 2022-2050, respectively. They were both chosen by considering the spin-up

periods of WRF and WRFHydro climate simulations, from which inputs of the NEMO were taken. Within the application of the ML model to estimate climate risks along the coastal municipalities of the Veneto region, the sea surface height parameter was retrieved from NEMO outputs. This parameter was temporarily corrected with the trend of mean sea level from satellite data from 1993 to 2020.

As further discussed in **Section 2.3.1.2**, in order to integrate a modelled data as input of the ML algorithm, it is necessary that the distributions of the modelled data and the data used to train and test the algorithm are similar over the reference period. The comparison of the value of SSH from the NEMO dataset and the CMEMS dataset over the reference period showed a good agreement in the central part of the distribution, but differences in the tails. In particular, it is observed that extreme SSH is underestimated in the NEMO model, which makes the absolute SSH values from the NEMO not suitable as input for the ML model. For this reason, datasets for the baseline and future scenarios were created using projected sea level rise trend from the NEMO model, and the variability of the CMEMS data (Tebaldi et al., 2021). Specifically, the CMEMS timeseries was split into the components related to trend and residual variations, which include seasonality, tides and weather-related variability. As a first step, the trend was removed from the timeseries. For each date in the future scenario timeframe, a date in the reference period was randomly sampled (with replacement), provided it was in the same calendar month and with the same moon phase, assigning the value of the residual sea level of this random datum to the projected date. Finally, the trend value for all dates was added. **Figure 18** shows the time series of daily maximum sea surface height (MSSH) over the coastal area of the Veneto Region, with an increasing trend of 3.85 mm/year over the 2009-2050 timeframe, in accordance with the results obtained within the *Work Package 3* of the AdriaClim project.

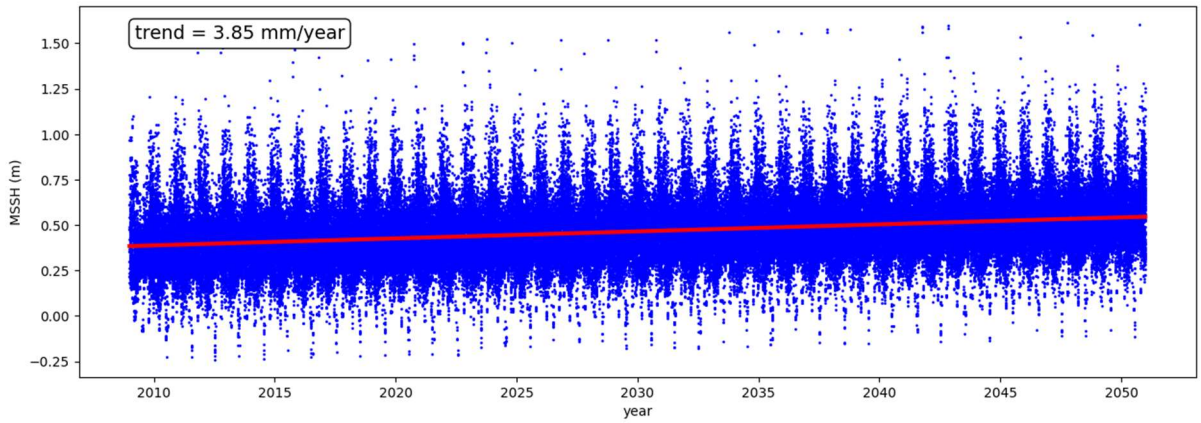

Figure 18: Time series of maximum daily sea surface height (MSSH) for the baseline and future using CMEMS dataset and the sea level rise trend generated from the AdriaClim-NEMO model under RCP8.5 climate change scenario.

2.3.1.2. Data analysis

In accordance with the ML algorithms applied in **Section 2.2** (i.e., daily impact estimation), it was possible to identify the list of features triggering extreme events, based on their temporal and spatial variability. Indicators related to *sea surface height, precipitation* and *wind* have been recognized as the cause of coastal impacts, in particular:

- MSSH: maximum daily sea surface height
- RX-1day: maximum daily cumulative precipitation in a month
- PRCPTOT: daily cumulative precipitation
- PRCPTOT_MAX_3: maximum daily cumulative precipitation in the previous 3 days
- VRFDd: maximum daily wind velocity
- Month: month related to the impact
- Municipality: location where the impact occurred

The objective of this analysis is to check the consistency of the *reference* and *baseline* in the reference timeframe (2009-2019). In particular, the data used to train, validate, and test the ML algorithms within the *reference*, must be as similar as possible to the modelled data of both *baseline* (2009-2019) and *future scenarios* (2020-2050). Therefore, the algorithm can be still applicable as long as the distributions (e.g., frequency and magnitude of extreme values) of the *reanalysis* and the *modelled* data are spatially and temporally comparable.

The ML algorithms used the same dataset (CMEMS) for both *reference* and *baseline* for the MSSH, hence, the distribution is the same in both. On the other hand, as detailed in **Section 2.3.1**, the atmospheric indicators (i.e., RX-1day, PRCPTOT, PRCPTOT_MAX_3, VRFDd) were retrieved from the CERRA dataset for the *reference* and from the AdriaClim-WRF model for both *baseline* and *future* scenarios. Ideally, the reference should be the same dataset used in the bias correction of the AdriaClim-WRF (i.e., UERRA). However, UERRA covers only the period up to 2015, which is insufficient compared to the reference timeframe of the assessment (i.e., 2009-2019). Therefore, CERRA, the next generation of the regional reanalysis for Europe, was used. **Figure 19** shows the distributions of both *reference* and *baseline* datasets for three selected atmospheric indicators within the reference timeframe 2009-2019 (i.e., VRFDd, PRCPTOT, RX-1day). Higher values of both wind and precipitation are observed in the baseline dataset compared to the reference. However,

the distributions of the two datasets are comparable, which allows further application of the machine learning algorithms to modelled data (**Section 2.3.2**).

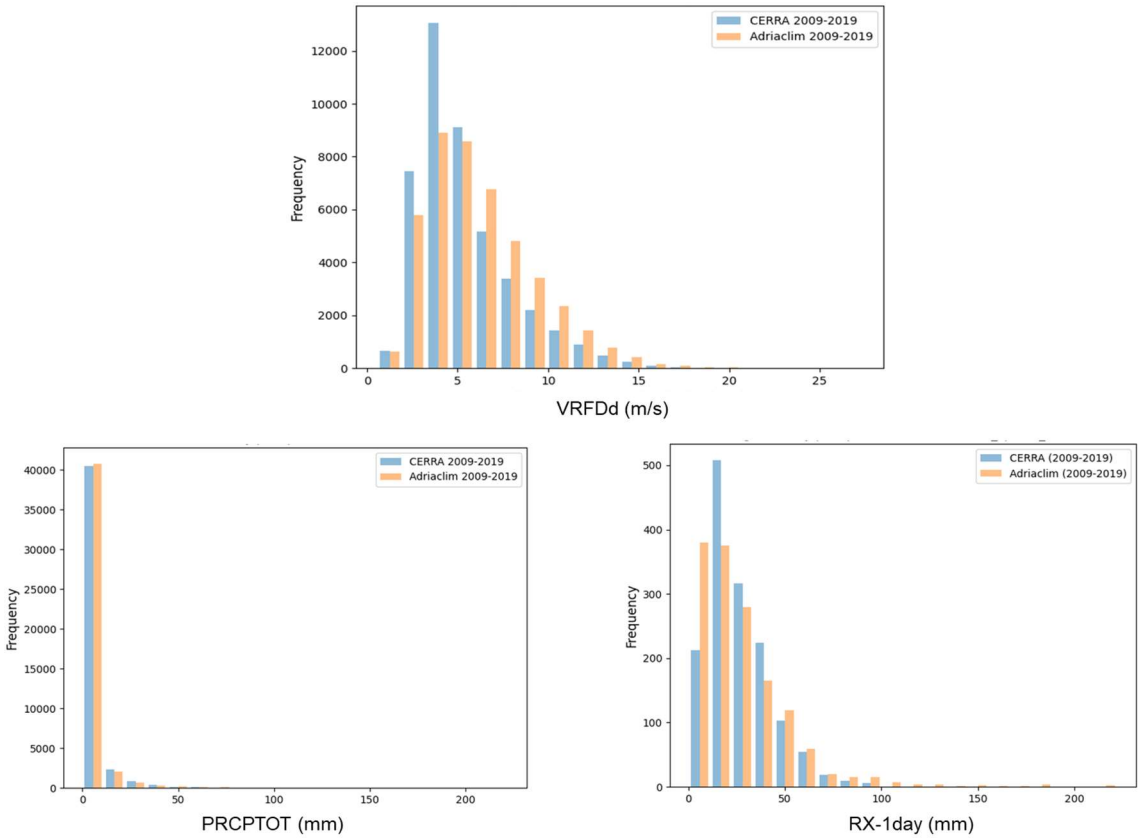

Figure 19: Distribution of wind velocity (VRFDd), total daily precipitation (PRCPTOT), and maximum daily precipitation in a month (RX-1day) from the CERRA and AdriaClim datasets within the reference period (2009-2019).

2.3.2. Method

Artificial Intelligence and Machine Learning (ML) algorithms offer a new path to address the analysis of multiple environmental hazards and to model future climate change impacts due to their ability to model complex feedbacks and non-linear interactions between different variables, without the need for an explicit modelling. In the frame of this study, a ML algorithm was used to estimate the number of days per year in which at least an impact occurs along the Veneto coastal area given the knowledge of daily local atmospheric and marine indicators.

The input data of the analysis is composed by a set of environmental features for each day in the timeframe 2009-2019 and for each municipality on the Veneto coastal area, and by a Boolean

variable representing the presence of an impact on the same day and location that will be used as output label (detailed in **Section 2.3.1**).

As the goal of this work is the estimate of the number of impact days, it seems natural to structure the dataset such that each sample corresponds to one year. In this case though, the dataset would have been composed by 10 samples (one per year), and with approximately 40000 features (i.e., 11 municipalities × 10 indicators × 365 days), which cannot be used to train any machine learning tool, as the number of input features is much bigger than the number samples.

To overcome this problem, several different approaches were considered, including time series, statistics, convolutional neural networks. Eventually, a novel two-tier approach was developed (**Figure 20**). In the first tier, a value of a risk score was obtained for each couple (day, municipality), while in the second tier these values were used to calculate the total number of days featured by the occurrence of impacts associated with extreme weather events per year. This method allowed the exploitation of the real-time relationship between indicators and impacts, using well-known ML algorithms. The novelty of the proposed approach does not rely on the implemented ML methods, but on the way these methods are combined.

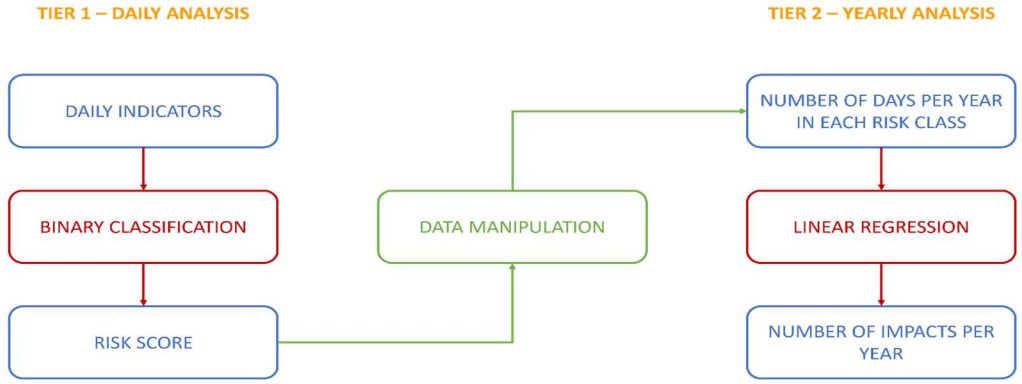

Figure 20: Scheme of the two-tier approach.

Tier 1 – Daily analysis

The goal of the first tier is to estimate, for each day and municipality, the risk score, which is a measure of the probability of an impact occurring at that location on that day.

Each sample of the input dataset is associated with a day and a municipality: the input features are the atmospheric and marine indicators (Table 1), and the output label is the presence/absence of impacts.

This is a binary classification problem on a skewed dataset (as the number of days with impact is about 1% of the total number of days).

A Multi-Layer Perceptron (MLP) algorithm, with sample weights to keep the minority class in the right account, has been trained, validated, and tested. The output of the application on a new input sample is the corresponding risk score, which is a measure of the probability of the occurrence of an impact on that (day, municipality).

It is worthwhile to note that the outcome of this algorithm is as reliable as its input data. When it comes to examining future climate projections, the results should be reliable on a daily basis, as the corresponding modelled data. However, their statistical distribution over several years, and hence the number of days with high values of risk score, is reliable.

Because of the skewness of the input data and the consequently use of weights in the codes, it is not possible to calculate the number of days with impacts per year as the sum of the risk scores. Similarly, it is not possible to set a threshold in the risk score, define any value with risk score above the threshold as day with impact and sum them up: in a binary classification on a skewed data if the recall is sufficiently high (i.e., most positive events are correctly identified), the precision is likely to be very low (i.e., there will be a high number of false positive). This makes the total amount of predicted positives an overestimate of the correct number of positives. These considerations led to the creation of a second algorithm that takes as input the daily risk scores and outputs the number of days with impact per year.

Tier 2 – Yearly analysis

The second tier is aimed at estimating the number of days per year in which at least one impact is expected along the Veneto coastal area using as input the knowledge of the daily risk scores previously calculated. As the goal is the estimate of the yearly frequency of impacts, it is natural to structure the dataset using yearly samples: the feature of each sample are the 365 values of the risk score for the 11 municipalities (i.e., approximately 4000 features), whereas the output label is the number of days with at list an impact on the Veneto coastal area. The total number of samples is 10 (i.e., the number of full years in the timeframe). As the number of features is much smaller than the number of samples, to create a ML algorithm it is necessary to reduce the number of features and increase the number of samples. The increase of the number of samples was obtained by the implementation of moving windows sampling: instead of considering 10 non-overlapping years, a year was defined as any interval of 12 consecutive months. Since samples adjacent in time are not independent from each other, making a random splitting a non-viable option, the data was split chronologically between train and test before the moving window process. To reduce the number of features, the risk scores of each sample were binned with a user-defined number of classes (i.e., risk classes), and the number of samples falling in each bin was calculated. The number of events

per year falling in each class are the features of the yearly samples. Finally, a linear regression algorithm with non-negative coefficients and zero-intercept was implemented estimating the number of annual impacts derived from the number of days in each risk class. The algorithm is then trained, validated and tested.

2.3.2.1. Estimation of annual risks for future hazard scenarios

The developed algorithms can be applied to modelled data, within the reference period and the future timeframe scenarios (i.e., until year 2050). Given that the distribution of indicators of *reanalysis* and *modelled* data in the reference period are similar enough, the ML algorithms have been applied to predict the yearly frequency of future impacts against RCP8.5 climate change scenarios. Therefore, this analysis will provide information on the relative importance of each potential hazard and of the iterative combination of them. In particular, in accordance with Teichert et al. (2016), where multiple stressors were iteratively included in the application until the real-world occurrence was achieved, **Figure 21** shows the combination of hazards selected to study the number of projected impacts per year for the coastal municipalities of the Veneto region.

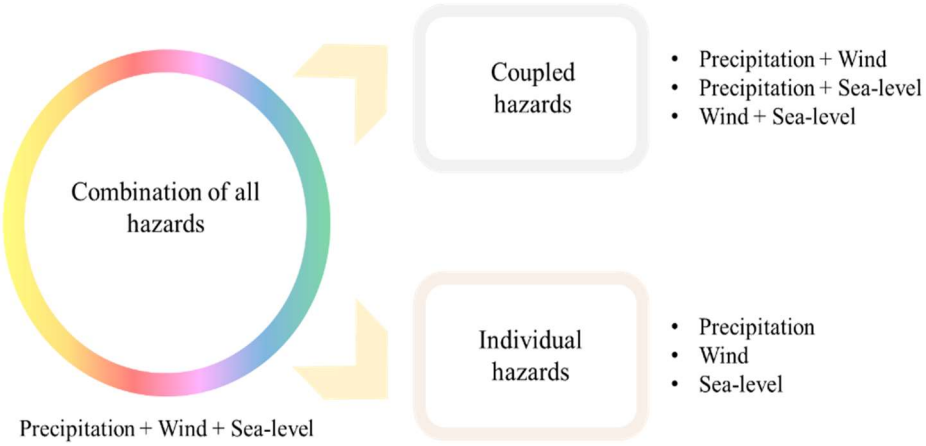

Figure 21: Iterative combination of the selected hazards to estimate future risks.

As detailed in **Section 2.2.3.3**, indicators of *precipitation*, *wind* and *sea-level* have been identified as responsible for the majority of coastal impacts. Accordingly, *Tier 2* of the developed ML algorithm was applied, investigating in the first place all hazards combined. However, in order to determine the most predominant indicator responsible for future risk trends, coupled hazards and, consequently, individual hazards have been examined. First, the average value of each indicator was set over the reference period (2009-2019) and then, for each type of selected hazard, the modelled

value of the same was fixed. Results of the iterative estimation of future annual risks are presented in **Section 2.3.3.3**.

2.3.3. Results and discussion

As described in **Section 2.3.2**, the following sections outline the resulting outputs of the proposed two-tier ML-based approach. The model validation and testing for the estimation of the annual occurrence of impacts is presented in **Section 2.3.3.1**. On the other hand, **Section 2.3.3.2** is devoted to the application of the two-tier approach with modelled data, in order to estimate the occurrence of impact risks in the future (**Section 2.3.3.3**).

2.3.3.1. Validation and testing of the two-tier approach to estimate the annual occurrence of impacts

The results of the two-tier approach to the training and test dataset for the estimate of the annual impact frequency from the knowledge of daily indicators is shown in **Figure 22**. There is a good agreement between both sets (i.e., between the number of predicted and recorded impacts). The least square error on the train set (i.e., the median of the squared distance between the number of predicted and recorded impacts) is 1.5, which means that the average error is approximately 10% of the number of predicted impacts. This result is quite satisfactory, given the uncertainty of the input data; the tested algorithm is now ready to be applied to new data.

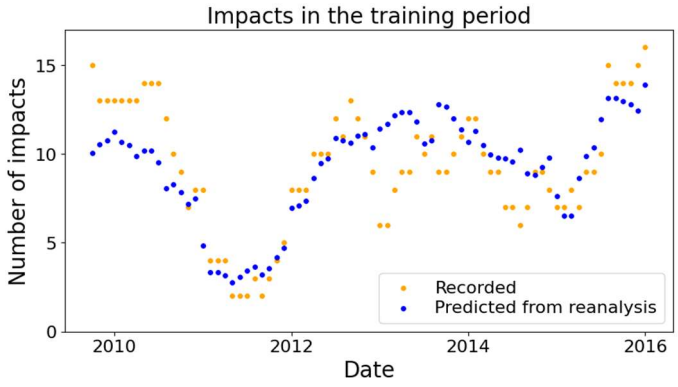

(a)

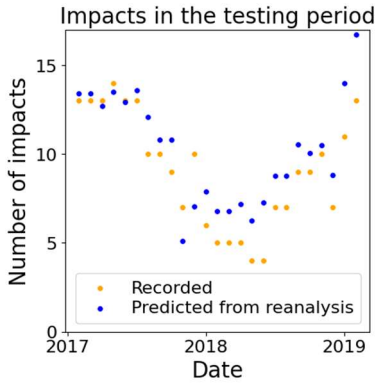

(b)

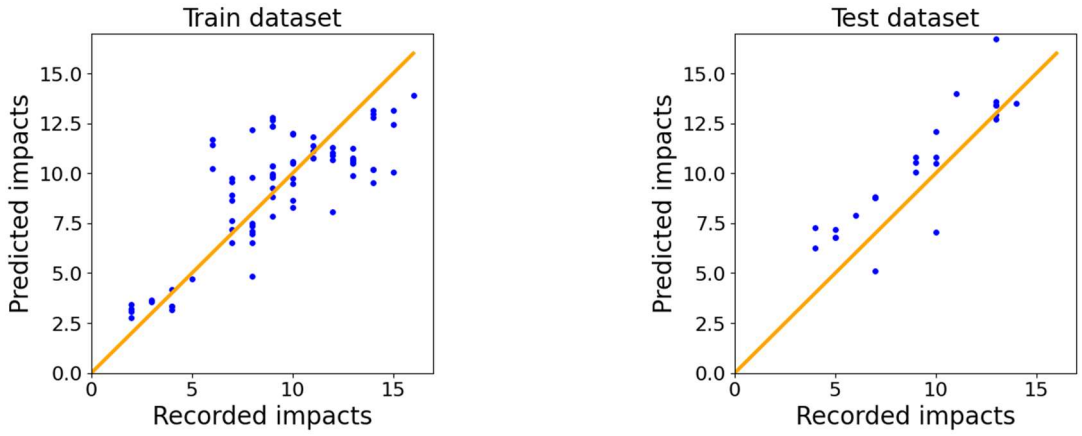

Figure 22: (a) comparison of predicted and recorded number of impacts for the train dataset; (b) comparison of predicted and recorded number of impacts over time for the test dataset; (c) predicted number of impacts versus recorded number of impacts for the train dataset; (d) predicted number of impacts versus recorded number of impacts for the test dataset.

2.3.3.2. Validation of the impact predictions

The Machine Learning (ML) model is then applied to the AdriaClim modelled dataset described in **Section 2.3.1.1**, after testing the distribution of the indicators. The AdriaClim model spanned over a 40-year period (i.e., 2010-2050). The period between 2009 and 2019 overlaps with the reference period, corresponding to the period in which impact data are available, thus identifying the studying period of the reanalysis data.

The first test run was hence the comparison of the collected number of impacts, the number of impacts calculated using the reanalysis data and the number of impacts calculated using the model. **Figure 23 s**hows how the AdriaClim model is not able to predict the yearly variability of the collected data, however the order of magnitude of the yearly impact is comparable. This result is in line with what can be expected from modelled data, as the actual timing of extreme events cannot be predicted, but the trend and the number of extreme events is approximately correct in the long run.

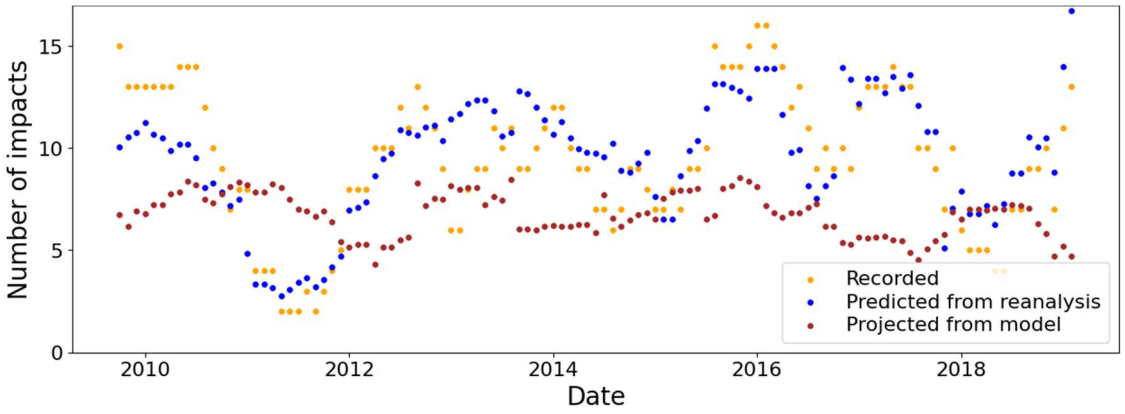

Figure 23: Comparison of recorded impacts, impacts predicted from the reanalysis data and impacts predicted from the AdriaClim model in the reference period.

2.3.3.3. Estimation of annual risks for future hazard scenarios

In order to estimate future annual risks (i.e., the potential yearly occurrence of impacts related to extreme weather events in the future climate change scenarios), the algorithm presented in **Section 2.3.2** was applied highlighting an increasing trend over the next 30 years. In particular, by fitting a linear regression model in the data, a 0.28 linear slope implies that every 3 or 4 years the number of risks along the coastal municipalities of the Veneto region increase by a unity in average (**Figure 24**). However, when a quadratic regression is applied (**Figure 25**), the increase of the number of impacts over time follows a parabolic trend (i.e., the slope of the fitted curve increases with time).

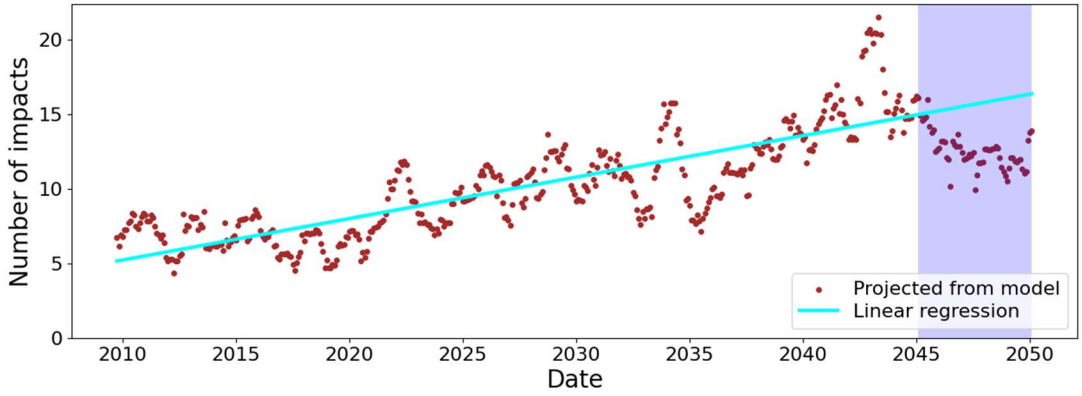

Figure 24: Resulting output of the estimation of annual risks.

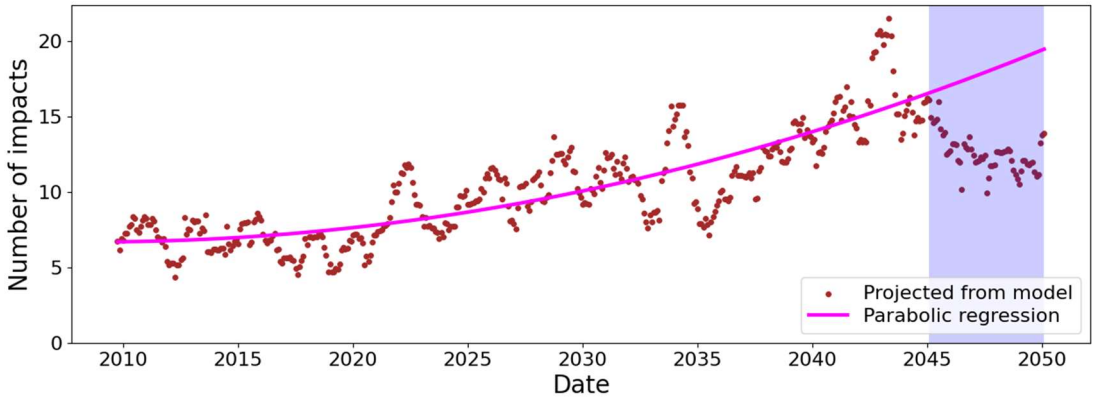

Figure 25: Resulting output of the estimation of annual risks.

Moreover, in order to better understand the contribution of the different hazards in the calculation of the annual occurrence, multiple sensitivity analyses were run, as described in **Section 2.3.2.1**, through a sensitivity analysis to better understand the contribution of different combinations of the selected hazards (i.e., precipitation, sea-level, wind intensity) under RCP8.5 scenarios. Because of the non-linearity of multi-risk analysis (there may be days in which each hazard is not enough to create an impact, but their combination is), and because there may be days when multiple hazards created an impact independently, the estimated risk caused by combined hazards is not the sum of the impacts of the single hazards.

Figure 26 highlights the different combinations of hazards. However, the final portion, concerning the last investigated period (after 2045), has been shaded in violet as it presents some criticalities, arising from the uncertainties of the model chain developed within the AdriaClim project (see **Section 2.3.1.1** for more details). For this reason, here the discussion will be focused on the future risk scenarios until year 2045.

When all the extreme hazards are considered (depicted in brown), there is an overall increase in future risks, with high and low peaks. It is of great interest to understand the reasons behind this double behaviour. Therefore, the individual hazards have been investigated.

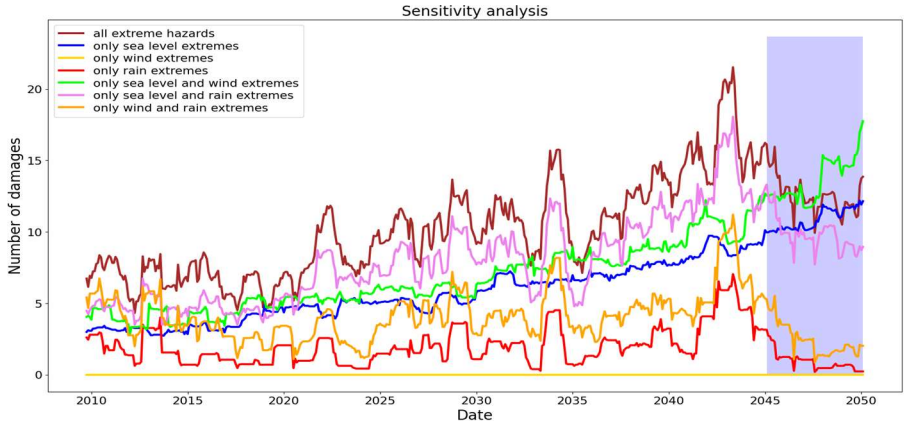

Figure 26: Sensitivity analysis: comparison of projected risks for different types of hazards.

The increasing trend of risks is mainly due to the trend of sea-level extremes (blue; **Figure 27**), and this can be explained by the fact that sea-level rise contributes to a slow but continuous increase of hazard-related phenomena, including coastal erosion and storm surge frequency (Mentaschi et al., 2018); Nicholls et al., 2007). On the other hand, wind extremes (yellow) seem not to produce impacts alone. However, the presence of the wind scenario coupled with the sea-level extremes (green) will trigger more impacts, as their combination is responsible for a higher increase of impacts (Marcos et al., 2019).

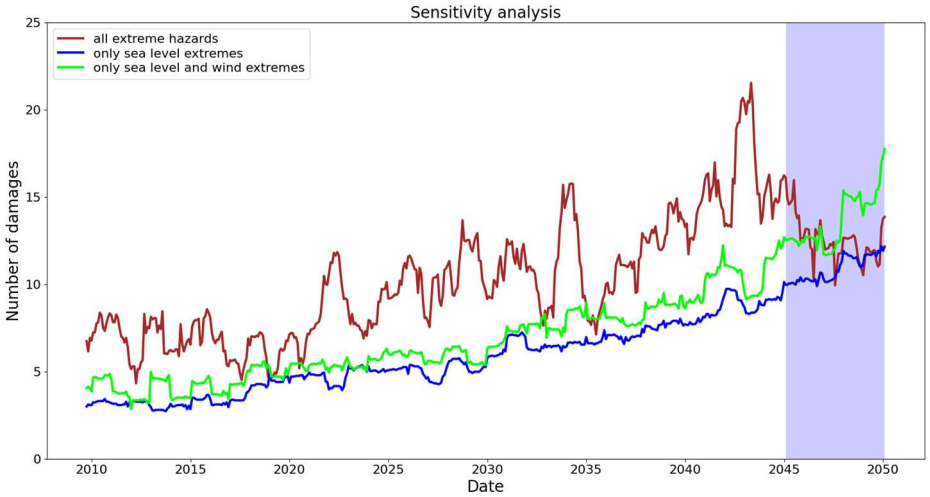

Figure 27: Future risk estimation (i.e., number of yearly impacts associated to extreme weather events) for sea-level and wind extremes.

At the same time, the high variability embodied by the peaks of minimum and maximum are associated with the impacts caused by extreme precipitation events (red; **Figure 28**). According to the previous analysis, the coupled combination of wind and precipitation scenarios (orange) will once again increase risks. This can be due to the thunderstorm's features, which often presents intense precipitation and winds (Jelic et al., 2021).

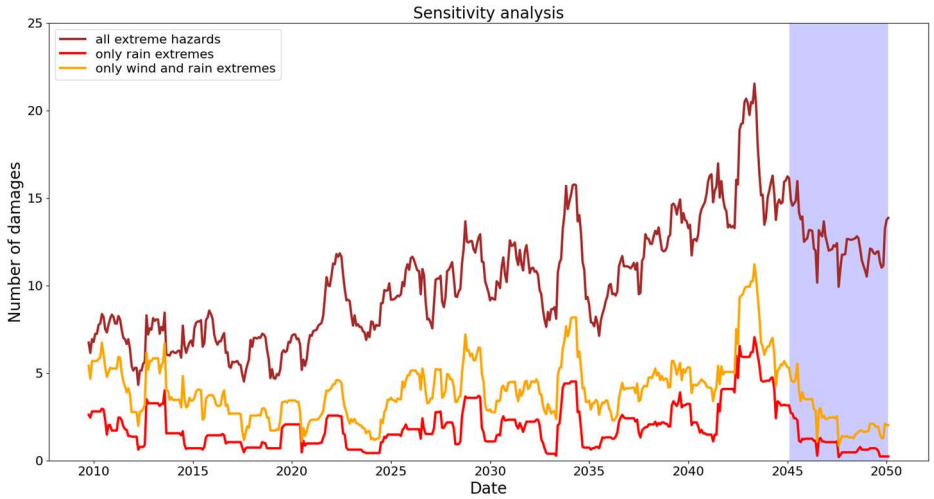

Figure 28: Future risk estimation (i.e., number of yearly impacts associated to extreme weather events) for precipitation and wind extremes.

2.4. Conclusions to Machine Learning approach

In this deliverable, a Machine Learning (ML) model was proposed to assess climate risks caused by extreme weather events in the Veneto case study. In order to fulfil this goal, a two-tier approach was developed. At first, the design of a ML algorithm allowed the evaluation of a risk score for each municipality given a set of observed environmental indicators, and allowed to understand the most important features accountable for the occurrence of daily coastal impacts in relation to the exposure and vulnerability characteristics of the investigated case study. Secondly, the estimation of annual climate risks was calculated by building an algorithm able to evaluate the number of days associated with the potential occurrence of annual impacts, which includes damages (e.g., agricultural losses, shoreline erosion, damage to buildings) and services interruption (e.g., blackouts, impaired viability), caused by extreme climate events. The model was then applied to both baseline (200-2019) and future climate change scenarios (2020-2050), by integrating the output data of the modelling chain developed within the Work Package 3 of the Interreg ITA-CRO

AdriaClim Project (*Deliverable D3.2.1*), thus supporting the comprehension of future climate change hazards' role in relation to the annual occurrence of impacts.

Several strategies were considered, and several algorithms have been implemented. First, all the algorithms were trained, validated and tested using both observations (i.e., ARPAV) and reanalysis data (i.e., CERRA). The correspondence between the observed and the predicted outcomes implies that the developed tools are reliable and ready to be used.

Once validated, the algorithms were used to better understand the phenomena that generate impacts. The feature importance analysis allowed the understanding, by using observed data, the contribution that each type of hazard plays in the creation of impacts. This analysis was also performed for groups of municipalities that share similar vulnerability and exposure factors, highlighting how these can amplify or mitigate the occurrence of impacts. Specifically, southern coastal areas (i.e., province of Rovigo), characterized by a larger natural area, experienced less damage, whereas more urbanized and more densely populated municipalities (e.g., Venice, Jesolo, Chioggia) were the most affected.

Consequently, the sensitivity analysis was performed by integrating the modelled data, thus providing insights on how different hazard factors will influence climate risk over the next 30 years. In particular, the upward trend in future climate risks will be predominantly driven by the continuous rise of sea-level and seasonal extreme precipitation, which will be further exacerbated by the presence of extreme wind events.

The developed algorithms followed the main criteria of robustness, replicability, transparency and explicability, as they were tested on new data, it uses mainly open-source python libraries, and identified the most important features for impact evaluation. Therefore, they could be a powerful instrument in the hands of local authorities and decision makers to predict impact occurrence and design adaptation plans. In particular, Tier 1 could be implemented to create early warning systems when applied to short-term weather forecasts, whereas the combined use of both algorithms is a useful tool for understanding the dynamics producing impacts and, consequently, defining adaptation and resilience strategies suitable for individual case studies. However, it is recommended to train and validate again the algorithms as the dataset is updated.

In fact, the most critical limitation of the study involved the quality of input data, especially impact data. These were retrieved from the *'Stato di crisi'* reports, which are often incomplete as they present a stronger qualitative component, rather than quantitative (i.e., the dataset lists the set of municipalities and dates affected by an extreme weather event, without reporting the actual date when each municipality was affected by a specific impact). The intensity of the observed impacts,

or even their precise number occurred in each day and in each municipality, is not recorded. This lack hinders the possibility of normalizing the impacts over local vulnerability and exposure factors (e.g., size of the municipality, population), hence bigger and more populated municipalities are more likely to be impacted. Moreover, impacts that did not trigger the *'Stato di crisi'* are missing, even if they created major damages or disruptions. Therefore, this information was manually cross-checked with local newspapers and integrated in the input dataset.

If more detailed information would (or will) be available (e.g., location, magnitude, economic damage), geographic, hydrographic and geological information could also be included in the analysis as indicators. Similarly socioeconomic dynamics (e.g., urbanization, population growth, migrations, tourism, economical activities) could be integrated to take into account the effect of their interaction with climatic drivers in exacerbating the risk and vulnerability towards disasters.

As a result, it is crucial that local authorities and the scientific community cooperate in the creation of a standardised impact dataset. Its existence could massively improve the quality of multi-risk studies, thus helping the scientific communities to disseminate their knowledge. In fact, if retrained with new data, the developed ML model can be easily applied to other case studies, characterized by other influencing indicators and assessment endpoints.

3. Spatial multi-criteria risk assessment approach for climate change adaptation and mitigation policies

Cities and territories are in a new strategic position to develop responses to multiple climate risks, as they can rely on new spatial information and advanced modelling operations to guide public decisions and the organisation of urbanised space. The loss of ecosystem quality affects several spatial dynamics, including the natural ability of the territory to mitigate the negative effects resulting from the tumultuous relationships between the configuration of human space and climatic phenomena, in particular: heat islands and urban and coastal flooding, caused by surface water runoff or sudden coastal storm surges.

It is well known how the impacts of climate change on cities and territories worldwide are evolving towards extreme weather phenomena, becoming more frequent and acute, and generating cumulative impacts and incremental phenomena that are particularly critical to the environment and human life. The sum of these events, combined with the fragility of an urbanised territory with an ever-increasing exposed value, amplifies the effects of climate change, making territories particularly vulnerable and scarcely resilient, with a consequent increase in human and environmental costs.

To counter this trend and to improve the quality of life in cities, many European and Italian experiences are experimenting with new ways of working in the direction of adaptation, exploiting the potential of scientific studies in the field of information and technology (Lerer et al., 2015; Morabito et al., 2015; Musco et al., 2016; Maragno, at al. 2020). Studies and research show that by assuming the reduction of vulnerability and risk as an intermediate objective to the achievement of territorial adaptation, it is possible to activate heterogeneous experiments useful for the collection of territorial issues and the construction of information layers supporting the recognition of different levels of climate resilience (Maragno, 2023).

From the point of view of the reduction of vulnerability related to the planning dimension, climate change places the city in a situation of information opportunity if one considers the analytical-exploratory experiments activated in the context of the emergency. The spatial assessment tool can therefore reduce 'the distance' that exists between the real representation of the impact and the ineluctable fatality of the concretisation of the climate change scenario. This process allows spatial planning to access new spatial information, positioning human settlements more consciously within the geographical logic of climate change.

By enriching the ordinary cognitive frameworks with new information levels (useful for reading and understanding the climatic phenomenon concerning the organisation of settlement structures), the

planning process is put in a position to orient adaptation choices in a more conscious and integrated way. In this phase, the challenge posed by climate change is inserted as a critical phenomenon, but also as an opportunity for a reinterpretation of the urban system itself.

The hypothesis formulated here, and which we attempt to test with an exploratory multi-attribute survey, is that climate change (CC) configures cross-sectoral and multi-level conditions at different spatial scales. The testing of a multi-vulnerability climate-oriented spatial assessment can guide planning and public decision-making in new policy domains.

The main objective is, therefore, to demonstrate how adaptation to climate change finds ample scope in the study and research of cognitive inertia linked to the new spatial observation services and the valorisation of a theoretical-operational (and cognitive) background capable of projecting deterministic assessment towards an approach based on an integrated hyper-assessment vision, facilitating the planning process.

Enhancing the Iuav experimentation in the 'city-climate' evaluation domain financed by the AdriaClim (Interreg Italy-Croatia) research project, a path is proposed that, starting from a multi-attribute exploratory procedure fed into a GIS environment, identifies plausible scenarios of territorial multi-vulnerability for the evaluation of 'morpho-climatic convergences' in spatial planning, management and regulation practices. The recognition of the cumulative impact condition is defined by the combination of appropriately semantically and metrically defined criteria, or environmental descriptors.

The test presents a two-stage assessment procedure:

- the first stage activates a multi-attribute exploratory procedure that helps to recognise the possible effects of climate change in a condition of multi-uncertainty underlying the semantic study of the three macro-descriptors declined to the morphological specificities of the places;
- the second stage instead involves associating the spatial information of the first with the exposure component (urban activities and functions from OpenStreetMap), generating a spatial and descriptive representation of the (Δ) qualitative-quantitative variations relative to the possibility of a given 'population' to be characterised by a multi-hazard.

The multi-vulnerability assessment returns possible conditions of territorial and social fragility related to the local climate response. The assessment considers the 'climate-territory' relationship in its spatial dimension and thus relates the effects of the climate phenomenon to the ecosystem performance of urban functions.

3.1. Multi-vulnerability assessment

To recognise the cumulative impacts based on the physical-morphological characteristics of the environment (spatial multi-vulnerability), a spatial multi-criteria methodology has been developed.

The definition of a multi-criteria methodology considers the characteristics of the morphological response to climatic impact and assists in orienting the evaluation of a set of urban planning measures.

The analysis and assessment methodology are justified by the following considerations:

a) the impacts that afflict the urban context are exacerbated by different morphological alterations;

b) the systematic use of digital technologies for the value recognition of the relationships between morphological components and settlement dynamics favours the spatialisation of the territory;

c) the use of an exposure component linked to the research and the use of open data sources facilitates a dynamic risk propensity assessment;

d) the implementation of a weighting algorithm based on a bilateral comparison among alternative hazards leads to the hierarchization of the decision, where the evaluation tends to take on a deliberative character.

The analytical-methodological procedure is based on the use of satellite-derived morphological data partly pre-packaged by the European project Copernicus, partly coming from the analysis of multispectral images of the Landsat 8 mission (USGS). Exploiting the data processed by Copernicus encourages the exploration and use of information layers that are already available, measured and validated by algorithms developed and improved within the project. The added value of these information models makes spatial analysis models open, continuously integrable and directly comparable. The increased potential for processing and elaborating data acquired from remote sensors favours the development of new and unprecedented survey techniques that can be easily updated with new information deposits from the processes of digitalisation of the territory. The use of new survey techniques in remote sensing solutions makes it possible to integrate the information deposits with new multi-source data and to provide scientific research with exhaustive and complete data, which are also indispensable to better direct the choice of information criterion concerning the survey question.

The work is developed following a qualitative-quantitative methodology aimed at illustrating investigation techniques capable of rendering a morphological behaviour of systemic impacts declined in a multiple-value context. The conceptual framework in **Figure 29** outlines the methodological functioning within which to move. It is articulated in three directions.

The methodological approach starts from a survey of vulnerabilities to climate change effects through a multi-criteria analysis in a GIS environment (heat in urban areas, urban flooding and coastal flooding), oriented to identify areas more or less predisposed to suffer possible impacts. In parallel, the analysis also focuses on the exposure of the study area through open-source data provided by the OpenStreetMap project. The intersection of the multi-vulnerability susceptibility and exposure data leads to the indication of areas potentially subject to a climate change-induced risk. The process can then be concluded by identifying the most affected and/or at-risk stakeholders to initiate a participatory urban planning approach for adaptation to CC.

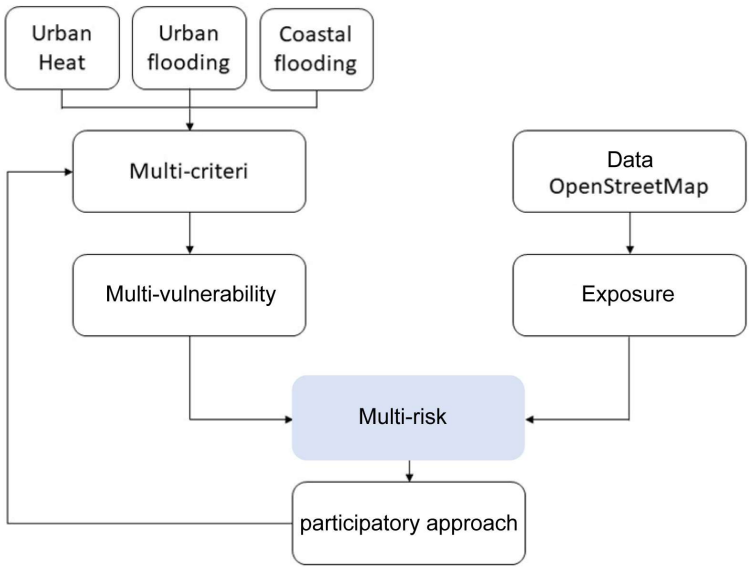

Figure 29 – Conceptual framework of work

3.1.1. Sources and data

The study uses different sources (Table 9). Some information refers to remote sensing elaborations and a wealth of spatial data already in the possession of the Municipal and Regional Administration (basic cartographic themes and general thematic cartography), others are part of the Copernicus

programme databases. All data used in the analysis process are freely available and constantly updated.

Table 9 - Information layers and base maps used for multi-vulnerability analysis and exposure assessment

Themes analysed	Description	Tipologia e risoluzione	Source
Vulnerability	Multispectral Satellite Image (30/07/2020): LC08_L1TP_191029_20200730_20200807_01_T1	Raster-Geotif-16 bits, 30 m	Landsat 8 (United States Geological Survey—USGS)
	Veneto Region Land Use Map updated 2018	Shapefile	Veneto Region
	DTM	Raster-Tif - 5 m	Veneto Region
	DTM	Raster-Tif - 0,25 m	Metropolitan City of Venice
	Imperviousness HRL (High-Resolution Layer)	Raster-Tif - 10 m	Copernicus Programme
	European Settlement Map (ESM 2015)	Raster-Tif - 2m	Copernicus Programme
Exposure	Point of interest	Shapefile	Openstreetmap

The existing correlation between structural and chemical-morphological parameters helps to define a planning dimension able to recognise spatial vulnerability as the outcome of cumulative impacts generated by CC (Wilby and Dessai, 2010; Wilby and Keenan, 2012). The recognition of a multi-vulnerability condition is defined by the combination of five criteria maps:

Vegetation Health Index (VHI):
indicator of vegetation health estimated based on the relationship between moisture values and thermal stress conditions (Maragno, 2021; Kogan, 1995). This indicator will be used to estimate sensitivity to impacts caused by heat waves and urban and coastal flooding. The maximum resolution of the VHI is 15m x 15m.

Imperviousness Density (IMD): freely downloadable data from the Copernicus program, returns the level of impervious soil with a spatial resolution of 10m x10m. The IMD helps to define areas that are highly sealed and therefore more sensitive to rising urban temperatures and less likely to absorb water from heavy cloudbursts and consequently increase the probability of urban flooding.

Runoff coefficient map (RCM): created through a schematization of land uses, starting from a re-classification of the Veneto Region land-use model (CCS 2018)[14]. Land uses to allow the estimation of the coefficients of absorption and surface runoff of rainwater, thus mapping the urban areas most prone and sensitive to the impacts generated by extreme weather events.

Digital Terrain Model (DTM): provided by administrative authorities (Veneto Region and Metropolitan City of Venice), it is a product resulting from LiDAR scanning on an aerial platform in 2014 and it has a resolution of 25 cm. The DTM returns the height of the ground surface without measuring natural elements (trees and shrubs) and anthropic elements (buildings and other structures). This data allows the identification of areas located at lower heights and therefore more sensitive to storm surges and mean sea level rise, if close to the coast.

European Settlement Map (ESM): provided by the Copernicus project as open data (the last 2015 version was released in 2019) in a raster format with a resolution of 2.5 metres. This information layer allows to detection the density of the built-up area as an element implicitly connected to the presence of a high concentration of population.

3.1.2. Definition of the weight vector using the AHP method

After normalising the criteria maps, the next step of the analysis is to assign a weight to each factor using an innovative spatial vulnerability assessment approach, based on the integration of the Analytic Hierarchy Process technique (AHP, Saaty, 1980) with the GIS environment for the development of a model able to consider and return the spatial interrelationships between the factors characterising the real decision-making context.

The AHP technique is used to organise the evaluation in a hierarchical form by expressing a preference judgement through the composition of pairwise comparisons between all the criteria contributing to the construction of the final decision. This process of weight assignment allows the decision-maker to arrive at a final choice that best satisfies the multitude of objectives by allowing the decision-maker to measure and synthesise the multitude of factors/criteria or sub-criteria (Eastman, 1999).

[14] Soil Cover Map, Veneto Region. 2018.

According to a comparison scale consisting of values ranging from 1 to 9, which summarises the level of importance of the criteria. The fundamental scale of absolute values is given below.

1/9	1/7	1/5	1/3	1	3	5	7	9
estremamente	fortemente	molto	moderatamente	ugualmente	moderatamente	molto	fortemente	estremamente
	meno importante					più importante		

Figure 30 – Saaty's reference scale for pairwise comparisons according to the AHP method

Table 10 shows the result of the normalisation of the preferences. The preferences indicate the relative desirability of the decision-maker of each of the five strategic levers used in the identification of the territorial areas differently predisposed to possible multi-vulnerability. Desirability is therefore expressed by employing a pairwise comparison.

Table 10 - Dominance coefficient matrix (consistency index of 0.04)

	Coeff_runoff	DTM	ESM	Imp	VHI
Coeff_runoff	1				
DTM	3	1			
ESM	1	1/5	1		
Imp	3	3	3	1	
VHI	1	1	1	1/5	1

Table 11 illustrates the vector of global priorities for the criteria considered in the hierarchical analysis. The values of the global priorities represent the starting point for the aggregation and final synthesis of the results of the hierarchical model. The most important criteria for determining the areas most likely to be subject to multi-impact were morpho-typological criteria, followed by the land-use factor, chemical-ecosystemic component and finally the population density component.

Table 11- Main driver of global priorities

	Derived weight
Coeff_runoff	0.1018
DTM	0.2412
ESM	0.0958
Imp	0.4404
VHI	0.1208

3.1.3. Multi-criteria evaluation outputs

The aggregation of the four sub-criteria was achieved by a weighted map algebra operation. The use of raster models together with appropriate techniques of weighted summation of variables (weighted linear combination) allows the construction of a raster map. Each pixel returns a value that represents the different predisposition of spatial elements to multi-vulnerability and therefore to possible impact and/or multi-impact **(Figure 31)**.

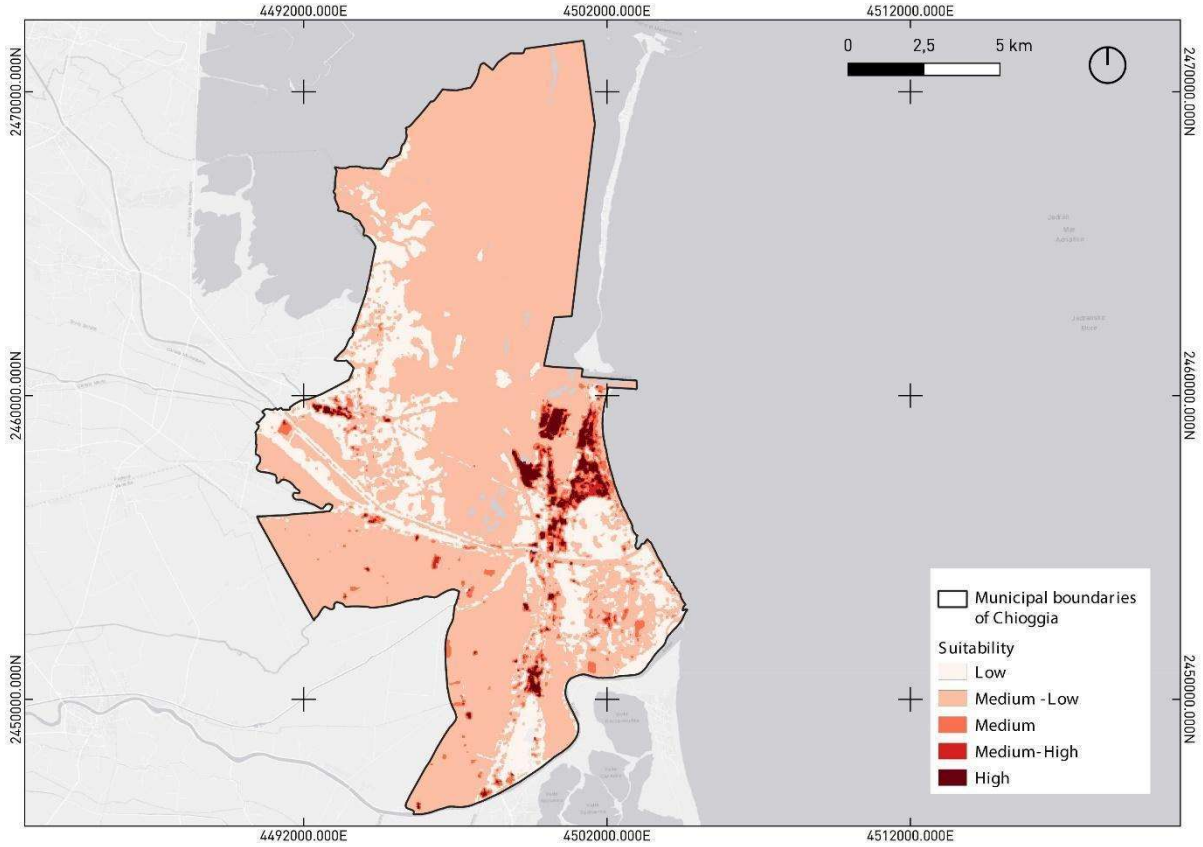

Figure 31. Predisposition to territorial multi-vulnerability in the Municipality of Chioggia (heat, hydraulic risk, flooding from intense.

3.2. Exposure assessment

3.2.1. Functional profile of the urban area

The variables that contribute to the definition of exposure exploits information directly linked to the geolocation of the functions of urban space, exploiting the use of Application Programming Interfaces (API) of OpenStreetMap (OSM). The geolocation returns a mapping of the activities and urban places of greatest environmental, cultural and socio-economic interest. In addition to the urban ecosystem phenomena of which it is an expression, the survey domain informs about the economic-social and cultural trends of the territories under analysis.

The OSM project can be considered as a participatory 'laboratory' built on the interaction of digital content produced by 2.0 users (user Generated Content, uGC) in the form of opinions on their

experiences of urban use and consumption, to create thematic cartographies designed to monitor the related updating processes of settlement processes. The OSM database is composed of geographical elements and places of interest linked to the daily life of users, appropriately surveyed and georeferenced by a collective mapping exercise.

The advantage of using this spatial information is that it contains the knowledge of the urban context with easily accessible and continuously updated points of interest, thus making it possible to spatially render different and heterogeneous socio-spatial patterns (or forms of city use). The OSM product is, therefore, able to enhance the skills and experience of users of urban space, acting as a link between the basic cartography and that of belonging, between the institutional product and the collective information of Web 2.0.

However, as the data mainly come from different volunteers or importing from other geographic data sources, there is currently no strict data quality control and this can lead to repeated or low accuracy data (Yang et al., 2018). A further issue advanced by Yang (2018) with respect to Openstreetmaps voluntary geographic information (VGI) data is the distribution of volunteers uploading data. Thus, there is a greater concentration of data in more densely populated areas.

Thus, the OSM database, being composed of geographical features, places of interest and social and economic structures, perfectly describes the population's use of the study area. Since population is the main indicator for assessing exposure to climate risks (Marin and Modica, 2017), the use of the Openstreetmap database is the most methodologically correct and innovative choice.

3.2.2. Description of OSM information and selection of tags

Using the OSM classification relative to the grouping and description of the various tags of the points of interest, twelve macro-categories were selected and inserted in as many layers in the Geographical Information System specifically implemented in the Qgis environment. The selection of the twelve macro-categories (following the OSM project) makes it possible to return a certain homogeneity and coherence of spatial information directly correlated to the morphological-functional profiles of the urban spaces under study.

Table 12 - Macrocategories and recognition sequence number

Macro-category	N°

Culture, entertainment and arts	1
Historical elements	2
Finance and communications	3
Gastronomy	4
Waste Management	5
Health infrastructure	6
Mobility	7
Shops	8
Administrative services	9
Leisure and sport	10
Tourism and accommodation	11

The final result a single shapefile file containing all the points of interest downloaded from OSM with the relative table of attributes that characterises their function.

Figura 32. Display of exposure database linked to OSM city functions

The reading of the data, both quantitative and qualitative, can be deepened through a spatial statistical investigation called hotspot analysis. The choice of this interpretation technique aims at studying densities (of activities and services) as the key to interpreting the urban phenomenon **(Figure 33)**.

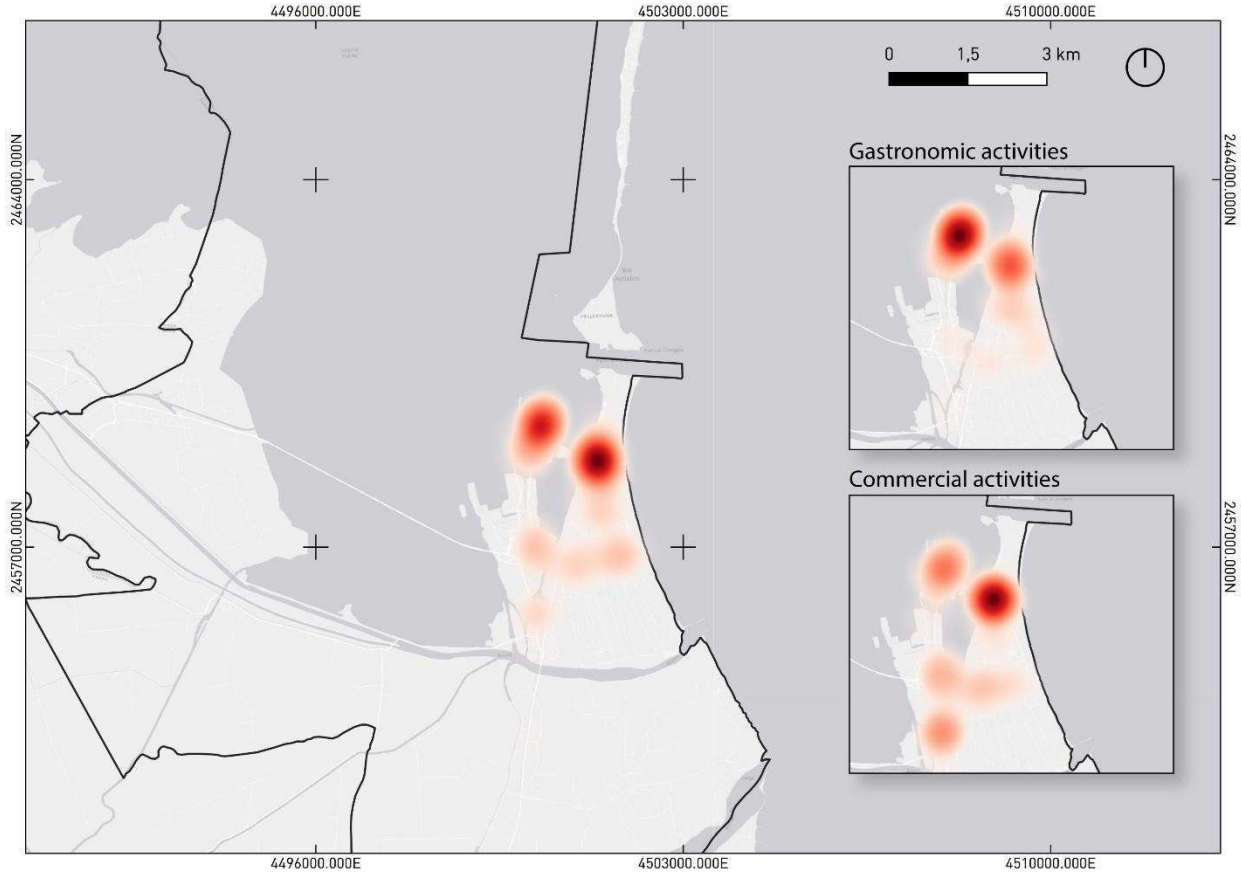

Figure 33. Output of exposure assessment using OpenStreetMap data. The area with the highest exposure/concentration of economic and social activities is identified.

3.3. Multi-vulnerability and exposure

By estimating the susceptibility to multi-vulnerability, it is possible to obtain an analysis matrix capable of assessing the elements (and functions) potentially exposed, effectively defining an urban risk orientation for each hazard considered.

The assessment of stakeholders affected by multi-vulnerability is therefore triggered through the relationship between the vulnerability variable and the exposure variable.

The evaluation consists of integrating the process of choosing spatial elements generated by non-additive procedures (exposure from OSM) with the weighted calculation of morphological-environmental components to support the multi-vulnerability estimation phase.

The spatial association between urban activities and vulnerability values also makes it possible to assess the activities that could be most affected by a significant convergence of impacts (from a risk analysis and assessment perspective), providing a critical behaviour of some physical-functional domains of the city in the face of potentially adverse climatic-environmental conditions.

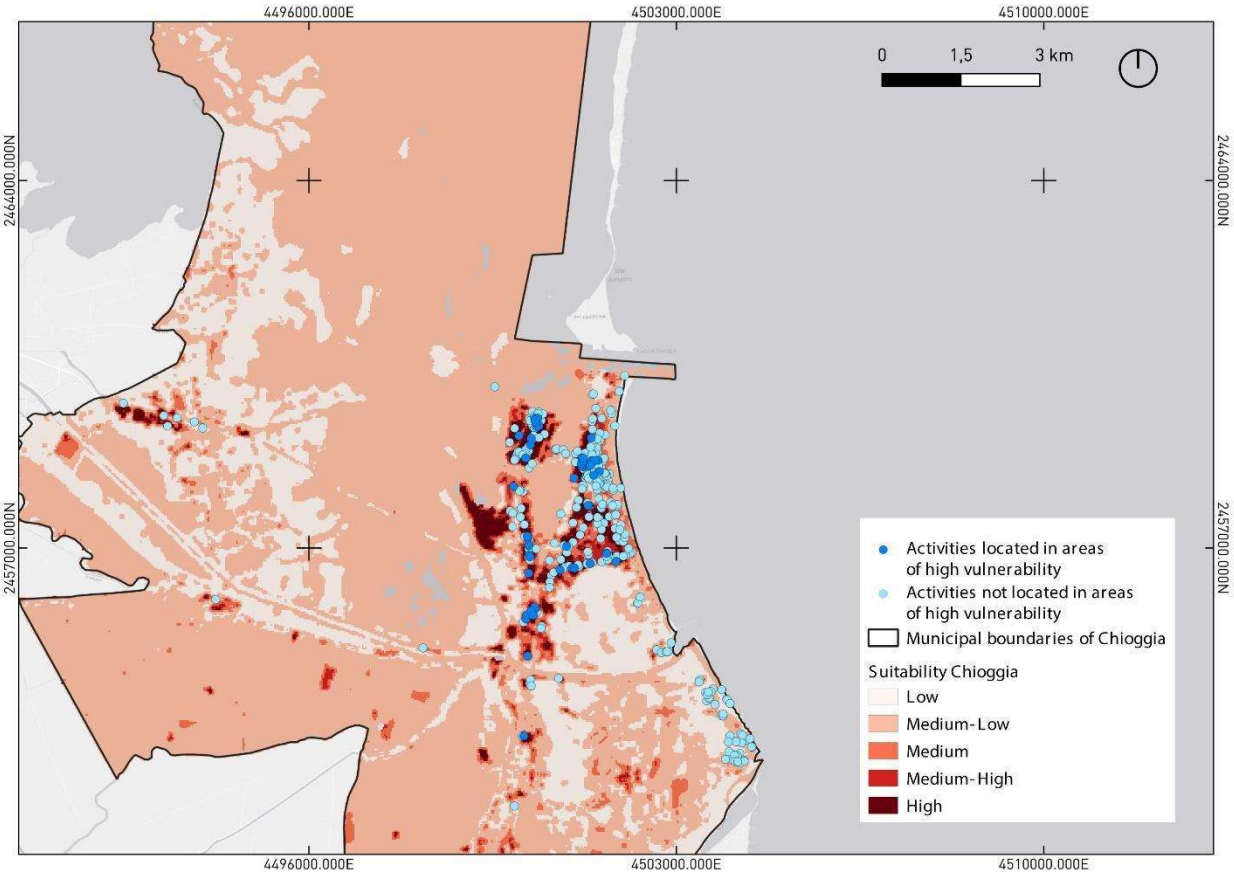

Figura 34. Identification of activities located in designated high vulnerability areas.

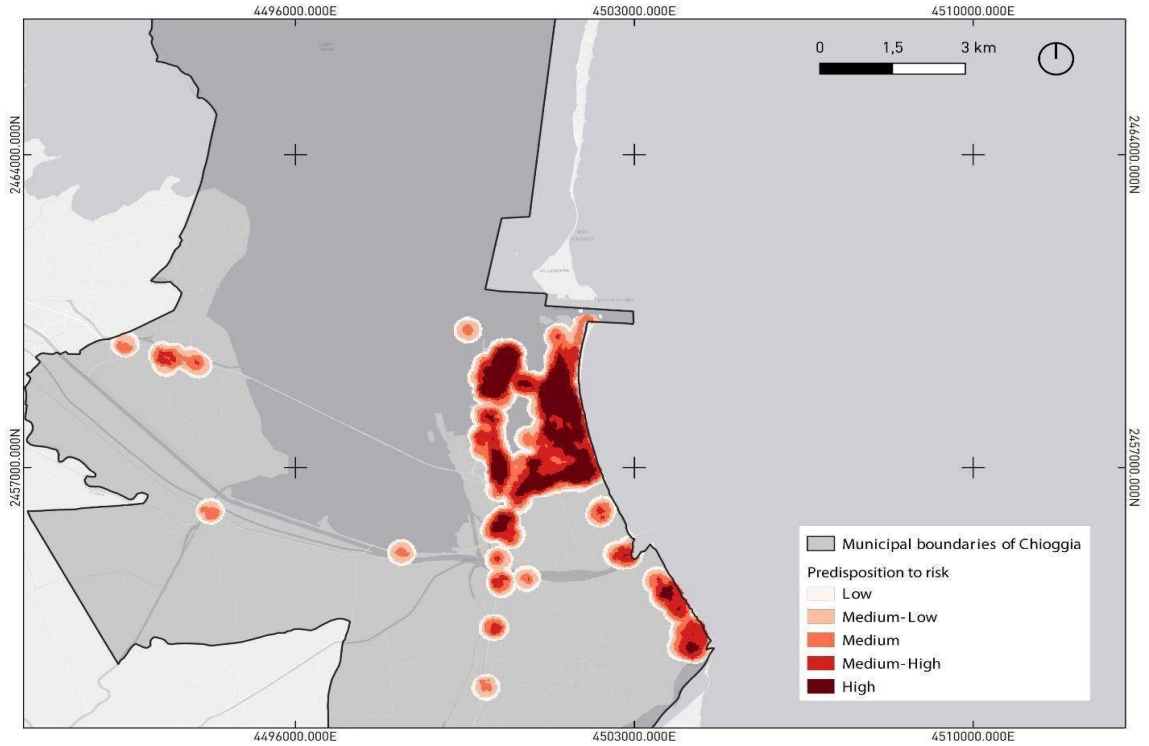

Figure 35. Assessment of risk-prone areas by weighted calculation of urban point functions for multi-vulnerability estimation

Table 13. Assessment results: distribution of multi-vulnerability by exposed assets and worst-case vulnerability condition

Macro cat - activities	Tot Activities - Chioggia	Activities in high vulnerability area	%
Culture, entertainment and arts	4	2	50,00
Historical elements	2	2	100,00
Finance and communications	20	14	70,00
Gastronomy	129	64	49,61
Waste Management	33	4	12,12

Health infrastructure	2	1	50,00
Mobility	79	19	24,05
Shops	107	56	52,34
Administrative services	2	1	50,00
Leisure and sport	14	1	7,14
Tourism and accommodation	34	23	67,65
Tot	426	187	

3.4. Outcomes of the multi-climate impact readiness analysis at municipal level

This section describes the results of the Iuav methodology.

Three different mappings are therefore reported for the three analysis municipalities. The first mapping refers to territorial multi-vulnerability and links the morphological aspects of the territory with potential climate impacts, the second refers to spatial exposure based on punctual data of urban activities and gives solidity to the process as it makes explicit the position and density of the economic values of the urban core, while the third mapping recombines the two previous ones by recalculating the total risk factor for the area in question. In addition, statistics are compiled for the presence of urban activities in areas subject to high and very high multi-risk. These activities have been grouped into twelve macro-categories[15] to improve the reading and understanding of the spatial context. Statistical analysis allows for more information profiles on the socio-economic fabrics most affected by climate impacts, helping local governments to adopt a diversified procedure for the design, implementation and management of interventions for urban regeneration and adaptation. On the other hand, the multi-risk tool allows for the activation of pluralistic approaches and up-to-date partnership forms that are already in place or under development.

[15] Gastronomy; Culture, entertainment and art; Historical objects; Leisure, recreation and sport; Waste management; Tourism and accommodation; Finance; Health; Communication; Transport; Administrative facilities; Shops and services; Schools.

3.4.1. Impact analysis for the Municipality of Jesolo

The territory of the Municipality of Jesolo, in **Figure 36**, is the result of a hybrid structure composed of canals and drains, urban centres and fishing valleys. Mechanical drainage and free-flowing areas drain entire agricultural compartments and natural sites located on the edge of the tourist backbone and districts for summer and temporary residences. The Piave, the Sile and the Adriatic enclose the municipality of Jesolo within its boundaries.

The Jesolo coastline is characterised by the density of economic activities and the type of uses that public space takes on in this strip behind the beach concessions. The urban functions and the speed of their rhythms respect the times dictated by the alternation of the seasons, resizing themselves from time to time according to the seasonal flow of tourists. The original urban layout, on the other hand, lies inland. Going up along the River Sile, the territory takes off its tourist garb to return to its ordinary layout. This is where the daily activities of residents take place and where the historic fabric returns to be the prevailing urban design and organisation.

The systematisation of variables for the observation and calculation of multi-risk generates a series of opportunities for the correct planning of interventions to defend against the impacts of climate change in contexts such as the Municipality of Jesolo. The mixed, heterogeneous territorial composition and the alternation of different uses and practices make this space an intense mixture of economic fabrics ranging from the seasonal tourist accommodation sector to the ordinary commercial network of retail outlets and micro-businesses. The spatial coding activities of the open-source data to which the multi-risk climate analyses are added take into account this precise dynamic that thickens and analyses the proximity between the activities of the urban economic space and the impacts that certain climatic drivers (UF, UHI, Ss) may generate as these factors add up.

The analysis conducted on Jesolo is developed from the interpretation and reinterpretation of land use and land cover classes. This information level makes it possible to link the decision-making phase to the location of the areas affected by the multi-hazard. Taking into account the composition of the land-use matrix, it is possible to extract the land-use classes that are most vulnerable to one or more climatic references drivers such as heat, flooding or storm surges. The following land use map **(Figure 36)** was revised according to the logic of the project to identify the study area but without neglecting the aspect related to the arrangement and alternation of agricultural, natural, coastal and urban plots.

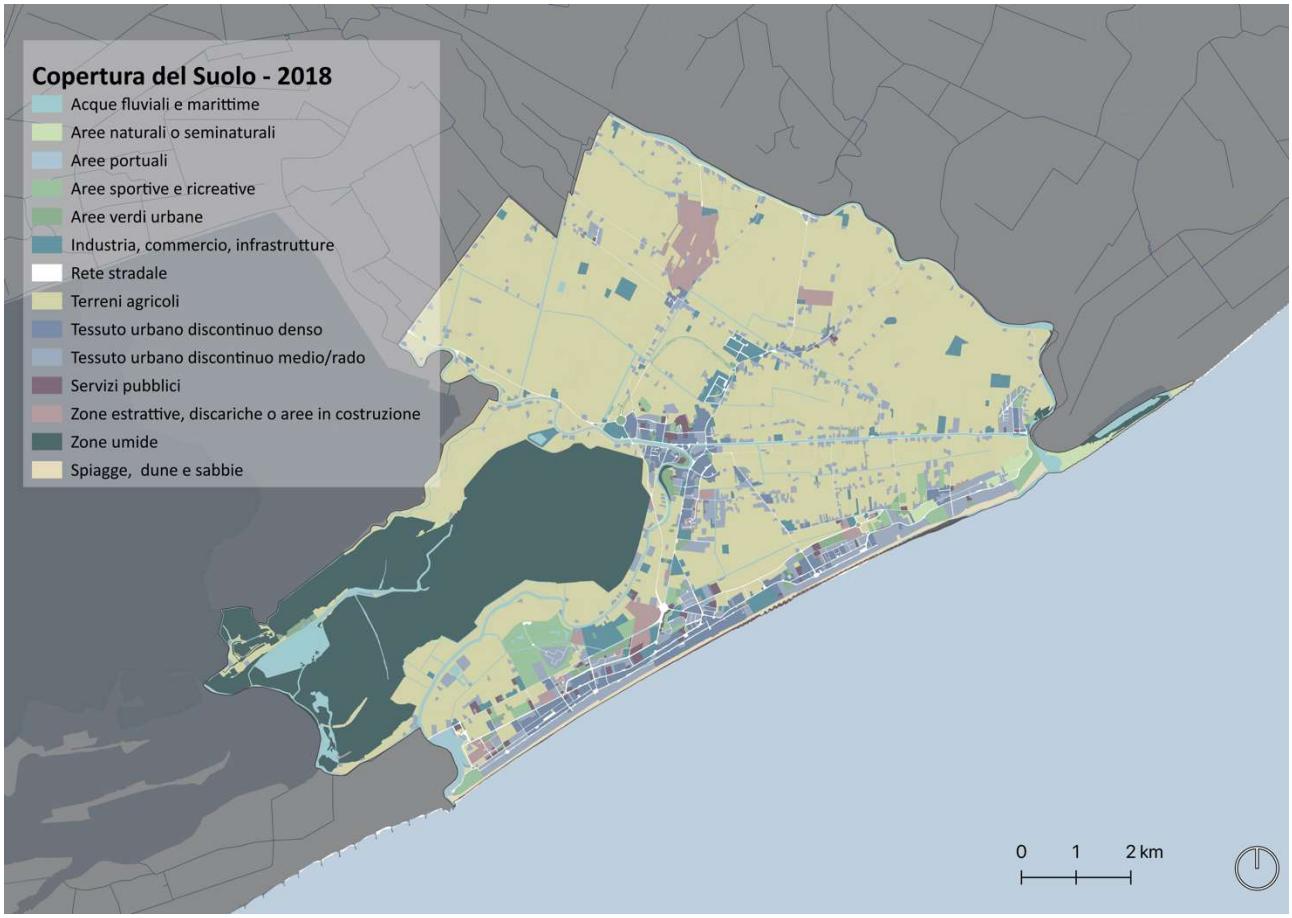

Figure 36. Study area of the Municipality of Jesolo. Aggregation of homogeneous land use and land cover classes based on CCS2018 RV.

The assessment of MV in **Figure 37** represents a phenomenon partly attributable to the progressive and complex sealing of soils. The central tissues of the city are the most prone to multi-vulnerability, which is prominent in correspondence with economic and commercial activities. In these classes, it is evident how planning models and urban morphologies can contribute significantly to the reduction of the mitigating capacity of the territorial ecosystem. Due to the density of flows, the rate of urbanisation and the strategic importance that the Jesolo pole represents for the entire Venetian area in terms of presence and occupational offer, it emerges that these are precisely the main areas in which to invest for the regeneration and climatic recalibration of neighbourhoods, streets and public space behind the dunes, without forgetting the indissoluble bond with the original nucleus behind the coast and its agricultural and, to a lesser extent, industrial/commercial vocation.

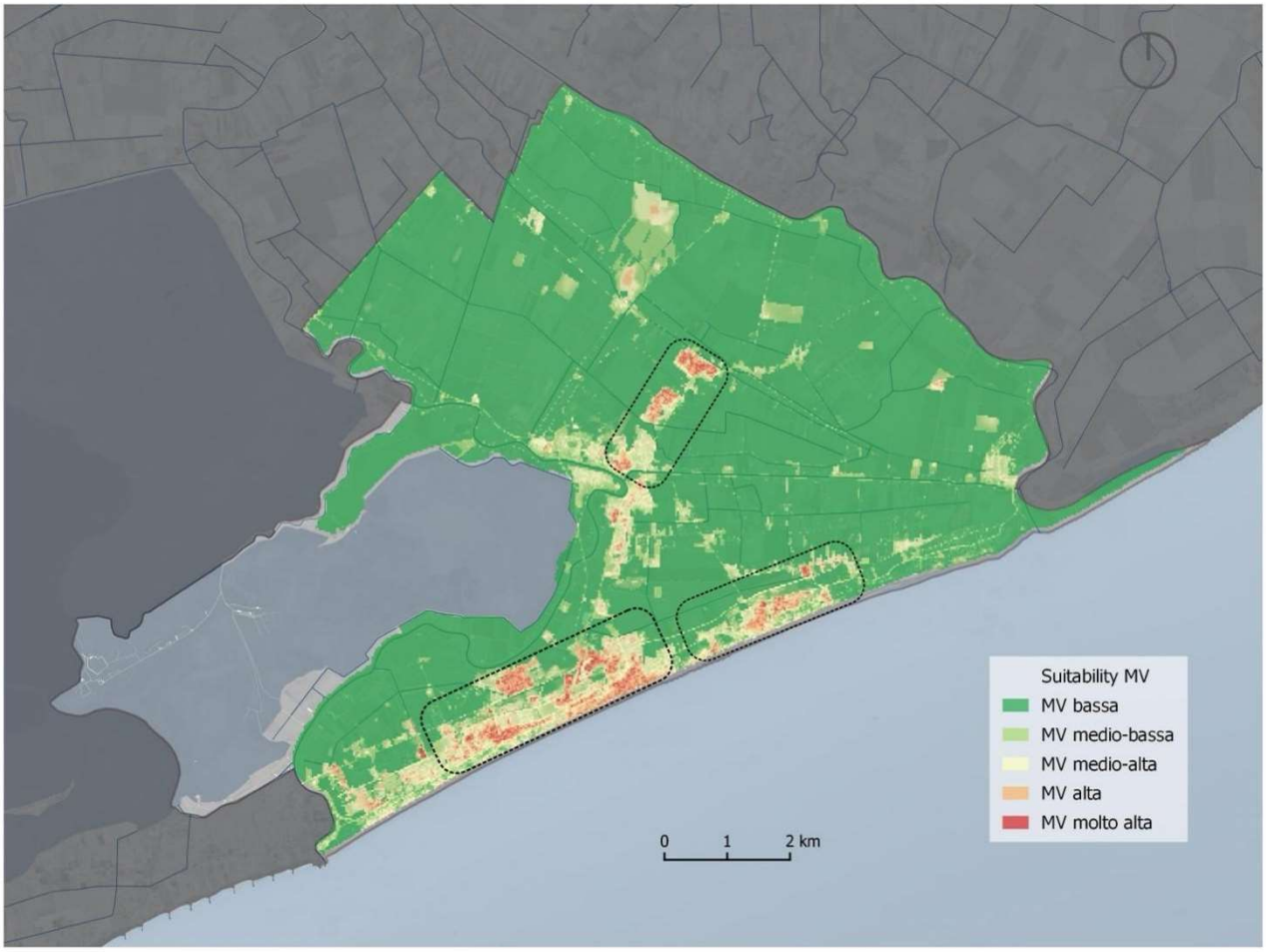

Figure 37. Multi-vulnerability map.

The domain of investigation informs not only the urban ecosystem phenomena of which it is an expression, but also social, tourism and cultural connective trends. A second level of processing concerns the spatial properties assumed by urban activities. This is an analysis methodology conducted with a statistical measure of density based on the 'exposure' layer. As can be deduced from the reading of **Figure 38**, density analysis allows for a better understanding of the distribution of the point data through a cluster representation.

The aggregation of these areas represents hot-spots for potential positive impacts in terms of adaptation to climate change and the revitalisation of the quality of urban space as well as the protection of visitors and residents against the impacts of climate drivers.

Figure 38. Exposure map.

The clustering operation makes it possible to observe the shape of the city and to identify functional areas with a certain regularity in the spatial distribution of urban activities. Most activities are concentrated in the urbanised districts (the central ones) and on the coastal strip.

The multi-risk assessment, resulting from the product between MV and exposure density, yields a spatial reality where it is the denser areas of the city that are most susceptible to climate multi-

impact. The results (largely predictable) are depicted in **Figure 39**, where the indicator takes high values corresponding to possible greater damage that multi-impact may cause to urban activities, concerning their continuity and distribution in the MV domain.

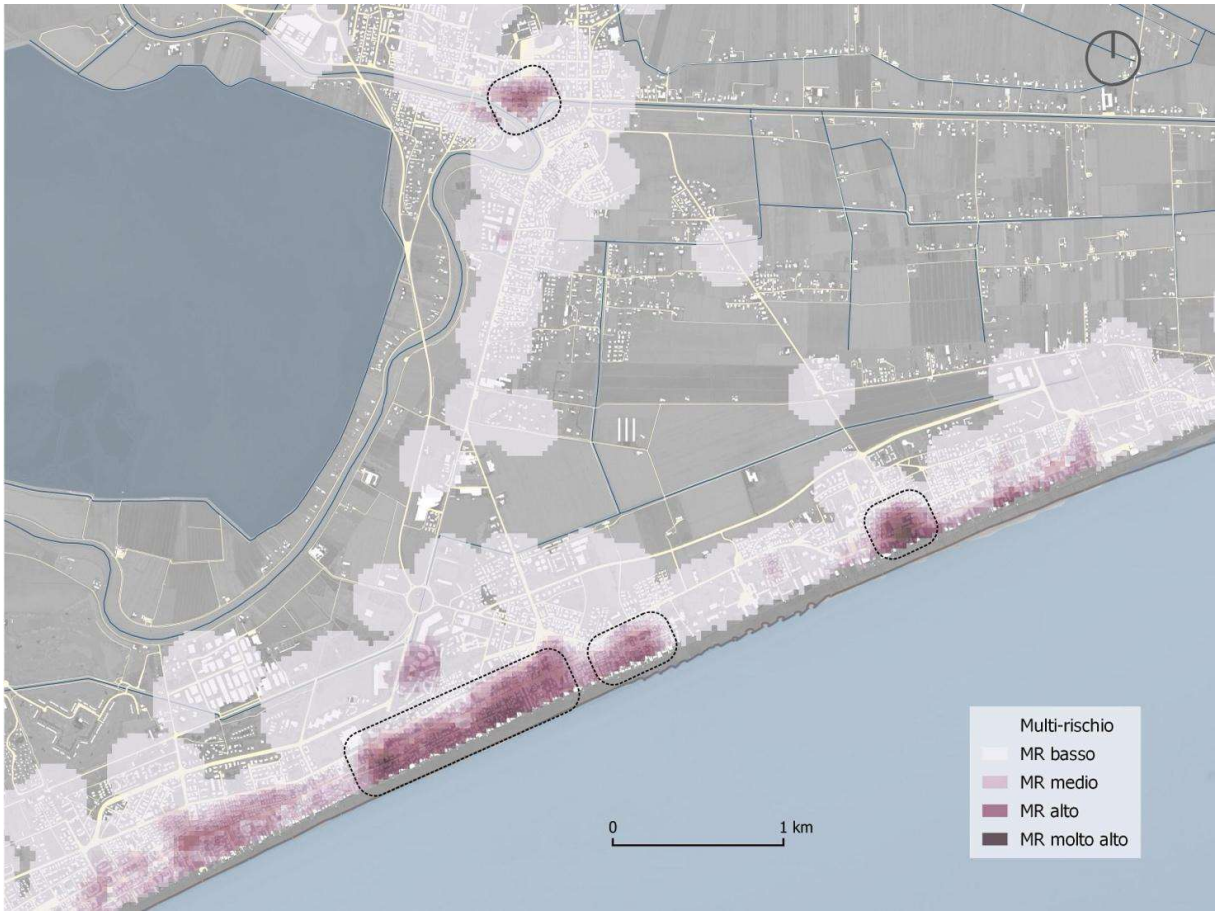

Figure 39. Multi-hazard map[16].

A point-by-point analysis of the data also provides information on the urban activities most exposed to climatic multi-hazard. In particular, **Table 14** shows significant percentages of high and very high multi-risk for the most central urban fabric of the city and commercial and artisan spaces. Finally, non-negligible incidences are also found in the finance and communications sector, health services and tourism activities (referring to accommodation and associated services). Based on the results,

[16] It represents the locations of the stratification of morphological vulnerabilities associated with the co-presence of a certain density of economic activities exposed to risk. The task of the multi-hazard is to recalibrate the adaptation process by employing physical, organisational and economic measures on the basis of priority areas of intervention.

we see how it is precisely the urban fabrics that, with their more or less dense residential or tourist characteristics, make the occurrence of climate impacts related to the intensification of phenomena more likely. The degree of exposure of urban areas is, of all land uses, the one that most brings out fragilities and at the same time potential future opportunities.

Table 14. Multi-risk assessment results for the municipality of Jesolo: distribution of the number of activities subjected to a high and very high risk level.

Macro-categories of activity	Number of activities in the macro-category		Activities subject to high and very high multi-hazard	
	n.	%	n.	%*
1- Culture, entertainment and the arts	10	1,18	5	50,00
2- Historical elements	3	0,36	0	0,00
3- Finance and Communications	22	2,61	11	50,00
4- Gastronomy	172	20,38	33	19,19
5- Waste Management	128	15,17	21	16,41
6- Health Services	23	2,73	3	13,04
7- Mobility	174	20,62	19	10,92
8- Shops	78	9,24	23	29,49
9- Administrative services	4	0,47	2	50,00
10- Leisure and sport	22	2,61	0	0,00
11- Tourism and accommodation	205	24,29	74	36,10
12- Schools	3	0,36	0	0,00
Total	**844**	**100%**	**191**	**22,63**

* Percentages of high and very high multi-risk of each macro-category, made up of one hundred total assets

3.4.2. Impact analysis for the municipality of Cavallino Treporti

Cavallino-Treporti is a coastal peninsula that separates the waters of the Venetian Lagoon from the Adriatic Sea. It brings with it evident morphological transformations that have occurred largely due to sea and river waters. To the north, fishing valleys and lagoon channels delimit this area as far as the Punta Sabbioni breakwater to the southwest. The beach has a strong power of attraction in terms of tourist and commercial flows.

The identities of this urban-territorial system are multiple **(Figure 40)**. Landscape units and small urbanisations alternate along the shoreline profile, outlining the rhythms of coexistence between traditional socio-cultural values, biodiversity hotspots and the hamlets of Cavallino-Treporti.

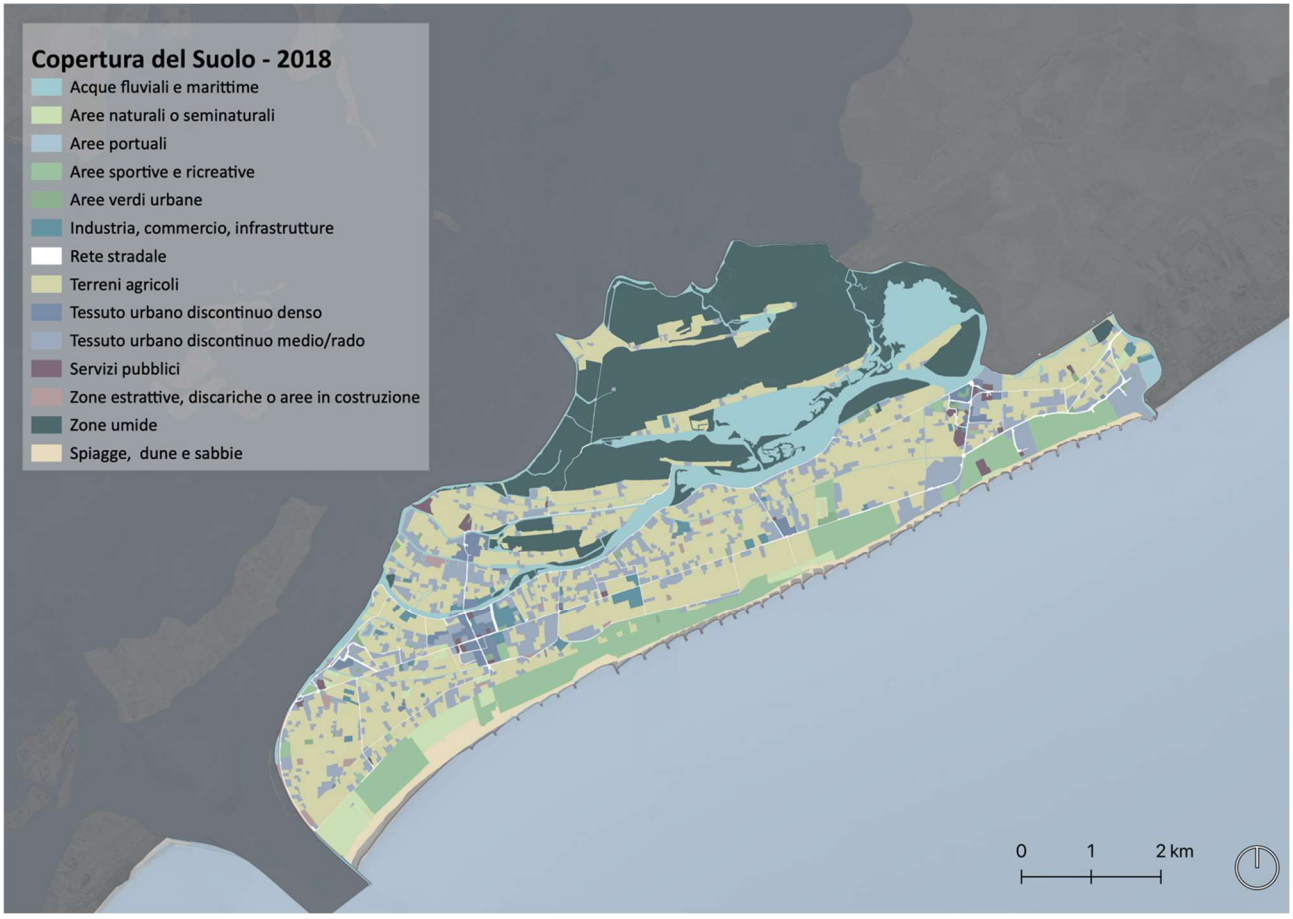

Figure 40. Cavallino Treporti Municipality study area. Aggregation of homogeneous land use and land cover classes based on CCS2018 RV

The MV assessment model developed later allows for the analysis of the spatial location of urban identity cores concerning precise morpho-climatological vulnerabilities, within a relationship that successively considers multiple forcings, such as the intensity of the disaster phenomenon and the co-presence of economic actors **(Figure 41).** In practice, making adaptations in territories requires adopting a systemic and comprehensive perspective of what is exposed. Once the urban pole to be protected has been identified, adaptation will take place after the approval of implementation programmes for the insertion of measures and solutions contained within the Abaco, in compliance with the requirements and characteristics demanded by the context and places. In the specific case study of the municipality of Cavallino-Treporti, the first result of the MV analysis suggests that it is precisely the four urban cores, Cavallino, Ca' Ballarin, Ca' Savio and Treporti, that are the spaces

within which adaptation should be most urgently stimulated: these cores, together with the entire coastal ridge, present areas of significant morpho-climatological multi-vulnerability.

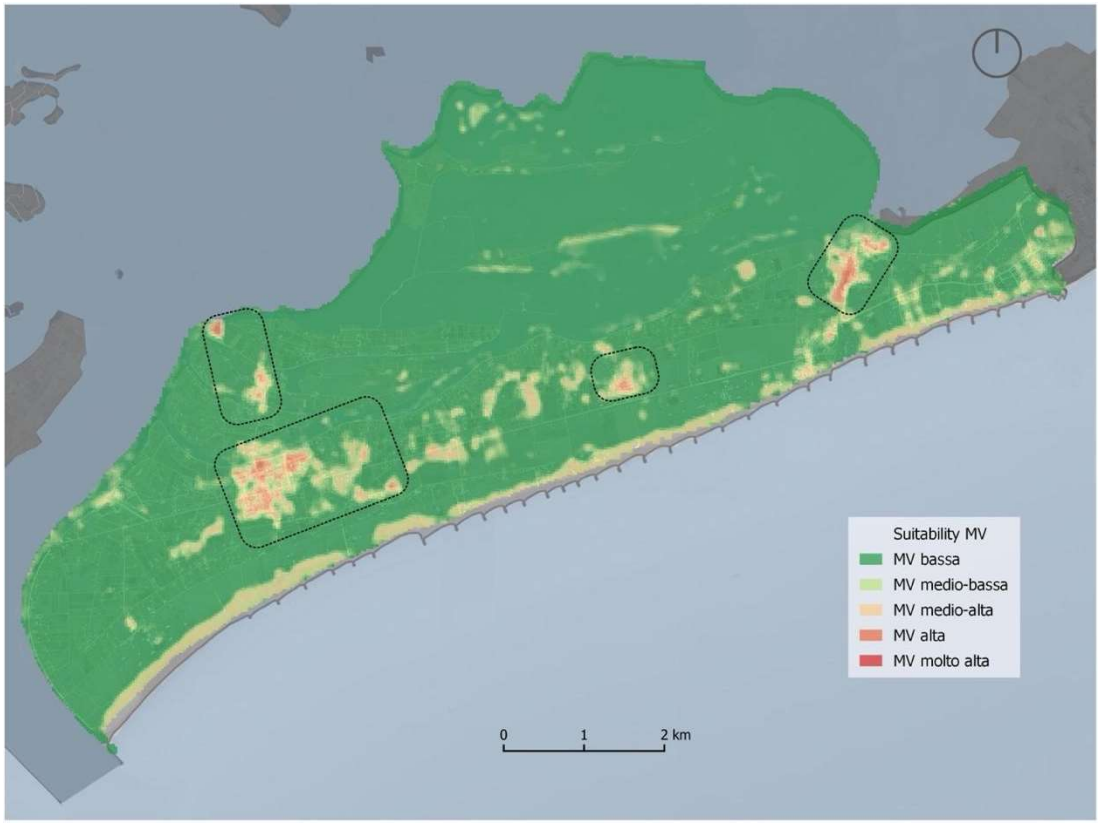

Figure 41. Multi-vulnerability map

Even though in Cavallino-Treporti the accommodation offered is mainly composed of equipped and green camping and tourist villages, there are also some scattered urbanisations. In this organic design, the original urban facilities are located behind the coast, inland, where agricultural areas and spots of small scattered urbanisations also alternate.

Figure 42: Exposure map.

The cores are distributed along the peninsula's ridge: the Via Fausta. The hamlets of Cavallino, Ca' Ballarin and Ca' Savio are connected by this linear infrastructure that extends along the entire coastal strip, as far as Punta Sabbioni. Except for Treporti, an urban core with a historical identity that is located further north, towards the fishing valleys beyond the lagoon channels, the entire coastal strip develops longitudinally to the coastline and enjoys a close relationship with the coastal front, the location of the main tourist activities.

As evidenced by the Kernel Density **(Figure 42)**, enterprises are mostly concentrated in the urban cores of the small hamlets and in the centre of Ca' Savio, leaving the seafront to campsites and villages.

The punctual localisation of activities concerns mainly Third Sector actors. The extraction of these 'open-source' data (e.g. location, type, address) makes it possible to arrive at a deep level of detail, the multi-risk, i.e. the parameter expressing the density of economic actors potentially affected by multiple impacts.

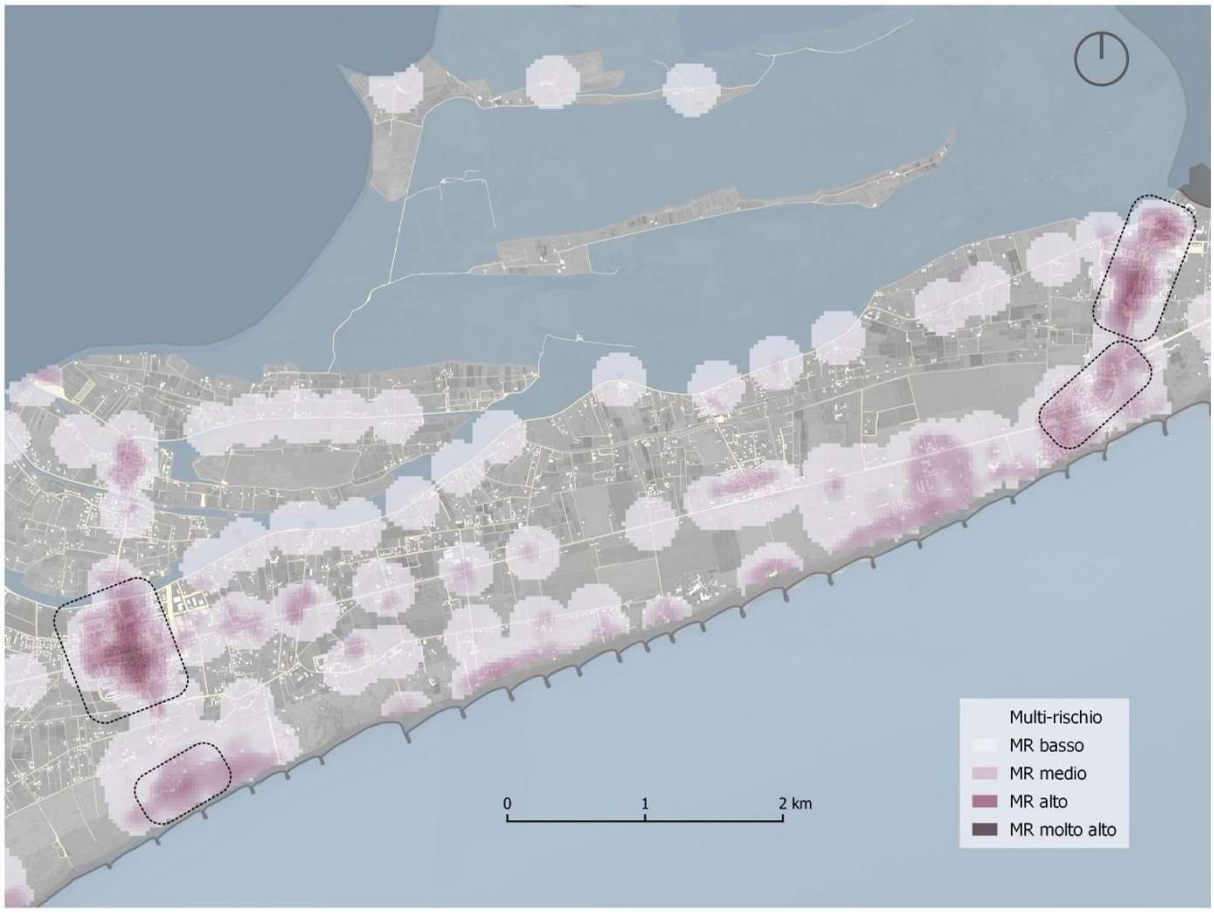

Figure 43. Multi-risk map.

Thus, by considering the typical fragilities of a coastal environment, MR lends robustness to the decision-making process, defining a picture of what urban functions are subject to the climate risks under analysis **(Figure 43)**.

From the analyses carried out on the Municipality of Cavallino-Treporti, a clear interpretative picture emerges, which translates into a confirmation of what has already been predicted in the regional and national climate change scenarios dedicated to coastal areas. The predisposition to risk in some areas is more marked than in others. It becomes generalised especially in those denser urban agglomerations where adaptive capacity is reduced and where, due to spatial organisation, economic operators are denser. Squares, avenues and boulevards are the places along which activities for the exchange of goods and services are distributed and interact with the local community and visitors. No less important is the number of activities at risk along the demarcation line with beaches. Sea storms and intense heat events, but also localised flooding and extreme weather events threaten these cores, concentrations of commercial and personal service businesses that occupy the very first coastal strip, sometimes also clustering within villages and campsites.

As can be seen from the summary table of the economic activities codified in Cavallino-Treporti, the model for the recombination of the factors in play (climatic and otherwise) highlighted a significant result: almost half of the mapped activities are affected by a certain level of risk, which can be defined as multi-risk when there is a convergence between sums of several factors. In operational terms, the model thus initiates a new phase for planning that is aware of and attentive to new climate variables that enter the process. The calibration of adaptation becomes an opportunity for the recombination of policy instruments as it could also be for regulations and implementation rules, which are considered closer to the operational level. As we will see later, the integration of climate action solutions occurs by combining the appropriate knowledge frameworks with urban retrofit techniques and strategies that are complemented by policy, information and warning programmes.

Due to the rules by which the territory of Cavallino-Treporti is organised, the model supports the planning of adaptation actions by concretising the location of the territorial areas and the economic actors involved by a certain risk factor. As it emerges from the reading of **Table 15**, out of the total 468 geo-coded activities, more than half are retail shops, gastronomy-related activities and finally LPT stations or stops. The characterisation by compartments, and macro-categories, allows us not only to coordinate interventions for adaptation according to the vision of the city of tomorrow but, above all, allows us to contribute to planning by adding an overall vision that takes into account the framework and context of reference. In both cases, whether it is an open space rather than a specific device capable of mitigating the impacts of climate on the city and the coast, what emerges most from reading the MR is the direct correlation with urban centres, even small to medium-sized ones.

Table 15. Multi-risk assessment results for the municipality of Cavallino-Treporti: distribution of the number of activities subjected to a high and very high risk level.

Macro-categories of activity	Number of activities in the macro-category		Activities subject to high and very high multi-hazard	
	n	%*	n	%**
1- Culture, entertainment and the arts	4	0,9	2	50,0
2- Historical elements	0	0,0	0	0
3- Finance and Communications	27	5,8	26	96,3
4- Gastronomy	120	25,6	67	55,8
5- Waste Management	89	19,0	38	42,7
6- Health Services	4	0,9	3	75,0
7- Mobility	120	25,6	51	42,5
8- Shops	77	16,5	56	72,7
9- Administrative services	1	0,2	1	100
10- Leisure and sport	10	2,1	6	60,0
11- Tourism and accommodation	16	3,4	10	62,5
12- Schools	0	0,0	0	0

Total	**468**	**100%**	**260**	**55**	
* percentage value obtained from the total number of activities in the municipality of Cavallino					
** percentage value derived from total assets within the macro-category of reference					

3.4.3. Impact analysis for the municipality of Porto Tolle

Porto Tolle is a municipality in the Province of Rovigo that is completely immersed in the territorial system of the Veneto Po Delta Regional Park. It is part of a valuable natural context, within which the conservation of ecosystem values is a priority and their complete functionality represents a cardinal element within the strategic and operational planning of the area **(Figure 44)**.

Within this local framework, climate change requires addressing additional issues with a cross-sectoral slant, which rises and overlap with ordinary management. To this end, the meta-criteria approach creates new evaluative elements with which individual phenomena related to localised impacts can be interpreted while maintaining a synoptic view (MV).

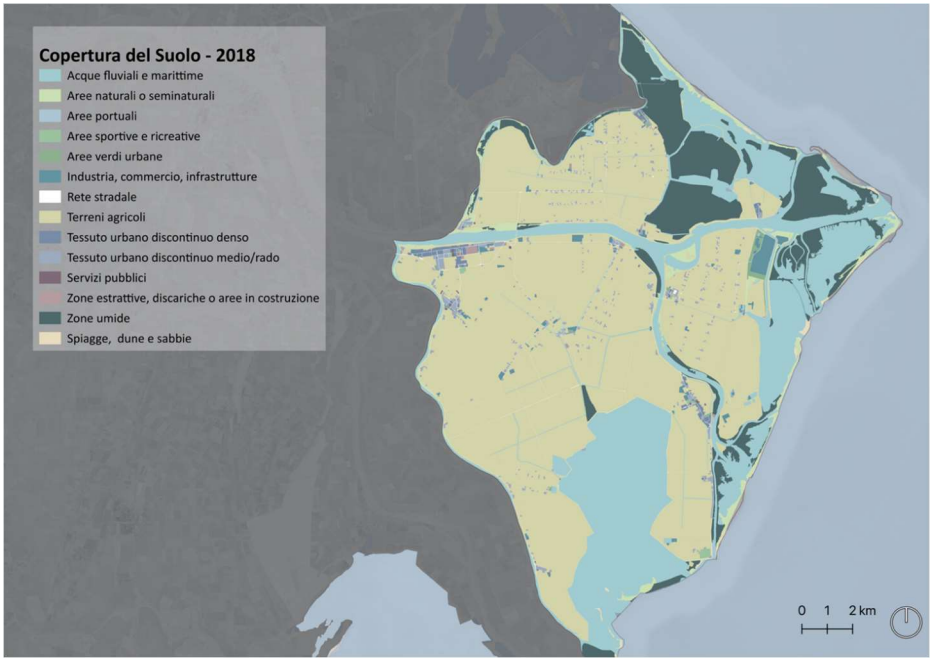

Figure 44. Porto Tolle Municipality study area. Aggregation of homogeneous land use and land cover classes based on CCS2018 RV.

This launches a new season for spatial planning and, as mentioned above, brings with it the need to review and expand policy instruments, coordinating climate action according to specific exposed factors.

Figure 45. Multi-vulnerability map

The case study of the Municipality of Porto Tolle, with its landscape richness sprinkled with small, independent and pulverised urbanisations, becomes an opportunity to investigate the multiple relations that lie between climate and project on a territorial scale **(MV, Figure 45)**: the location of the areas affected by risk also becomes one of the planning drivers of the territorial matrix as well as a new information level ready to direct attention towards a new planning paradigm.

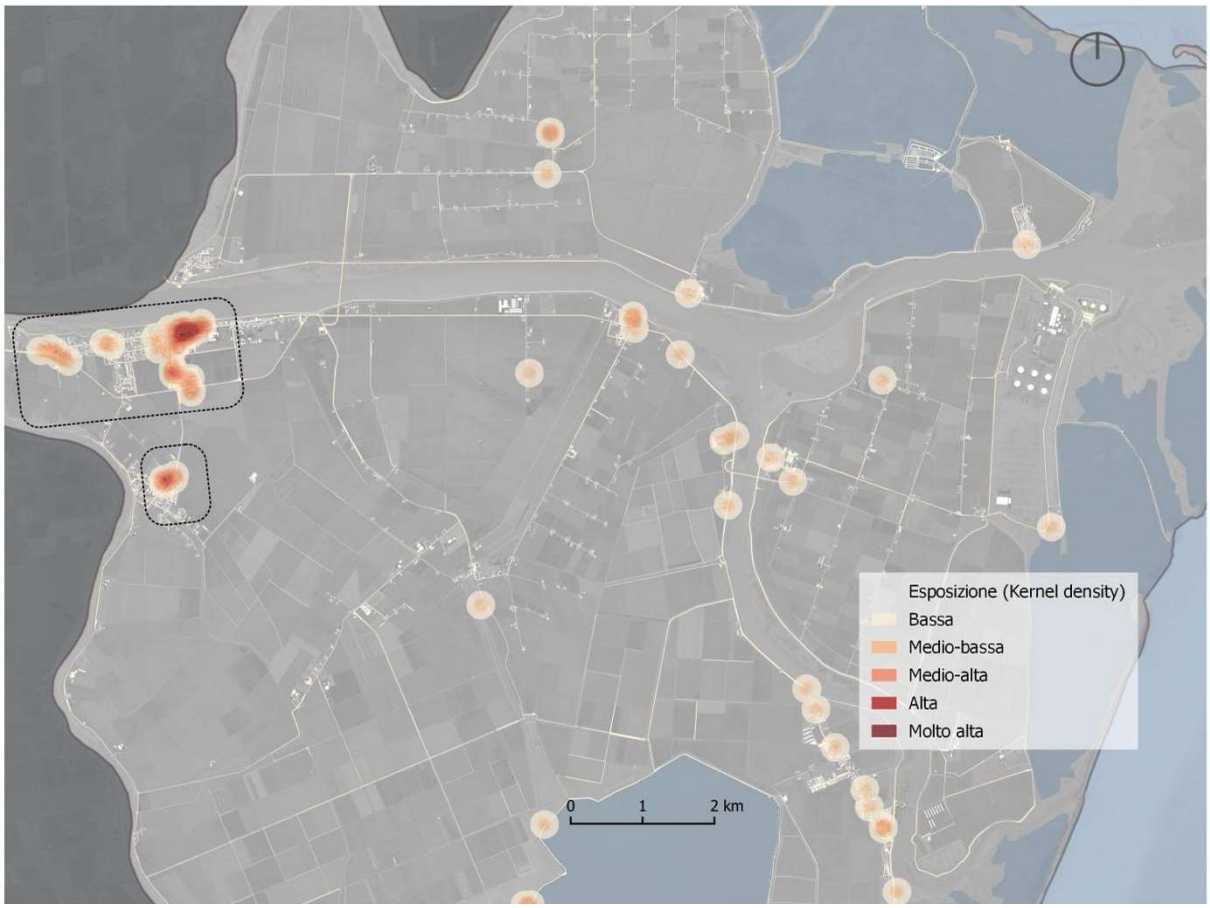

Figure 46. Exposure map

The micro-enterprise activities involved in the AdriaClim project are mainly concentrated in the small centres of the municipality's hamlets, particularly in the main town Ca' Tiepolo and the neighbouring hamlet of Donzella. **(Figure 46).**

Analyses conducted on the Municipality of Porto Tolle reveal a climatic picture whose management requires a coordinated spatial vision given the municipality's considerable territorial extension. The risk hotspots **(Figure 47)** appear in the urban centres with the densest residential tissues, where there are dense economic operators and areas vulnerable to flooding, heat waves and, sea storms along the coast. Contrade, hamlets and boulevards are the dimensions according to which the relationship between the actors characterising the local nucleus and interacting with the tourists of the Po Delta coastal front takes place.

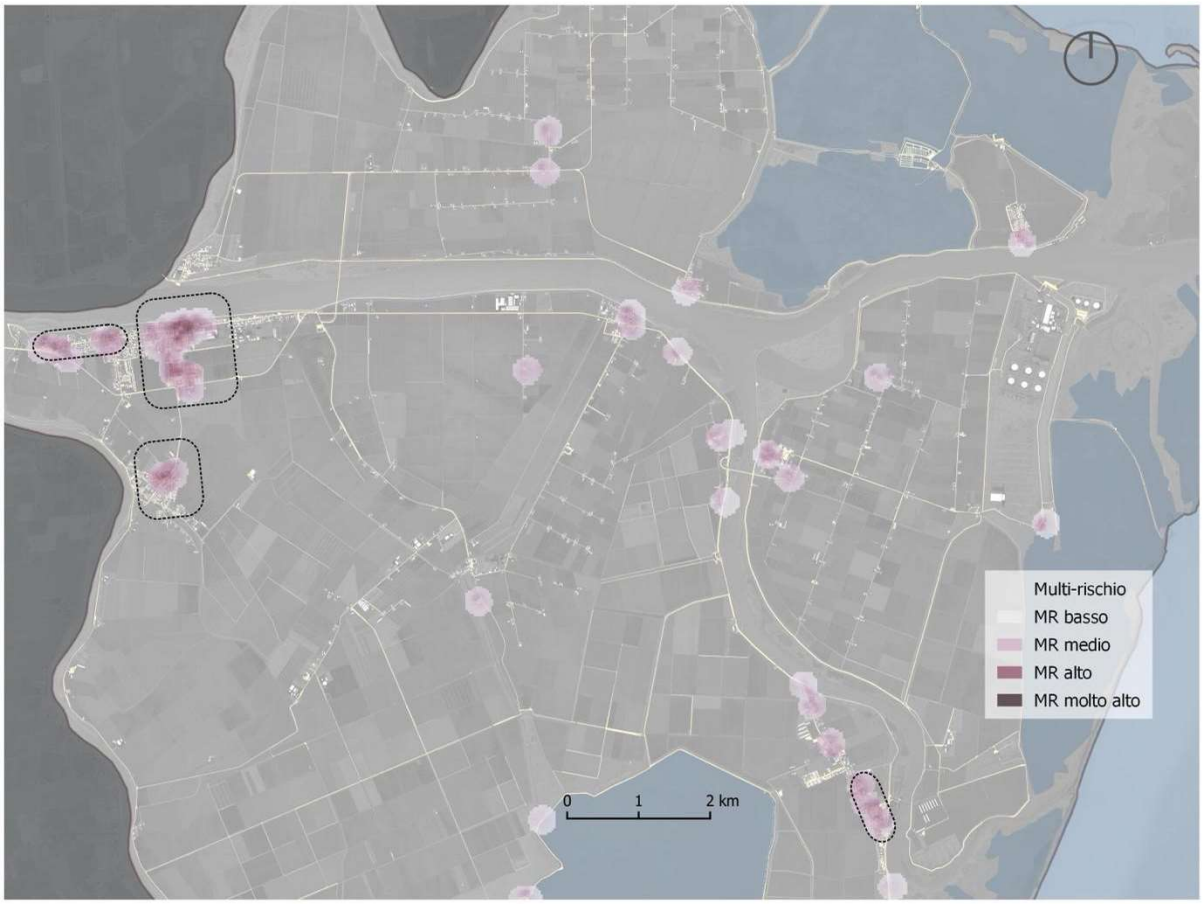

Figure 47. Multi-risk map.

As can be seen in Summary **Table 16**, again the model returns an important result: more than half of the activities mapped by OpenStreet Map are exposed to risk from multiple factors. In essence, climate change adaptation, to be effective concerning the challenges at hand, needs to review the rhythms and rules of open space and urban morphologies, even in small towns and villages.

As we will see later, the integration of climate action solutions occurs by thinking about the application of intervention techniques with the pursuit of objectives of a strategic nature.

Taking into consideration the punctiform territorial framework of the Municipality of Porto Tolle, we can see how some macro-categories require a priority framework of intervention to the remaining classes; although present in a smaller number for the prevalent categories, historical elements (cat. 2), shops (cat. 8), administrative services (cat. 9) and finally tourist facilities (cat. 10) are fully involved in the portions of territory considered at risk. To guide the programming of interventions also for the Municipality of Porto Tolle, the model, therefore, supports the calibration of the ex-post phase by defining a hierarchy of intervention among the economic categories; in essence, adaptation is posed as an open question, whose interpretative reading of the context is enriched with the progressive inclusion of the territorial and climatic variables of interest. The choice and use of certain devices will take place voluntarily, in a differentiated manner according to the morphology of the places, the needs given by the socio-economic context of the area, and respecting the fragility and balance of the natural ecosystems present.

Table 16. Multi-risk assessment results for the municipality of Porto Tolle: distribution of the number of activities subjected to a medium-high risk level.

Macro-categories of activity	***Number of activities in the macro-category***		***Activities subject to high and very high multi-hazard***	
	n	***%****	***n***	***%****
1- Culture, entertainment and the arts	*1*	*1,15*	*1*	*100*
2- Historical elements	*7*	*8,05*	*7*	*100*

3- Finance and Communications	*3*	*3,45*	*2*	*67*
4- Gastronomy	*25*	*28,74*	*14*	*56*
5- Waste Management	*2*	*2,30*	*2*	*100*
6- Health Services	*0*	*0,00*	*0*	*0*
7- Mobility	*31*	*35,63*	*18*	*58*
8- Shops	*3*	*3,45*	*3*	*100*
9- Administrative services	*2*	*2,30*	*2*	*100*
10- Leisure and sport	*6*	*6,90*	*5*	*83*
11- Tourism and accommodation	*7*	*8,05*	*4*	*57*
12- Schools	*0*	*0*	*0*	*0*
Total	***87***	***100%***	***58***	***66%***
** percentage value derived from the total number of activities in Porto Tolle*				
*** percentage value derived from total assets within the macro-category of reference*				

- Bibliography

Adolphson M. (2010), "Kernel densities and mixed functionality in a multicentred urban region", *Environment and Planning B-Planning & Design,* 37: 550–566.

Baldi, P. (2012). Autoencoders, Unsupervised Learning, and Deep Architectures. *Proceedings of Machine Learning Research*, 27:37-49.

Barbi, A., Cagnati, A., Cola, G., Checchetto, F., Chiaudani, A., Crepaz, A., & Robert-Luciani, T. (2013). *Atlante climatico del Veneto. Precipitazioni-Basi informative per l'analisi delle correlazioni tra cambiamenti climatici e dinamiche forestali nel Veneto. Regione del Veneto, Mestre, Italy.*

Barbi, A., Monai, M., Racca, R., & Rossa, A. M. (2012). Recurring features of extreme autumnall rainfall events on the Veneto coastal area. *Natural Hazards & Earth System Sciences*, *12*(8), 2463–2477. https://doi.org/https://doi.org/10.5194/nhess-12-2463-2012

Barriopedro, D., García-Herrera, R., Ordóñez, C., Miralles, D. G., & Salcedo-Sanz, S. (2023). Heat Waves: Physical Understanding and Scientific Challenges. *Reviews of Geophysics*, *61*(2). https://doi.org/10.1029/2022RG000780

Bezzi, A., Pillon, S., Martinucci, D., & Fontolan, G. (2018). Inventory and conservation assessment for the management of coastal dunes, Veneto coasts, Italy. *Journal of Coastal Conservation*, *22*(3), 503–518. https://doi.org/https://doi.org/10.1007/s11852-017-0580-y

Breiman, L. E. O. (2001). *Random Forests*. 5–32.

Cahyana, N., Khomsah, S., & Aribowo, A. S. (2019). Improving Imbalanced Dataset Classification Using Oversampling and Gradient Boosting. *5th International Conference on Science in Information Technology (ICSITech)*, 217–222. https://doi.org/10.1109/ICSITech46713.2019.8987499

Camuffo, D. (2021). Four centuries of documentary sources concerning the sea level rise in Venice. *Climatic Change*, *167*(3–4), 1–16. https://doi.org/https://doi.org/10.1007/s10584-021-03196-9

Cavalieri, C. (2020). Extreme-city-territories. Coastal geographies in the Veneto region. *Journal of Urbanism: International Research on Placemaking and Urban Sustainability*, 1–19.

Chang, C. C., & Lin, C. J. (2001). Training v-support vector classifiers: Theory and algorithms. *Neural Computation*, *13*(9), 2119–2147. https://doi.org/10.1162/089976601750399335

De Ruiter, M. C., Couasnon, A., van den Homberg, M. J. C., Daniell, J. E., Gill, J. C., & Ward, P. J. (2020). Why We Can No Longer Ignore Consecutive Disasters. *Earth's Future*, *8*(3), e2019EF001425. https://doi.org/https://doi.org/10.1029/2019EF001425

Ertekin, S., Huang, J., Bottou, L., & Giles, L. (2007). Learning on the border: active learning in imbalanced data classification. *Proceedings of the Sixteenth ACM Conference on Conference on Information and Knowledge Management (CIKM '07)*, 127–136.

Eastman J.R. (1999), Multi-criteria evaluation and GIS. Geographical information systems 1, 493–502.

Ferrarin, C., Lionello, P., Orlić, M., & Al., E. (2022). Venice as a paradigm of coastal flooding under multiple compound drivers. *Scientific Reports*, *12*, 5754. https://doi.org/https://doi.org/10.1038/s41598-022-09652-5

Ferrarin, C., Roland, A., Bajo, M., Umgiesser, G., Cucco, A., Davolio, S., Buzzi, A., Malguzzi, P., & Drofa, O. (2013). Tide-surge-wave modelling and forecasting in the Mediterranean Sea with focus on the Italian coast. *Ocean Modelling*, *61*, 38–48. https://doi.org/https://doi.org/10.1016/j.ocemod.2012.10.003

Fritzsche K., Schneiderbauer S., Bubeck P., Kienberger S., Buth M., Zebisch M., Kahlenborn W. (2014), The vulnerability sourcebook: concept and guidelines for standardised vulnerability assessments, Deutsche Gesellschaft für Internationale Zusammenarbeit (GIZ) GmbH.

Gatrell A., Bailey T., Diggle P., Rowlingson B. (1996), "Spatial point pattern analysis and its application in geographical epidemiology", *Transactions of the Institute of British Geographers*, 21: 256–74.

Goodfellow, I., Bengio, Y., & Courville, A. (2016). *Deep Learning*. MIT Press.

Halsnæs, K., & Trærup, S. (2009). Development and Climate Change: A Mainstreaming Approach for Assessing Economic, Social, and Environmental Impacts of Adaptation Measures. *Environmental Management*, *43*(5), 765–778. https://doi.org/https://doi.org/10.1007/s00267-009-9273-0

He, C., Wang, R., & Chen, X. (2021). A Tale of Two CILs: The Connections Between Class Incremental Learning and Class Imbalanced Learning, and Beyond. *IEEE/CVF Conference on Computer Vision and Pattern Recognition (CVPR) Workshops*, 3559–3569.

Hersbach, H. et al. (2020). The ERA5 Reanalysis. *Quarterly Journal of the Royal Meteorological Society*. https://doi.org/10.1002/qj.3803

IPCC (2014), Climate Change 2014: Impacts, Adaptation, and Vulnerability, Cambridge.

Jelic, D., Telišman Prtenjak, M., Malecic, B., Belušic Vozila, A., Megyeri, O. A., & Renko, T. (2021). A New Approach for the Analysis of Deep Convective Events: Thunderstorm Intensity Index. *Atmosphere*, *12*(7), 908. https://doi.org/https://doi.org/10.3390/atmos12070908

Joint Research Centre, Institute for Prospective Technological Studies, Nicholls, R., & Richard, J. (2012). *Impacts of climate change in coastal systems in Europe : PESETA-coastal systems study*. https://doi.org/doi/10.2791/3558

King, G., Honaker, J., Joseph, A., & Scheve, K. (2001). Analyzing Incomplete Political Science Data: An Alternative Algorithm for Multiple Imputation. *American Political Science Review*, *95*(1), 49–69. https://doi.org/10.1017/S0003055401000235

L'Hévéder, B., Li, L., & Sevault, FlorenceSomot, S. (2013). Interannual variability of deep convection in the Northwestern Mediterranean simulated with a coupled AORCM. *Climate Dynamics*, *41*(3), 937–960. https://doi.org/https://doi.org/10.1007/s00382-012-1527-5

Lam, R., Sanchez-Gonzalez, A., Willson, M., Wirnsberger, P., Fortunato, M., Pritzel, A., Ravuri, S., Ewalds, T., Alet, F., Eaton-Rosen, Z., Hu, W., Merose, A., Hoyer, S., Holland, G., Stott, J., Vinyals, O., Mohamed, S., Battaglia, P., & contribution, equal. (2022). *GraphCast: Learning skillful medium-range global weather forecasting*.

Lange, S., Volkholz, J., Geiger, T., Zhao, F., Vega, I., Veldkamp, T., Reyer, C. P. O., Warszawski, L., Huber, V., Jägermeyr, J., Schewe, J., Bresch, D. N., Büchner, M., Chang, J., Ciais, P., Dury, M., Emanuel, K., Folberth, C., Gerten, D., … Frieler, K. (2020). Projecting Exposure to Extreme Climate Impact Events Across Six Event Categories and Three Spatial Scales. *Earth's Future*, *8*(12), e2020EF001616. https://doi.org/https://doi.org/10.1029/2020EF001616

Lee, S., Kang, J. E., Park, C. S., Yoon, D. K., & Yoon, S. (2020). Multi-risk assessment of heat waves under intensifying climate change using Bayesian Networks. *International Journal of Disaster Risk Reduction*, *50*, 101704. https://doi.org/https://doi.org/10.1016/j.ijdrr.2020.101704

Legambiente. (2012). *Il consumo delle aree costiere italiane. La COSTA VENETA, da Bibione a Porto Tolle: l'aggressione del cemento e i cambiamenti del paesaggio*.

Lerer S., Arnbjerg-Nielsen K. and Mikkelsen P. (2015), 'A Mapping of Tools for Informing Water Sensitive Urban Design Planning Decisions—Questions, Aspects and Context Sensitivity', *Water*, 7(12), pp. 993–1012. doi: 10.3390/w7030993.

Lionello, P., Barriopedro, D., Ferrarin, C., Nicholls, R. J., Orlic, M., Reale, M., Umgiesser, G., Vousdoukas, M., & Zanchettin, D. (2020). Extremes floods of Venice: characteristics, dynamics, past and future evolution. *Natural Hazards and Earth System Sciences*, *November*, 1–34. https://doi.org/https://doi.org/10.5194/nhess-2020-359

Limonta G., Paris M. (2017), "Riconoscere e monitorare la potenziale fragilità dei sistemi commerciali urbani: una proposta per la Regione Lombardia", in *Atti della XIX Conferenza Nazionale SIU*, Planum Publisher, Milano-Roma, pp. 1042-1051.

Liu, F. T., Ting, K. M., & Zhou, Z.-H. (2008). Isolation Forest. *Eighth IEEE International Conference on Data Mining*, 413–422. https://doi.org/10.1109/ICDM.2008.17

Maalouf, M., & Trafalis, T. B. (2011). Rare events and imbalanced datasets: an overview. *Researchgate.Net*, *3*(4), 375–388. https://doi.org/10.13140/RG.2.1.4088.1367

Maragno D., Pozzer G., dall'Omo C. F. (2023), Supporting metropolitan Venice coastline climate adaptation. A multi-vulnerability and exposure assessment approach. *Environmental Impact Assessment Review*, *100*, 107097.

Marcos, M., Rohmer, J., Vousdoukas, M. I., Mentaschi, L., Le Cozannet, G., & Amores, A. (2019). Increased extreme coastal water levels due to the combined action of storm surges and wind waves. *Geophysical Research Letters*, *46*, 4356–4364. https://doi.org/https://doi.org/10.1029/2019GL082599

Marin, G., Modica, M., 2017. Socio-economic exposure to natural disasters. Environmental Impact Assessment Review 64, 57–66. https://doi.org/10.1016/j.eiar.2017.03.002

MATTM. (2017). *Piano Nazionale di Adattamento ai Cambiamenti Climatici PNACC*.

Mentaschi, L., Vousdoukas, M. I., Pekel, J. F., Voukouvalas, E., & Feyen, L. (2018). Global long-term observations of coastal erosion and accretion. Scientific Reports, 8(1), 1–11. https://doi.org/10.1038/s41598-018-30904-w

Morabito M. et al. (2015) 'Urban-hazard risk analysis: Mapping of heat-related risks in the elderly in major Italian cities', *PLoS ONE*, 10(5), pp. 1–18. doi: 10.1371/journal.pone.0127277.

Musco F. et al. (2016), 'Mitigation of and adaptation to UHI phenomena: The Padua case study', in Counteracting Urban Heat Island Effects in a Global Climate Change Scenario. Springer International Publishing, pp. 221–256. doi: 10.1007/978-3-319-10425-6_8.

Murtagh, F. (1991). Multilayer perceptrons for classification and regression. Neurocomputing, 2(5–6), 183–197. https://doi.org/https://doi.org/10.1016/0925-2312(91)90023-5

Nicholls, R. J., Wong, P. P., Burkett, V. R., Codignotto, J. O., Hay, J. E., McLean, R. F., Ragoonaden, S., & Woodroffe, C. D. (2007). Coastal systems and low-lying areas. In P. J. van der L. and , M.L. Parry, O.F. Canziani, J.P. Palutikof & E. C.E. Hanson (Eds.), Climate Change 2007: Impacts, Adaptation and Vulnerability. Contribution of Working Group II to the Fourth Assessment Report of the Intergovernmental Panel on Climate Change (pp. 315–356). Cambridge University Press, Cambridge, UK.

Paolo Tarolli, Luo, J., Straffelini, E., Liou, Y.-A., Nguyen, K.-A., Laurenti, R., Masin, R., & Vicenzo D'Agostino. (2023). Saltwater intrusion and climate change impact on coastal agriculture. PLOS Water, 2(4), E0000121. https://doi.org/https://doi.org/10.1371/journal.pwat.0000121

Regione del Veneto. (2012). Analysis of ICZM practice in Italy: Veneto.

Ribeiro M., Losenno C., Dworak T., Massey E., Swart R., Benzie M., Laaser C. (2009), 'Design of guidelines for the elaboration of Regional Climate Change Adaptations Strategies', *Ecologic Institute, Vienna, Austria*.Saaty, T.L., 1980. The Analytic Hierarchy Process. McGraw-Hill, New York.

Richman, M. B., & Leslie, L. M. (2018). The 2015-2017 Cape Town Drought: Attribution and Prediction Using Machine Learning. Procedia Computer Science, 140, 248–257. https://doi.org/https://doi.org/10.1016/j.procs.2018.10.323

Rivera-Velasquez, M. F., Fallico, C., Guerra, I., & Straface, S. (2013). A Comparison of deterministic and probabilistic approaches for assessing risks from contaminated aquifers: An Italian case study. Waste Management & Research, 31(12), 1245–1254. https://doi.org/https://doi.org/10.1177/0734242X13507305

Rizzi, J., Gallina, V., Torresan, S., Critto, A., Gana, S., & Marcomini, A. (2016). Regional Risk Assessment addressing the impacts of climate change in the coastal area of the Gulf of Gabes (Tunisia). Sustainability Science, 11(3), 455–476. https://doi.org/10.1007/s11625-015-0344-2

Ruol, P., Martinelli, L., & Favaretto, C. (2018). Vulnerability analysis of the Venetian littoral and adopted mitigation strategy. Water, 10(8), 984.

Ruol, P., & Pinato, T. (2016). Gestione Integrata della Zona Costiera - Studio e monitoraggio per la definizione degli interventi di difesa dei litorali dall'erosione nella regione Veneto" Adozione linee guida.

Ruti, P. M., Somot, S., Giorgi, F., Dubois, C., Flaounas, E., Obermann, A., Dell'Aquila, A., Pisacane, G., Harzallah, A., Lombardi, E., Ahrens, B., Akhtar, N., Alias, A., Arsouze, T., Aznar, R., Bastin, S., Bartholy, J., Beranger, K., Beuvier, J., … Vervatis, V. (2016). MED-CORDEX

INITIATIVE FOR MEDITERRANEAN CLIMATE STUDIES. American Meteorological Society, 1187–1208. https://doi.org/10.1175/BAMS-D-14-00176.1

Saaty T.L. (1980), *The Analytic Hierarchy Process*, McGraw-Hill, New York.

Schlef, K. E., Moradkhani, H., & Lall, U. (2019). Atmospheric Circulation Patterns Associated with Extreme United States Floods Identified via Machine Learning. Scientific Reports, 9(1), 7171. https://doi.org/https://doi.org/10.1038/s41598-019-43496-w

Simmons , A., et al . (2020). Global stratospheric temperature bias and other stratospheric aspects of ERA5 and ERA5.1. ECMWF Technical Memorandum Number, 859, 40. https://doi.org/10.21957/rcxqfmg0

Simpson, N. P., Mach, K. J., Constable, A., Hess, J., Hogarth, R., Howden, M., Lawrence, J., Lempert, R. J., Muccione, V., Mackey, B., New, M. G., O'Neill, B., Otto, F., Pörtner, H.-O., Reisinger, A., Roberts, D., Schmidt, D. N., Seneviratne, S., Strongin, S., … Trisos, C. H. (2021). A framework for complex climate change risk assessment. One Earth, 4(4), 489–501. https://doi.org/10.1016/j.oneear.2021.03.005

Stocchi, P., & Davolio, S. (2017). Intense air-sea exchanges and heavy orographic precipitation over Italy: The role of Adriatic sea surface temperature uncertainty. Atmospheric Research, 196, 62–82. https://doi.org/https://doi.org/10.1016/j.atmosres.2017.06.004

Sutanto, S. J., Vitolo, C., Di Napoli, C., D'Andrea, M., & Van Lanen, H. A. J. (2020). Heatwaves, droughts, and fires: Exploring compound and cascading dry hazards at the pan-European scale. Environment International, 134, 105276. https://doi.org/10.1016/j.envint.2019.105276

Tao, F., Rötter, R. P., Palosuo, T., Gregorio Hernández Díaz Ambrona, C., Mínguez, M. I., Semenov, M. A., Kersebaum, K. C., Nendel, C., Specka, X., Hoffmann, H., Ewert, F., Dambreville, A., Martre, P., Rodríguez, L., Ruiz-Ramos, M., Gaiser, T., Höhn, J. G., Salo, T., Ferrise, R., … Schulman, A. H. (2018). Contribution of crop model structure, parameters and climate projections to uncertainty in climate change impact assessments. Climate Change Biology, 24(3), 1291–1307. https://doi.org/https://doi.org/10.1111/gcb.14019

Tebaldi, C., Ranasinghe, R., Vousdoukas, M., Rasmussen, D. J., Vega-Westhoff, B., Kirezci, E., Kopp, R. E., Sriver, R., & Mentaschi, L. (2021). Extreme sea levels at different global warming levels. Nature Climate Change, 11(9), 746–751. https://doi.org/https://doi.org/10.1038/s41558-021-01127-1

Teichert, N., Borja, A., Chust, G., Uriarte, A., & Lepage, M. (2016). Restoring fish ecological quality in estuaries: Implication of interactive and cumulative effects among anthropogenic stressors. Science of The Total Environment, 542(Part A), 383–393. https://doi.org/https://doi.org/10.1016/j.scitotenv.2015.10.068

Tilloy, A., Malamud, B. D., & Joly-Laugel, A. (2022). A methodology for the spatiotemporal identification of compound hazards: wind and precipitation extremes in Great Britain (1979–2019). Earth System Dynamics, 13(2), 993–1020. https://doi.org/10.5194/esd-13-993-2022

Torresan, S., Critto, A., Dalla Valle, M., Harvey, N., & Marcomini, A. (2008). Assessing coastal vulnerability to climate change: Comparing segmentation at global and regional scales. Sustainability Science, 3(1), 45–65. https://doi.org/https://doi.org/10.1007/s11625-008-0045-1

Torresan, S., Critto, A., Rizzi, J., Marcomini, A., Mendez, F. J., Leschka, S., & Fraile-Jurado, P. (2012). Assessment of coastal vulnerability to climate change hazards at the regional scale: the case study of the North Adriatic Sea. Natural Hazards & Earth System Sciences, 12(7).

Torresan, S., Critto, A., Rizzi, J., Zabeo, A., Furlan, E., & Marcomini, A. (2016). DESYCO: A decision support system for the regional risk assessment of climate change impacts in coastal zones. Ocean & Coastal Management, 120, 49–63. https://doi.org/https://doi.org/10.1016/j.ocecoaman.2015.11.003

Tripathibr R., Sahoobr R., Guptabr V., Sahoo V. (2013), 'Developing Vegetation Health Index from biophysical variables derived
using MODIS satellite data in the Trans-Gangetic plains of India', *Emirates Journal of Food and Agriculture*, 25 https://doi.org/10.9755/ejfa.v25i5.11580

Umgiesser, G., Bajo, M., Ferrarin, C., Cucco, A., Lionello, P., Zanchettin, D., Papa, A., Tosoni, A., Ferla, M., Coraci, E., Morucci, S., Crosato, F., Bonometto, A., Valentini, A., Orlić, M., Haigh, I. D., Nielsen, J. W., Bertin, X., Fortunato, A. B., … Nicholls, R. J. (2021). The prediction of floods in Venice: methods, models and uncertainty (review article). Natural Hazards & Earth System Sciences, 21, 2679–2704. https://doi.org/https://doi.org/10.5194/nhess-21-2679-2021

Ungaro F., Calzolari C., Pistocchi A., Malucelli F. (2014), 'Modelling the impact of increasing soil sealing on runoff coefficients at regional scale: a hydropedological approach', *Journal of Hydrology and Hydromechanics,* 62, https://doi.org/10.2478/johh-2014-0005

Van Aalst, M. K. (2006). The impacts of climate change on the risk of natural disasters. Disasters, 30(1), 5–18. https://doi.org/https://doi.org/10.1111/j.1467-9523.2006.00303.x

Wilby R.L., Dessai S. (2010), 'Robust adaptation to climate change', Weather 65, https://doi.org/10.1002/wea.543

Wilby R.L., Keenan R. (2012), 'Adapting to flood risk under climate change', *Progress in Physical Geography: Earth and Environment*, 36, https://doi.org/10.1177/0309133312438908

Yang S., Shen J., Konečný M., Wang Y., Štampach R. (2018, June), 'Study on the Spatial Heterogeneity of the POI Quality in OpenStreetMap', *Proceedings of the 7th International Conference on Cartography and GIS, Sozopol, Bulgaria* (pp. 18-23).

Yu, H., Lu, N., Fu, B., Zhang, L., Wang, M., & Tian, H. (2022). Hotspots, co-occurrence, and shifts of compound and cascading extreme climate events in Eurasian drylands. Environment International, 169, 107509. https://doi.org/10.1016/j.envint.2022.107509

Zanuttigh, B., Simcic, D., Bagli, S., Bozzeda, F., Pietrantoni, L., Zagonari, F., Hoggart, S., & Nicholls, R. J. (2014). THESEUS decision support system for coastal risk management. Coastal Engineering, 87, 218–239. https://doi.org/10.1016/j.coastaleng.2013.11.013

Zennaro, F., Furlan, E., Simeoni, C., Torresan, S., Aslan, S., Critto, A., & Marcomini, A. (2021). Exploring machine learning potential for climate change risk assessment. *Earth-Science Reviews*, *220*, 103752. https://doi.org/10.1016/J.EARSCIREV.2021.103752